



Grant Agreement No.: 226479

SafeLand

Living with landslide risk in Europe: Assessment,
effects of global change, and risk management strategies

7th Framework Programme
Cooperation Theme 6 Environment (including climate change)
Sub-Activity 6.1.3 Natural Hazards

Deliverable D2.10

Identification of landslide hazard and risk "hotspots" in Europe

Work Package 2.4 - Identification of landslide hazard and risk "hotspots" in
Europe

Deliverable/Work Package Leader: ICG / NGI

Revision: Final

1 May, 2010

Rev.	Deliverable Responsible	Controlled by	Date
0	ICG	UPC	01.11.2010
1		JRC	31.01.2011
2			

SUMMARY

Hotspots of landslide hazard and risk were identified by three GIS based analysis that cover all of Europe with the same approach and locally validated with available landslide inventories. The results show clearly where landslides pose the largest hazard in Europe and the objective approach allows a ranking of the countries by exposed area and population. In absolute numbers Italy is the country with the highest amount of area and population exposed. Relative to absolute number of inhabitants and area, the small alpine countries such as Lichtenstein score highest where as much as 40% of the population is exposed. It is obvious that the type and quality of the input data is decisive for the quality of the results. Especially the estimation of extreme precipitation needs improvement. The numbers are preliminary and only based on the results from one of three applied hazard models.

Note about contributors

The following organisations contributed to the work described in this deliverable:

Lead partner responsible for the deliverable:

International Centre for Geohazards (ICG), Oslo, Norway

Team:

- Christian Jaedicke, (Work Package leader)
- Kjetil Sverdrup-Thygeson, (GIS)
- Helge Smebye, (GIS)
- Egil Syre, (GIS)
- Bjørn Vidar Vangelsten, (Risk)
- Farrokh Nadim, (Supervisor)
- Bjørn Kalsnes, (Coordinator)

Partner responsible for quality control:

Universitat Politecnica de Catalunya (UPC), Barcelona, Spain

Other contributors:

- AMRA Scarl (Tonino Santo, landslide inventory).
- Eidgenössische Technische Hochschule Zurich
- Geological Institute of Romania (Raluca-Mihaela Maftai; validation)
- Joint Research Centre (Miet Van Den Eeckhaut and Javier Hervás; hazard model 2 and review of the deliverable)
- Max-Planck-Gesellschaft zur Förderung der Wissenschaften e.V.
- TRL Limited (Jessica Smith; validation)
- Università degli Studi di Firenze (Veronica Tofani; validation)
- Université de Lausanne (Marc-Henri.Derron; hazard model 3)

CONTENTS

1	Introduction	6
2	Data used.....	9
2.1	Digital Elevation Model.....	9
2.2	Geology.....	10
2.3	Glaciers	10
2.4	Lakes and rivers	10
2.5	Land use	10
2.6	Landslide events.....	10
2.7	Precipitation	11
2.8	Seismicity.....	11
2.9	Snow cover.....	11
2.10	Soil moisture	12
2.11	Soil cover	12
2.12	Infrastructure.....	12
2.13	Temperature	13
2.14	Coping capacity / Vulnerability.....	13
2.15	Population	13
3	Models	14
3.1	ICG model.....	14
3.2	JRC model.....	14
3.3	UNIL model.....	14
4	Validation.....	15
5	Results	16
5.1	Results from the ICG model	16
5.2	Results from the JRC model	20
5.3	Results from the UNIL model.....	24
6	Discussion.....	28
6.1	Input data	28
6.2	Applied methods	28
6.3	Model validation	28
6.4	Risk assessment	29
7	Conclusions	32
8	References	33
9	Appendix A – Data Input	34
9.1	Digital Elevation Model.....	34
9.2	Geology.....	34
9.3	Glaciers	35
9.4	Lakes and rivers	35

9.5	Land use	36
9.6	Landslide events.....	37
9.7	Precipitation	37
9.8	Seismicity.....	38
9.9	Snow cover.....	38
9.10	Soil cover	39
9.11	Soil moisture	39
9.12	Infrastructure.....	40
9.13	Population	41
9.14	Project extent	41
10	Appendix B – Model descriptions.....	42
10.1	ICG model.....	42
10.1.1	Model for Landslide Hazard Evaluation	42
10.1.2	Data preparation	43
10.1.3	Slope factor S_r	43
10.1.4	Lithology factor S_l	46
10.1.5	Land cover index S_v	47
10.1.6	Precipitation trigger factor T_p	48
10.1.7	Seismic trigger factor T_s	49
10.1.8	Categorisation of landslide hazard	50
10.2	JRC model.....	51
10.2.1	Introduction	51
10.2.2	Data preparation	51
10.2.3	Model for Landslide Susceptibility Evaluation	52
10.2.4	Model for Landslide Hazard Evaluation	53
10.3	UNIL Model.....	56
10.3.1	Introduction	56
10.3.2	Data and Methods	56
10.4	Risk assessment	60
10.4.1	Discussion	61
10.4.2	Evaluation of physical exposure	62
11	Appendix C – Model validation.....	64
11.1	Answers from Romania (GIR).....	65
11.2	Answers from Italy (UNIFI)	67
11.2.1	Introduction	67
11.2.2	ICG Precipitation Model.....	67
11.2.3	ICG Seismic Model.....	72
11.2.4	JRC Precipitation Model.....	75
11.2.5	JRC Seismic Model.....	76
11.3	Answers from Scotland (TRL).....	77
11.3.1	Imagery Examined	77
11.3.2	Areas Examined	77
11.3.3	Bervie Braes, Stonehaven, Aberdeenshire	80
11.3.4	ICG Precipitation Model.....	82
11.3.5	JRC Precipitation Model.....	92
11.3.6	ICG Seismic Model.....	96
11.3.7	JRC Seismic Model.....	97

11.3.8 UNIL Rock fall Model	98
11.4 Answers from Norway (ICG)	104
12 Appendix D – Model results.....	106
12.1 Results from the ICG model	107
12.2 Results from the JRC model	109
12.3 National fact sheets	111

1 INTRODUCTION

Landslide hazard and risk in Europe become a public concern just after a recent local catastrophe such as the widespread flooding and landsliding in Switzerland and Austria, in the summer of 2005, or the events in Messina (Italy) in autumn 2009, in Madeira January 2010 in (Figure 1-1) or southern Italy in February 2010. Every year numerous landslides occur all over Europe and experts know to a certain degree which parts of the continent are most exposed to landslide hazard.

Nevertheless, landslide events, as the examples mentioned above, do not necessarily point out the areas with highest landslide risk. Often, landslides occur unexpectedly and the decisions where investments should be done to prevent future events are based on hasty need for showing action and political will.

A uniform and objective analysis of landslide risk for Europe would give an overview over the exposed areas and allow a simple ranking of areas where the invested money will yield the highest protective effect for humans and infrastructure.

The project team hopes to provide a new and more objective tool to assess landslide risk in Europe.



Figure 1-1: The scars left by landslides on 22. February 2010 on the slopes of Curral das Freiras, a village in the interior of Madeira, Portugal (Helder Santos / AP).

The objective of this Work Package is to perform a first-pass analysis of landslide hazard at European scale to identify the landslide hazard and risk "hotspots", i.e. where hazard and risk are highest. The results of this Work Package provide support for the choice of the case study sites in the SafeLand project. They also make it possible to visualize, on a European scale, the expected changes in the landslide hazard pattern for different global change scenarios (SafeLand Area 3).

The scale of the analysis ranges from 30 x 30 m (ICG, UNIL) to 900 x 900 m (JRC) where landslide hazard is estimated by three different models applying an appropriate combination of the parameters representing susceptibility factors (slope, lithology, soil moisture, vegetation cover, etc.) and triggering factors (extreme precipitation and seismicity). The weights of different susceptibility and triggering factors are calibrated against the information available in landslide inventories. Originally, the models are developed based on a first shot approach to develop the methods and processing to run the models smoothly. Second, the models will be improved by adjusting weights of the different susceptibility factors to yield the most realistic results.

The intersection of the landslide hazard "hotspots" with population density and infrastructure density maps provides a first-pass estimate of landslide risk "hotspots".

For understanding landslide risk, one has to consider three consecutive assessments (i.e. susceptibility, hazard and risk), which are finally combined to achieve an estimate of the risk.

- 1) The physical environment in itself gives the basis for the susceptibility to landslides. This category includes the terrain (steep, flat), geology, soils, vegetation and land use. These factors decide if the area is capable to produce a landslide but do not give any estimate of the likelihood of an event.
- 2) The likelihood of an event is determined by a trigger. This trigger can be the effect of water (precipitation and snow melt), seismic activity or human activities such as excavation or blasting in the landslide-prone terrain. The most common trigger is heavy rainfall that exceeds the normally experienced rain events in an area. This study considers both seismicity and precipitation as triggers.
- 3) Landslides as a natural process present no danger or threat in themselves. One can assume that globally most landslides are never detected. First in the interaction with human activities, landslides show their devastating power. The presence of humans, their infrastructure and possessions is usually described as the exposure. That is, once the areas where a landslide hazard exists are identified, one has to study how many people and assets are located in these hazard zones as well as how vulnerable these people and assets are. For example, a wooden shack would be much more easily destroyed by a landslide than a solid house with concrete foundations.

The combination of hazard and vulnerability leads to the risk. This can be described in a mathematical way as:

$$\text{Risk} = (\text{susceptibility} \times \text{trigger}) \times (\text{vulnerability} \times \text{exposure})$$

with $\text{susceptibility} \times \text{trigger} = \text{hazard}$.

A high quality hazard assessment is a more complex task than assessing susceptibility in terms of models, data availability and resource use. Introducing a trigger creates instant challenges. Precipitation extremes are often not even captured by the standard meteorological

network and the correct threshold of the amount of water actually needed to produce slides is very different from region to region.

Even more complicated is the study of risk. For a true estimate, one should sum up all the assets that can be destroyed in a landslide event. This can range from a road with cables and pipes to entire houses with their content. On a European scale, this kind of approach is not applicable. Therefore, only two types of elements at risk are considered in this study, the number of people living in landslide exposed areas and the accumulated number of kilometres of national and international roads and railroads. The analysis helps identifying where in Europe the risk hotspots are located and allows comparison of the risk level between the countries included in the analysis.

Landslide hazard can be mitigated by both physical countermeasures (such as slope stabilisation, reforestation and water management) and non-physical countermeasures (such as evacuations and road closures). Many known landslide areas in Europe already have such warning and other mitigation systems in place. As data collection with such information on a European scale is close to impossible, this is not considered by the model used in this analysis resulting in overestimation of the risk for these areas. As an alternative, the human development index could be used for Europe as a measure for the ability to manage the landslide hazard in a given area and situation.

The terms and definitions used in this report are in accordance with the SafeLand project handbook (deliverable D8.1).



Figure 1-2: As long as landslide events only affect natural environments, the risk for human assets is low

2 DATA USED

The basic challenge for a comparative hazard and risk analysis for Europe is the need for homogeneous datasets. Locally and nationally, detailed maps of population, development index, geology etc. are available. They are unfortunately of very little use for a European analysis. Often the applied methods for creating the maps are different from one country to another and in some cases the methods are not publicly available at all. Local data is therefore applicable for the verification of the European model, but not as input to the model.

Homogenous datasets are difficult to access, with many datasets only covering the countries within the European Union. The alternatives are global datasets which may lack accuracy and in many cases are not well suited to study differences between European countries. The first challenge for this project was therefore to use the limited resources in an optimal way to gather the best possible datasets for each input parameter. The applied models are flexible and results can be improved using newer and better datasets as they become available.

In this chapter the available datasets are described briefly with respect to their contribution to the landslide hazard and risk. More details can be found in appendix A.

2.1 DIGITAL ELEVATION MODEL

The topography is the most important factor for landslide susceptibility. In flat terrain, the gravitational forces are too weak to move land masses. With increasing inclination, the terrain becomes more susceptible to landsliding. Natural loose geological material is usually stable up to slope angles of 27 degrees. In terrain steeper than 30 degrees, rocks and other loose materials fall continuously and does not create deposits which can form larger landslides. Above 45 degrees usually only rock falls and large rock avalanches occur.

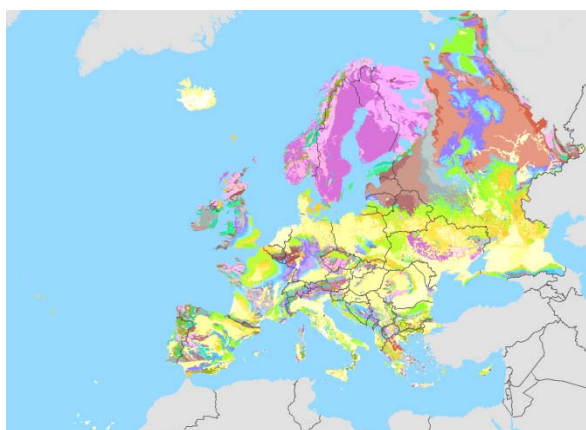


Figure 2-1: Map showing the geology of the study area

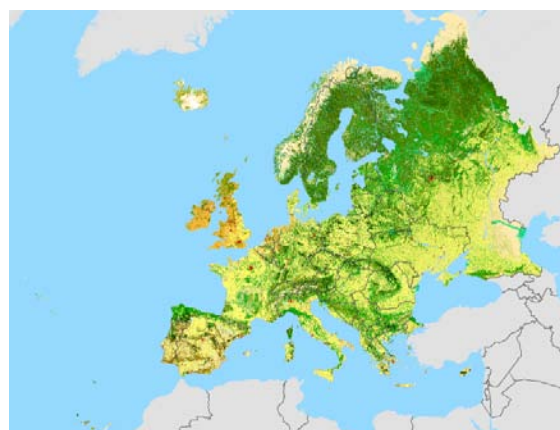


Figure 2-2: Map showing the land cover of the study area

2.2 GEOLOGY

The geology of any location gives information about the strength of the available material that could form a landslide. Young and weak sedimentary deposits have a higher potential for landslides than old hard base rock. A European geological map was used to classify the type of rock (sediment, igneous, metamorphic) and age of the rock according to how it impacts on landslide susceptibility (Figure 2-1).

2.3 GLACIERS

Glaciated areas are normally not active with respect to landslides and information on the location of glaciers can be used to exclude these areas from the analysis (Figure 2-4).

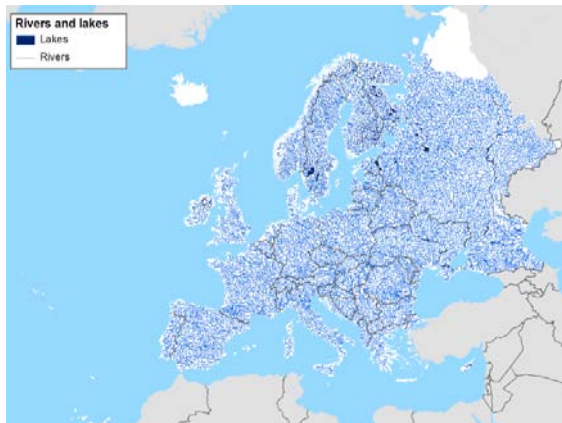


Figure 2-3: Map showing the rivers and lakes



Figure 2-4: Map showing glaciated areas

2.4 LAKES AND RIVERS

Lakes and rivers give information on the location and amount of water that normally is present on the surface. Such information can help identifying hazard zones for example for torrents and debris flows which usually follow the path of existing creeks and minor streams (Figure 2-3).

2.5 LAND USE

Land use data yields information on the type of surface and its effect on landslide susceptibility. The data is usually reclassified into urban areas, water bodies, forest and farm land (Figure 2-2).

2.6 LANDSLIDE EVENTS

For the calibration and the validation of the models results databases of historical landslide events are essential. Such databases exist in many European countries but are exceedingly difficult to access. In many cases no national databases, but local collections, often on paper

only, are available. Scientific inventories often concentrate on a special type of landslides and leave out the total picture. In other countries landslide inventories are unavailable due to strict data sharing policies and are not available for research purposes. For validation of the hazard model in this study, national data for Romania and Norway and local datasets for the Barcelonnette (France) , Italy and some locations in Scotland were used.



Figure 2-5: Only three digital landslide inventories were available for the present study

2.7 PRECIPITATION

Precipitation is a key trigger for landslides with shallow landslides often being released by short time extreme events while deep seated landslides are often triggered by long lasting intense rain fall. Data related to such events are scarce and pose a big challenge to landslide hazard modellers. Currently, European maps are only available for monthly mean precipitation, but efforts are being made by several European agencies to obtain estimates of expected extreme precipitation. An example is shown in Figure 10-8.

2.8 SEISMICITY

Seismicity is the second key trigger for landslides next to precipitation. In many regions of the world, earthquakes have triggered some of the largest known landslides. In this analysis separate hazard models were developed for precipitation and seismic triggered landslides.

2.9 SNOW COVER

The seasonal snow cover can be used as an indicator of land areas that are not likely to produce landslides during winter time. Assuming that e.g. some areas in the northern part of Europe are covered by snow for four months of the year and that landslides are not likely in this period, one can reduce the temporal probability of landsliding by $\frac{1}{3}$.

2.10 SOIL MOISTURE

Type of soil, precipitation and land use all have significant influence on the amount of water that is available in the soil. The effect on landsliding can be twofold. High soil moisture decreases the stability of the soils due to high pore pressure. Very low soil moisture on the other hand would lead to cracks and channels in the soil, which again form a starting point for landsliding and erosion as soon as high precipitation intensity hits the soil.

2.11 SOIL COVER

The type of soil and its thickness above bedrock is essential information for landslide modelling. This type of data is available for many of the European countries, but a homogenous dataset covering all of Europe is missing. Therefore, soil cover could not be used in the analysis and its results would certainly improve significantly if such a dataset would become available.

2.12 INFRASTRUCTURE

The consequence of landsliding depends of the amount of human assets present in the affected area. Such assets can be buildings, constructions, roads, railways or other infrastructure in addition to the humans themselves. Roads and railways are readily available datasets and can easily be used in the analysis of risk. Individual buildings cannot be addressed on a European scale, but population maps (section 2.15) give an indication of the number of people that are exposed to landslide hazard (Figure 2-6).

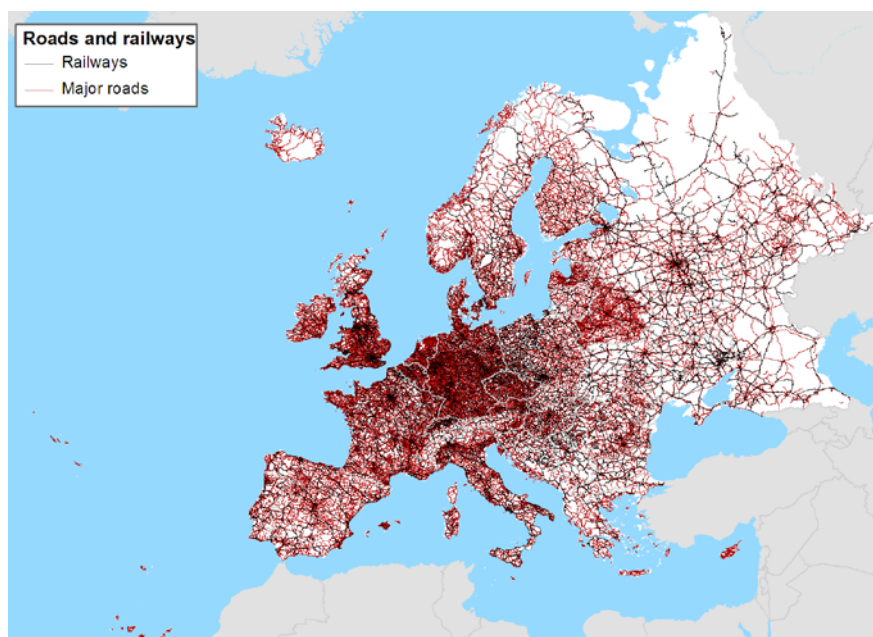


Figure 2-6: Network of European road and railways

2.13 TEMPERATURE

The mean annual temperature can be used as an indication similar to soil moisture and snow cover. The data was not applied in the current models.

2.14 COPING CAPACITY / VULNERABILITY

The consequences of landslide events often depend on the fast and effective response of the local and national authorities. This ability is highly dependent on the level of organisation in the society concerned. A country or region with weak administrative structures will have more difficulties with coping with a landslide event than regions where the civil response is well organised and prepared for the various types of natural events threatening the society. Various types of indicators and systems of indicators exist to assess a society’s vulnerability and coping capacity related to natural phenomena. In this study a formulation similar to the one used in the “Natural Disaster Hotspots – A Global Risk Analysis” (Dilley et. al, 2005) was attempted, but a reliable calibration based on loss data for Europe was not possible. Therefore the Human Development Index for each country is used as a rough indication of resilience and coping capacity.

2.15 POPULATION

Maps of population distribution give valuable information on where landslide hazard intersects with human activity. The existing global dataset is used to analyse how many individuals are exposed to landslide hazard in Europe in total and in each individual country (Figure 2-7).

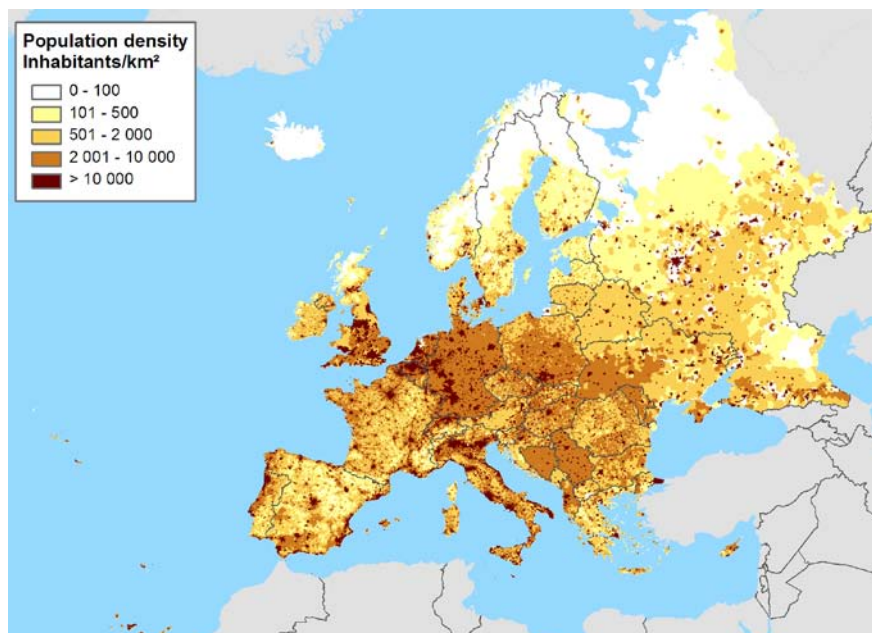


Figure 2-7: Population density in Europe

3 MODELS

Modelling landslide hazard and risk can be done on many different scales. Detailed modelling to assess and mitigate the hazard for selected buildings or infrastructure is an engineering task performed on a daily basis in Europe.

On a global scale, the Hotspots project (Nadim et al., 2006) tried to identify the most exposed areas for landslides and snow avalanches. This type of analysis was also tested on selected areas such as South East Asia, the Caribbean and Himalayas. On a European scale, this project makes the first attempt to assess the landslide hazard and risk in Europe in an objective and homogenous way to allow comparison and ranking of the affected countries.

In SafeLand, three models were applied independently. The input data were the same datasets as described in appendix A, but all three contributors were free to choose which datasets they used in their final model. The models are described in detail in appendix B, but a short version is given in the following sections.

3.1 ICG MODEL

The ICG model is described in detail in several publications. In general, the model is based on the combination and weighting of different gridded data layers. Each layer is classified according to its supposed effect on landsliding. For example, weak sedimentary geology is classified into a higher susceptibility class than hard plutonic geology. The classified layers are then multiplied and weighted relatively to each other to generate a hazard index for each pixel on the map. The grid used for this study is about 30 x 30m, since this is the resolution of the digital elevation model covering the major part of Europe (areas north of 60° N are not covered by the 30m digital elevation model outside of Norway) even if other applied grids have a much coarser resolution.

3.2 JRC MODEL

The JRC landslide hazard model contains two steps. First, landslide susceptibility was estimated using the statistical model logistic regression. Secondly, the obtained classified landslide susceptibility map was confronted with precipitation and seismic data respectively to obtain two qualitative hazard maps, one for hydrologically-triggered landslides and one for seismically-triggered landslides. Important is that these maps were produced for slides and flows only and that rock falls were not included in the modelling. The grid used for this study is about 900 x 900m, since this is the resolution of the digital elevation model available for the complete study area.

3.3 UNIL MODEL

The UNIL model estimates rock fall susceptibility by identifying possible source areas for rock falls and then calculates the estimated run out length for each source pixel. The resulting susceptibility is then related to a release probability of the rocks from the source areas. UNIL performed a basic risk analysis by estimating the exposed population in each European country.

4 VALIDATION

The validation of two models (ICG, JRC) was done against existing data from documented historical landslide events. Such data was available from Norway, France, Italy, Scotland and Romania. A short evaluation form with eight questions was sent to the partners in these countries to the model results against their data and experience. The questions focused on the ability of the models to identify the regions most affected by landslides and how any discrepancies could be explained. On a European scale one cannot expect the models to fit perfectly on a local scale. But they should catch the pattern within an area of several square kilometres. Key findings from the validation exercise are listed in the Discussion chapter below. Further details of the validation analysis can be found in appendix C.

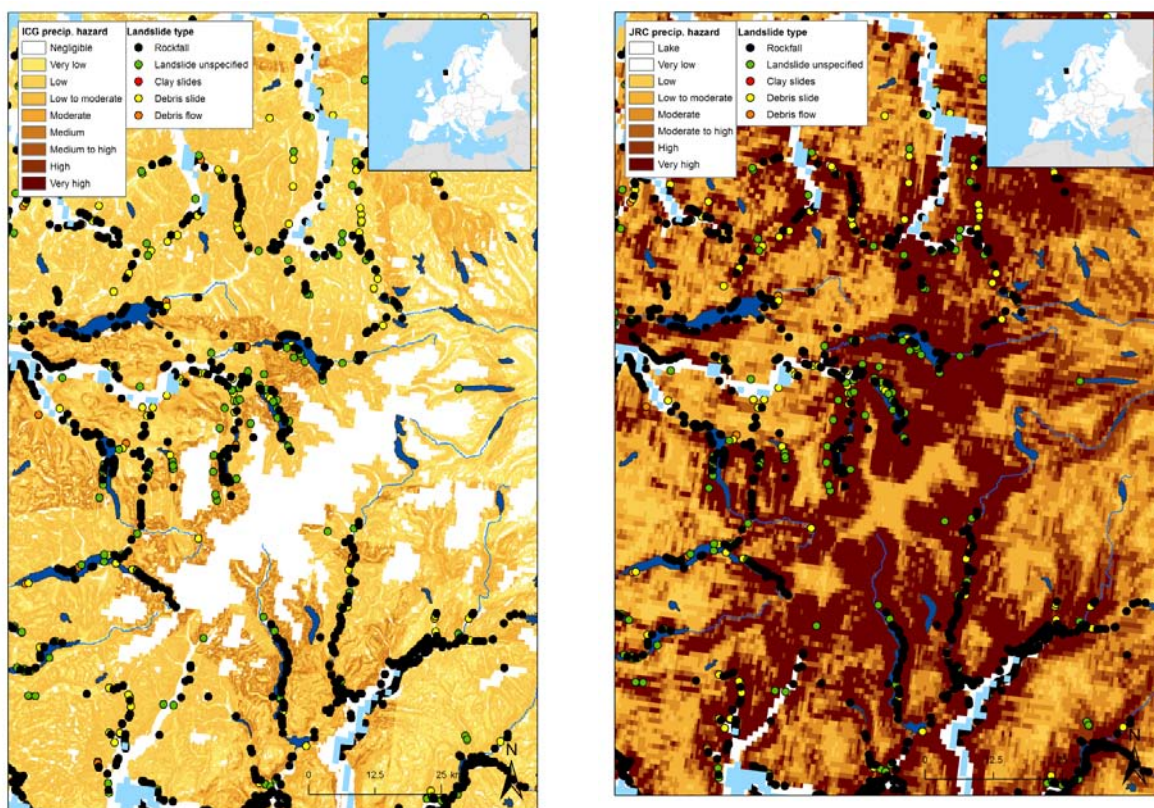


Figure 4-1: Example for results from the ICG and JRC landslide hazard models for precipitation. Both models cover the recorded events reasonably well, but the JRC model shows generally a higher hazard values than the ICG model.

5 RESULTS

The analysis covers 44 countries and the extent of the study is roughly defined according to the physical boundaries of Europe. This area encompasses 9.7 million km² of land area and 729 million inhabitants.

5.1 RESULTS FROM THE ICG MODEL

The maps in Figure 5-1 and Figure 5-2 show the landslide hazard for Europe both for precipitation- and earthquake-induced landslides estimated by the ICG model. A distinct difference can be observed between the two maps, where the precipitation-induced landslides cover in some degree all mountainous areas in Europe, while the earthquake-induced landslides are much more concentrated in the south-eastern part of Europe and Iceland, where the seismic hazard is known to be high. The main mountain ranges are well reproduced and the results look reasonable on a European scale.

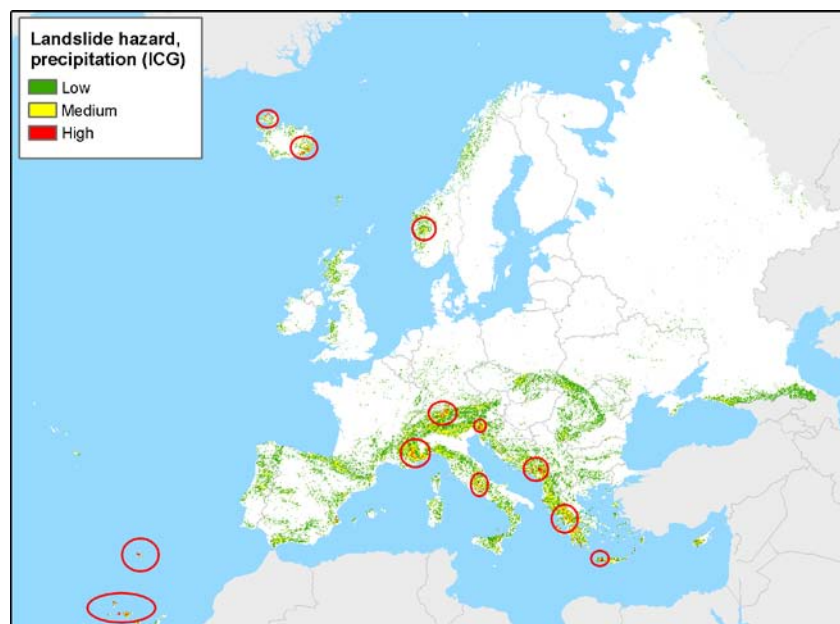


Figure 5-1: Landslide hazard caused by precipitation (results from the ICG model). Red circles show possible hotspots

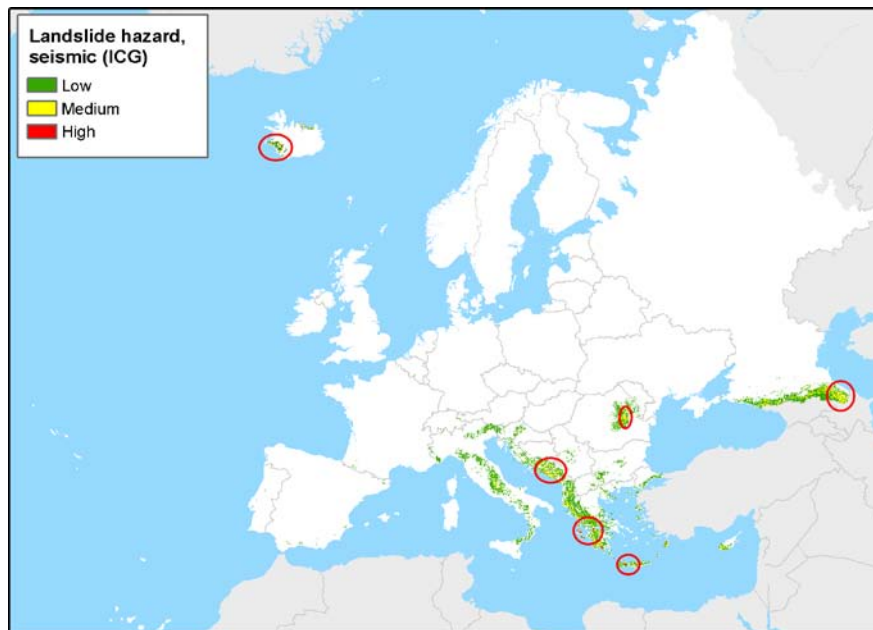


Figure 5-2: Landslide hazard caused by seismicity (results from the ICG model). Red circles show possible hotspots

For precipitation-induced landslides the results from the hazard model were used to estimate the exposure of population and infrastructure to the hazard. For this purpose the affected land areas, number of people and kilometres of roads and railways were counted for each of the 44 countries in this study.

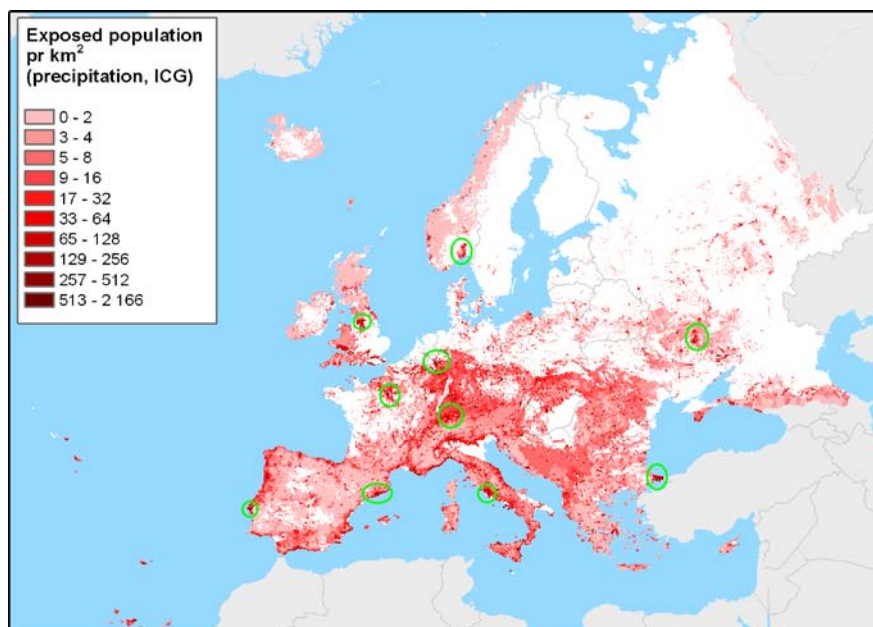


Figure 5-3: Exposure map for Europe with possible hotspots marked in green.

Looking at all 44 countries a total number of 167 000 km² are exposed to medium or high landslide hazard. This is 1.7% of the land area of Europe. In these areas live 8.2 million people, which represent 1.1% of the total number of European inhabitants. Focusing on the areas with high hazard one finds 17 000 km² and 1.3 million people exposed (0.2%).

The hazard map in Figure 5-1 shows the areas of highest hazard represented by the mountain regions of the Pyrenees, northern and south eastern Alps, Italy, the Balkan, western Norway and Iceland. On the other hand, the European exposure map in Figure 5-3 shows the highest exposure in the densely populated areas around cities that are surrounded by mountains, such as Barcelona, Lisbon and Rome. The exposure map clearly shows that the highest level of risk is not necessary correlated to the hazard but much more dependent on the distribution of population in Europe.

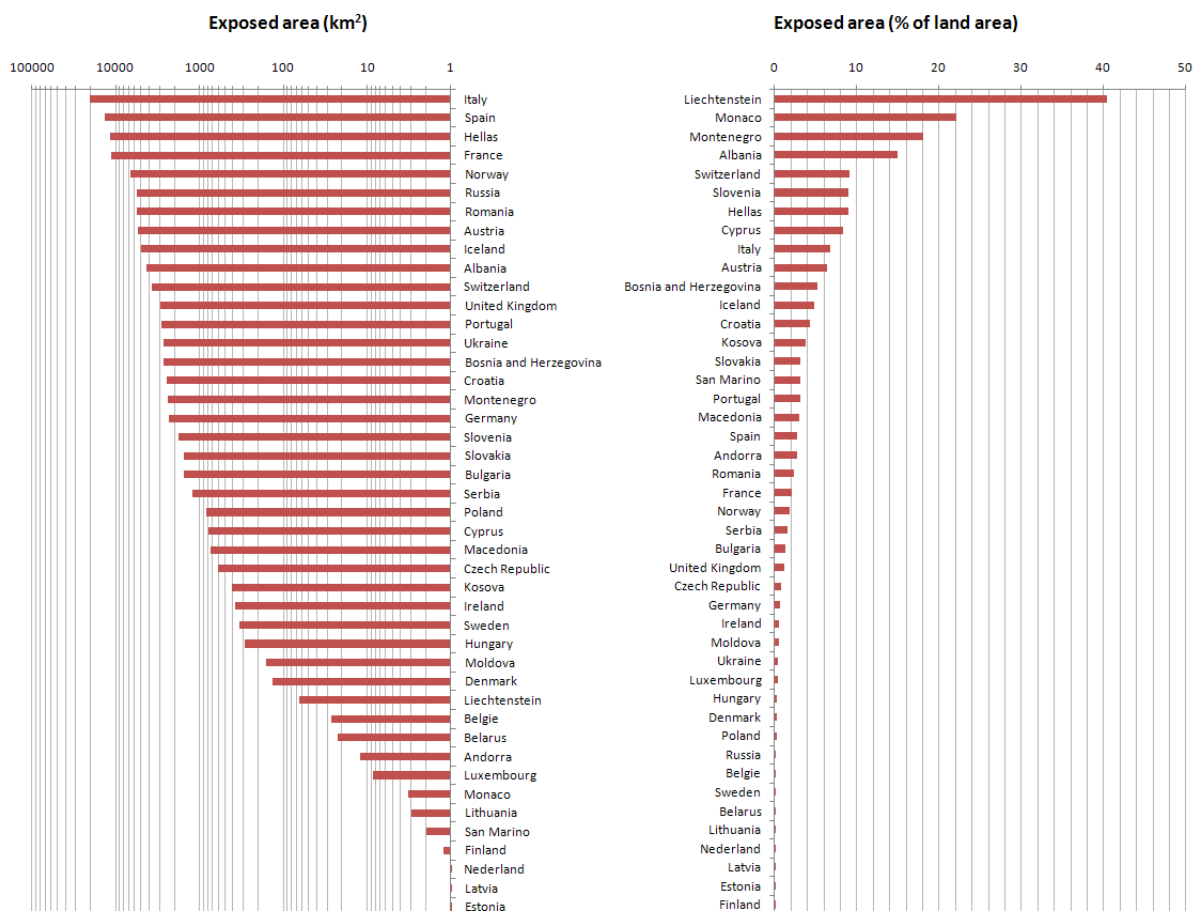


Figure 5-4: Total and relative number of exposed area in the countries within the study area

Ranking countries by exposed land area (i.e. relative exposure), one finds that Lichtenstein is the country with the highest percentage of exposed land area (40%), while Italy features most terrain exposed to landslide hazard in total numbers (20 000 km², Figure 5-4).

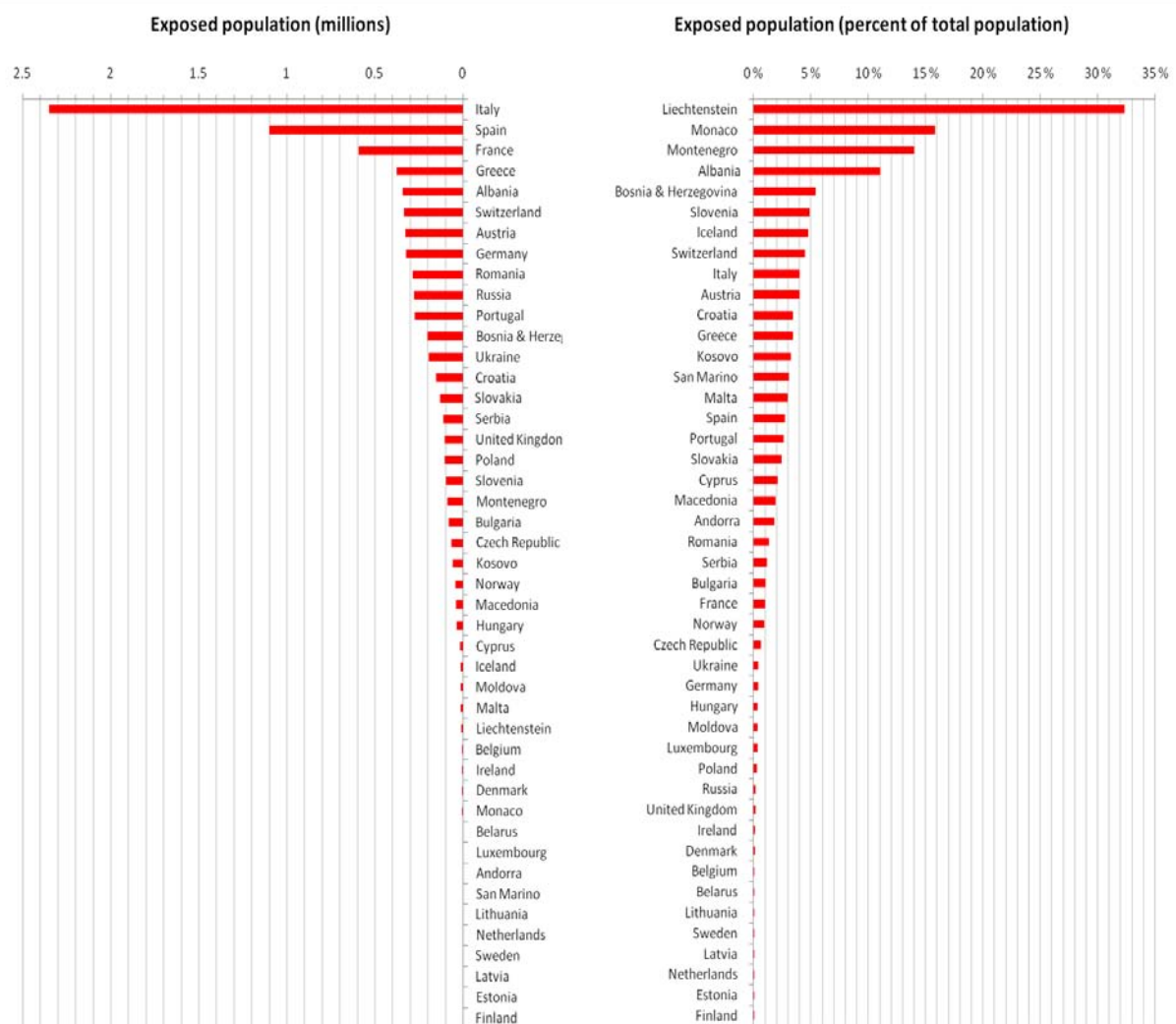


Figure 5-5: Total and relative number of exposed people in the countries within the study area

The countries with the highest level of exposed people can be found in the mountainous areas (Figure 5-5). Small countries like Montenegro and Liechtenstein score high on the relative hazard as a large portion of their population actually live in the mountains. Italy has the highest total number of exposed people, but due to large areas of low or negligible landslide risk in the country Italy moves down to ninth place on the list of countries ranked by relative exposure (exposed divided by total population). In total numbers Italy has more than 2.3 million people living in landslide terrain (Figure 5-5). That is nearly 1/5 of the total amount of people exposed in Europe.

The ten countries with the highest number of exposed people represent 77% of the total number of people exposed to landslides in Europe. On the other end of the scale are the countries with very little topography (e.g. Netherlands, Latvia) or countries where the mountainous areas are not inhabited (e.g. Finland).

In terms of exposed infrastructure Italy tops the list of countries both for roads (6 597 km) and railways (2 274 km). Second is France while Germany ranges on 4th place. Relative to the total length of roads and railways, the smaller countries again score highest with Montenegro and Liechtenstein on top of the list. In Greece 10% of the roads are exposed and Switzerland features ca. 9%. In Montenegro almost 40% of the 187 km of railways are exposed while in Switzerland 9% of its total 4 600 km is exposed.

Looking at Europe as a whole, 2.6% of the road network and 1.8% of the railways are exposed to landslide hazard following the results from the ICG model.

5.2 RESULTS FROM THE JRC MODEL

The results from the JRC model are shown in Figure 5-6 and Figure 5-7 for precipitation and seismic triggers respectively. Clearly the mountainous areas in the Alps, Scotland, West-Norway and Pyrenees are pointed out as being areas with high landslide hazard due to precipitation triggered slides. In addition, areas in the Balkans and Caucasus are highlighted. On the other hand, areas in central Italy are not clearly depicted by the model.

The seismic trigger on the other hand points out central Italy, the whole southern rim of the Caucasus, North – East Italy, the Balkans and small parts of Iceland.

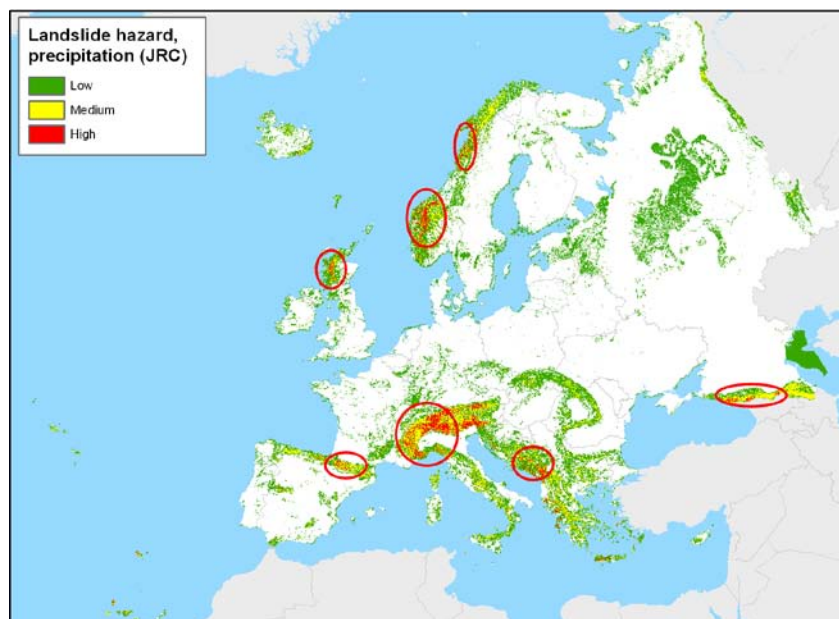


Figure 5-6: Landslide hazard caused by precipitation (results from the JRC model).
Red circles show possible hotspots

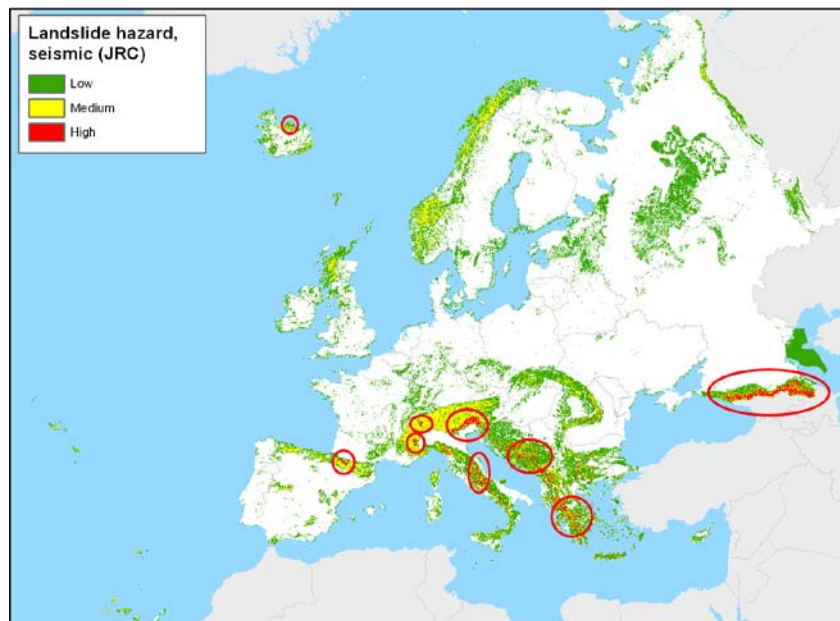


Figure 5-7: Landslide hazard caused by seismicity (results from the JRC model). Red circles show possible hotspots

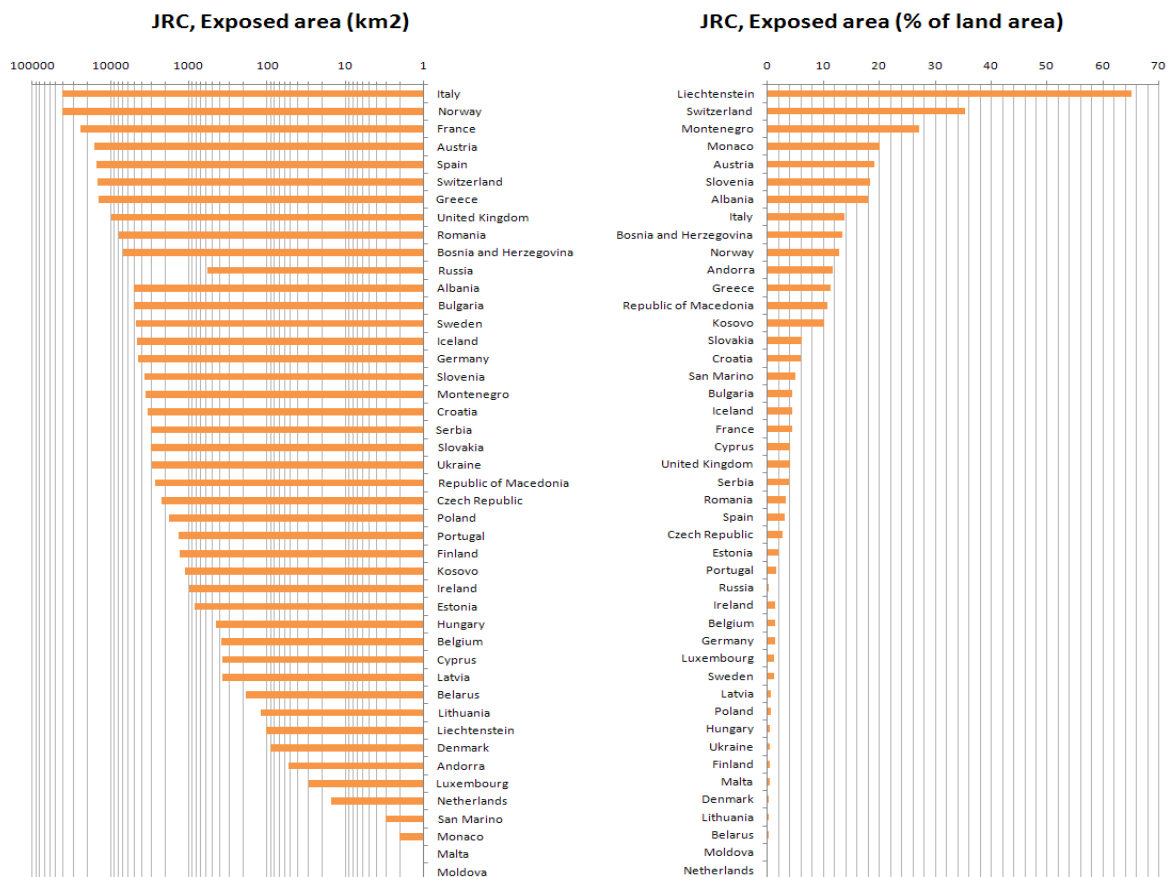


Figure 5-8: Total and relative number of exposed area in the countries within the study area

Ranking the countries according to area exposed to precipitation-induced landslides (Figure 5-8), Italy, Norway and France top the list with Switzerland on a 6th place. Relative to the total land area, the small alpine countries dominate, but also for Switzerland (2) and Austria (5) a large fraction of the land seems to be exposed to landslide hazard.

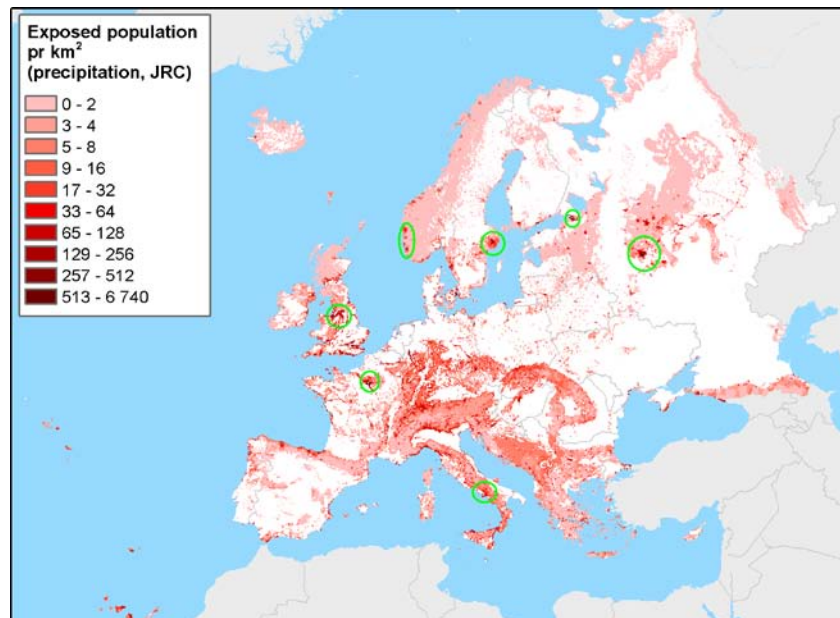


Figure 5-9: Exposure map for Europe with possible hotspots marked in green.

With regard to the amount of exposed population, Italy clearly scored highest with over 3.5 million people exposed. France and Switzerland are second and third respectively. In relative number, the small alpine countries show the highest percentage of exposed people. But also relative large countries as Switzerland and Austria show over 10% exposed population. Even, if Scotland is pointed out as one of the hazard hotspots, the exposure for the United Kingdom as a whole is the lowest in the ranking.

The exposure map in Figure 5-9 shows clearly high risk hotspots in areas that are known to feature low landslide hazard, for example the urban centers of Paris, Stockholm and St. Petersburg. Most likely, the population density here plays a far more important role than the landslide hazard.

In total, the results from the JRC model indicate 255 000 km² (2.6%) and 15.4 (2.1%) million people as exposed to precipitation-induced landslides. 42 000 km (3.3%) of the road network and 18 500 km of the railway system are located in exposed areas.

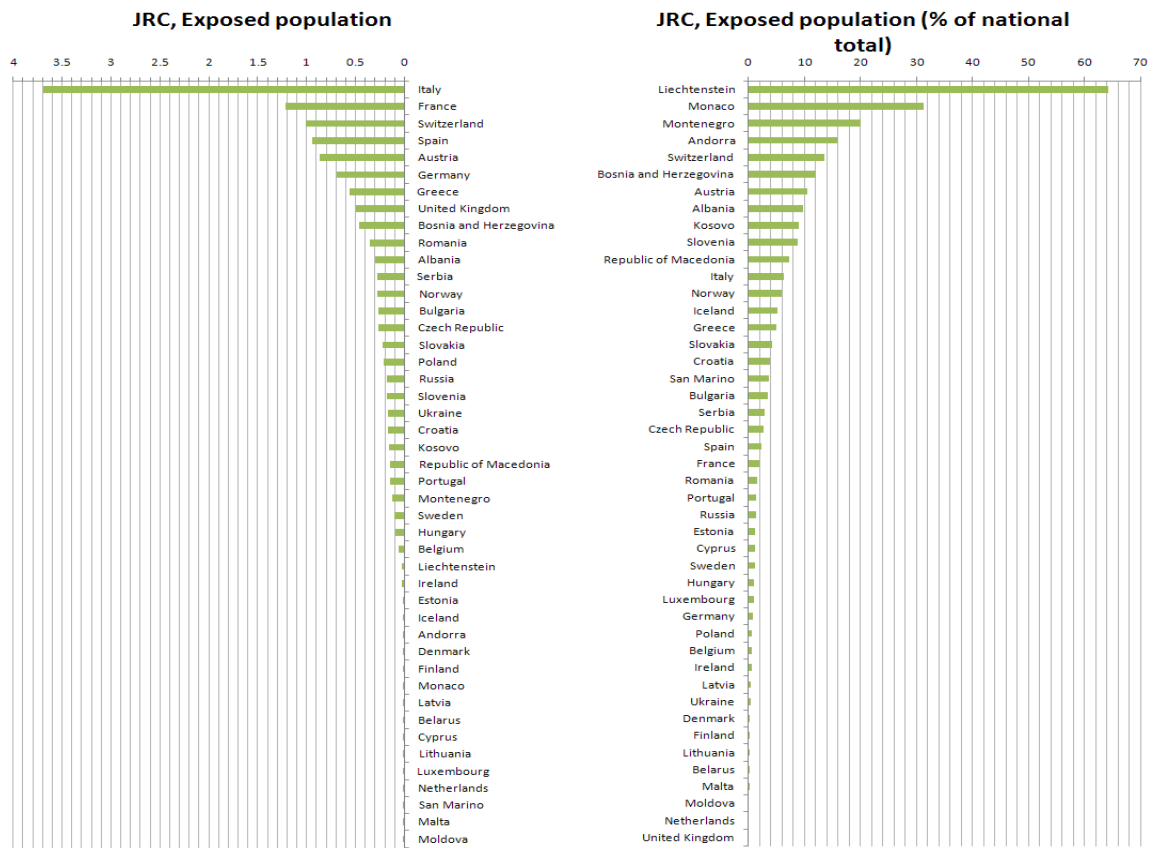


Figure 5-10: Total and relative number of exposed people in the countries within the study area

5.3 RESULTS FROM THE UNIL MODEL

A susceptibility map for rock fall was drawn for the entire Europe up to latitude 60° North (Figure 5-11). The resolution of the final product is 100 m (grid cell size). This dataset will be made freely available as vector shapefile. Such a map can be used for instance to detect important transportation corridors (motorways or railways) crossing zones potentially affected by rock falls. This is the case of the Gotthard motorway (Figure 5-12), one of the major roads crossing the Alps (around 5 million cars and 1 million trucks each year). In May 2006, eleven blocks of around 10 m³ reached this motorway, making two fatalities. The road had to be closed for 1 month.

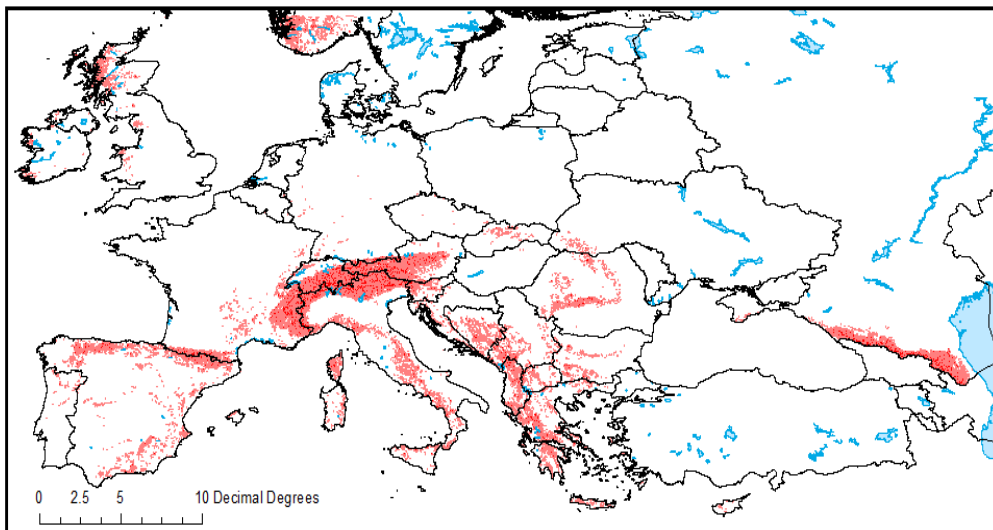


Figure 5-11: Overview of the rock fall susceptibility map for Europe

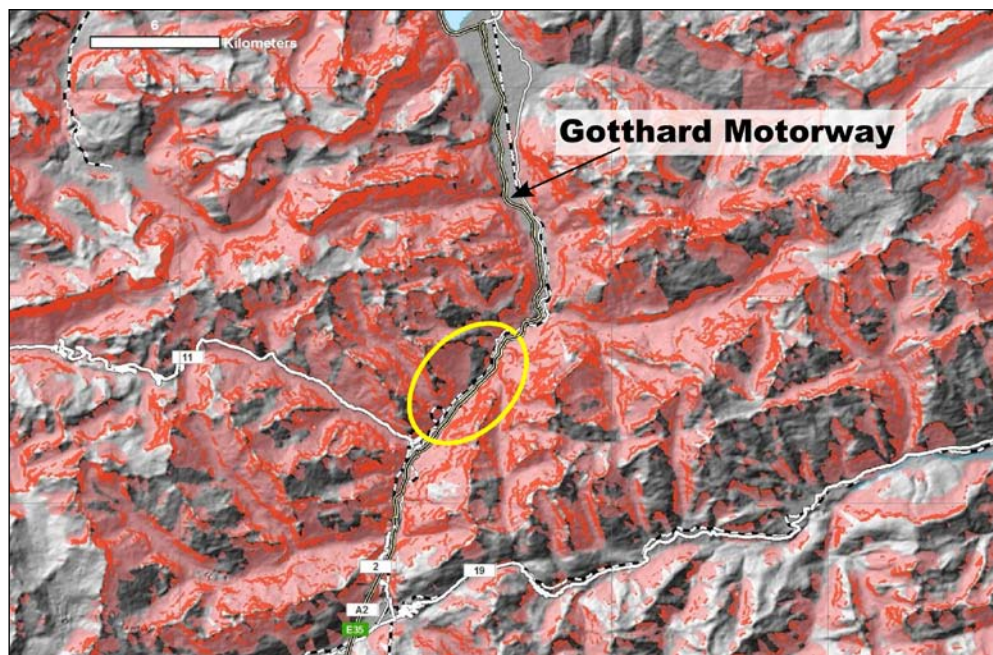


Figure 5-12: Extract of the rock fall susceptibility map in the area of the Gotthard (Switzerland). The motorway passes through a susceptible zone (yellow circle), that was strongly affected in 2006 by rock falls

The slope activity index (SAI; see appendix B) map displays a rough qualitative indicator of the propensity of an area to suffer from rock falls (Figure 5-13). This index is based only on the slope angle distribution and can thus be used even if only a DEM is available.

Presently the SAI has to be considered as a first attempt to define a simple indicator of rock fall activity based on geomorphic features. In the future, such indexes should be developed in a way that can be linked with a probability of event.

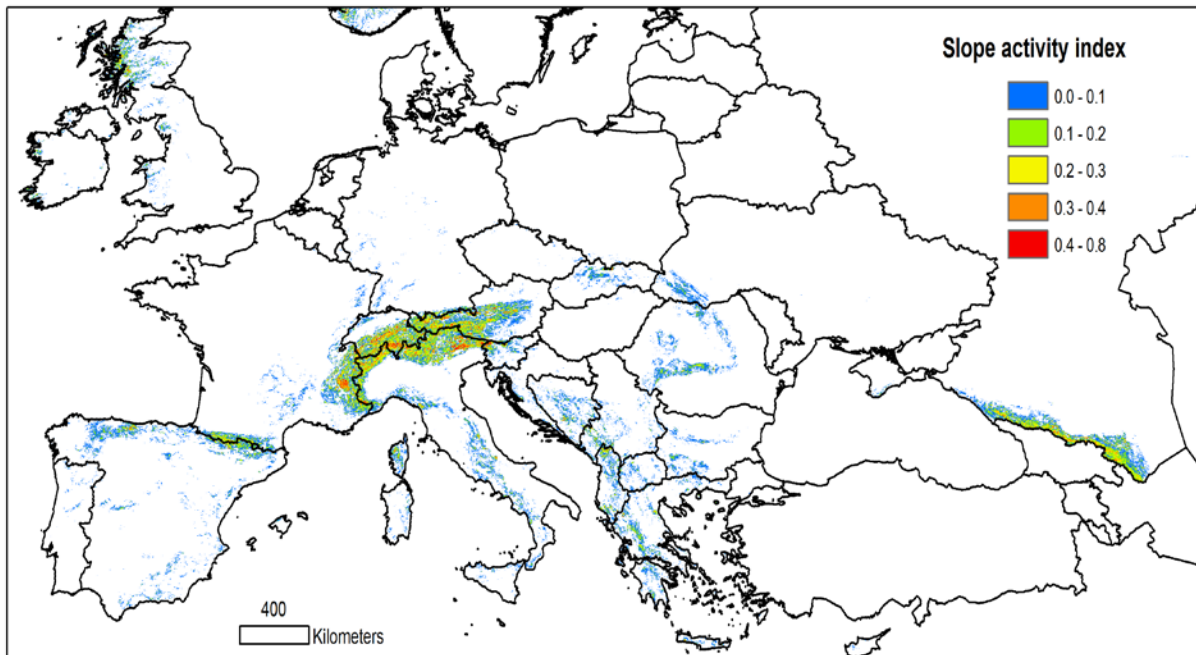


Figure 5-13: Slope activity index (SAI) map for Europe

The final simplified risk map shows the number of potentially exposed people per 100 km². It takes into consideration the susceptibility to rock fall, the “regional” steepness (through the slope activity index) and the population density. Of course areas with high mountain ranges and a locally high population density, like in the Alps or Pyrenees (particularly Andorra), are locations with high risk indexes (Figure 5-14). Interestingly, some very densely populated areas, out of high mountain ranges, such as Palermo and Naples, have intermediate SAI but very high risk index (Figure 5-15). This tends to show that this simplified risk index is able to properly balance its “hazard” and “element at risk” components.

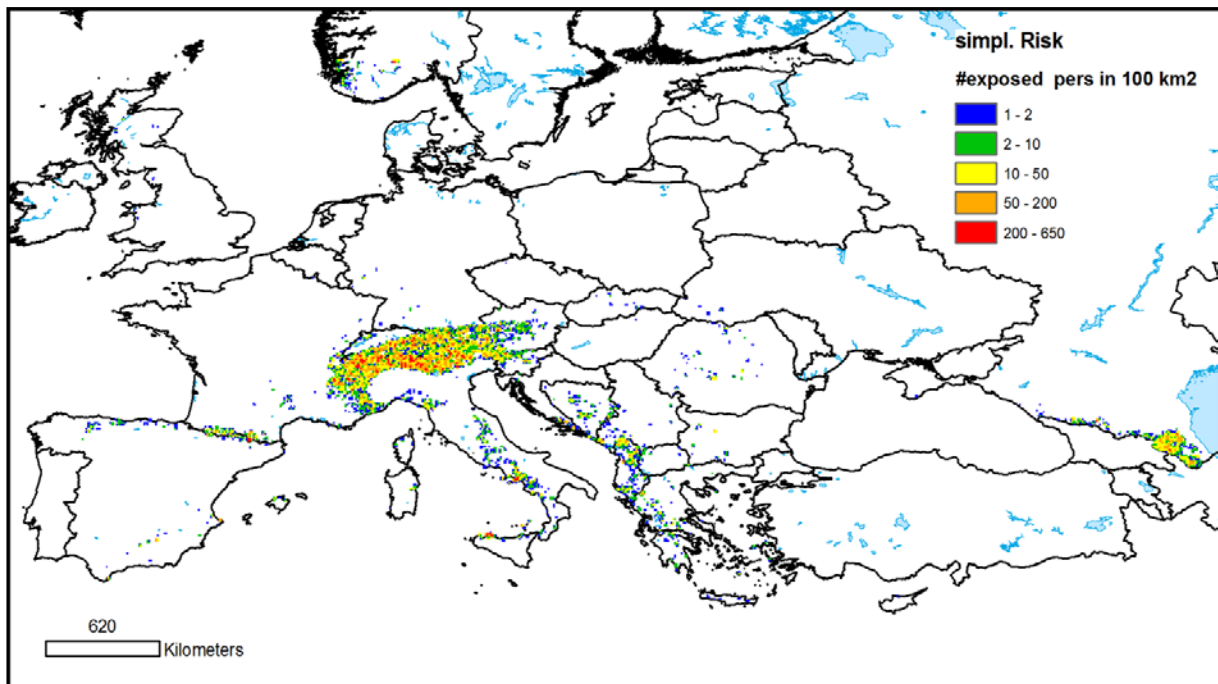


Figure 5-14: Simplified risk map of Europe. Number of people potentially exposed to rock fall in 100/km².

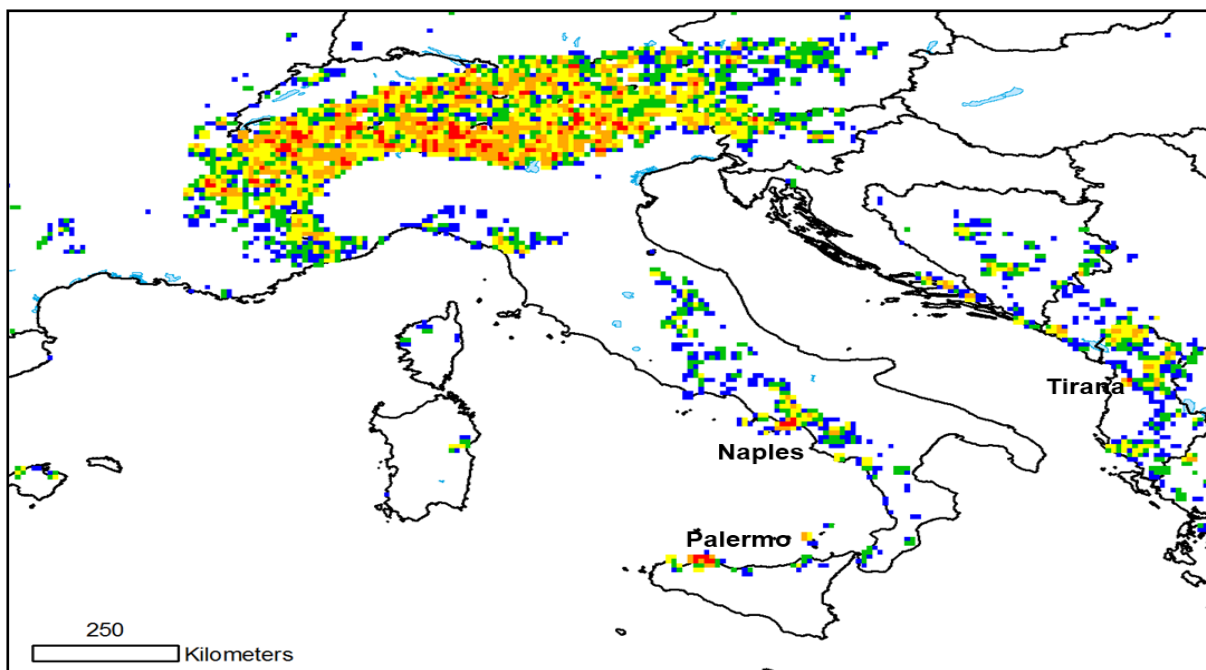


Figure 5-15: Detail of simplified risk map of Europe

Figure 5-16 shows the number of people potentially exposed to rock fall by country. Unsurprisingly, alpine countries have a high rating (Italy, Switzerland, France, Austria, Slovenia). The high score of Russia is clearly due to the Caucasus mountain range, in particularly its eastern part where the population density is higher. In Albania, a large part of the territory is in the Dinaric Alps, explaining its relatively high number of exposed people. Andorra is of course a well known “micro-hotspot”.

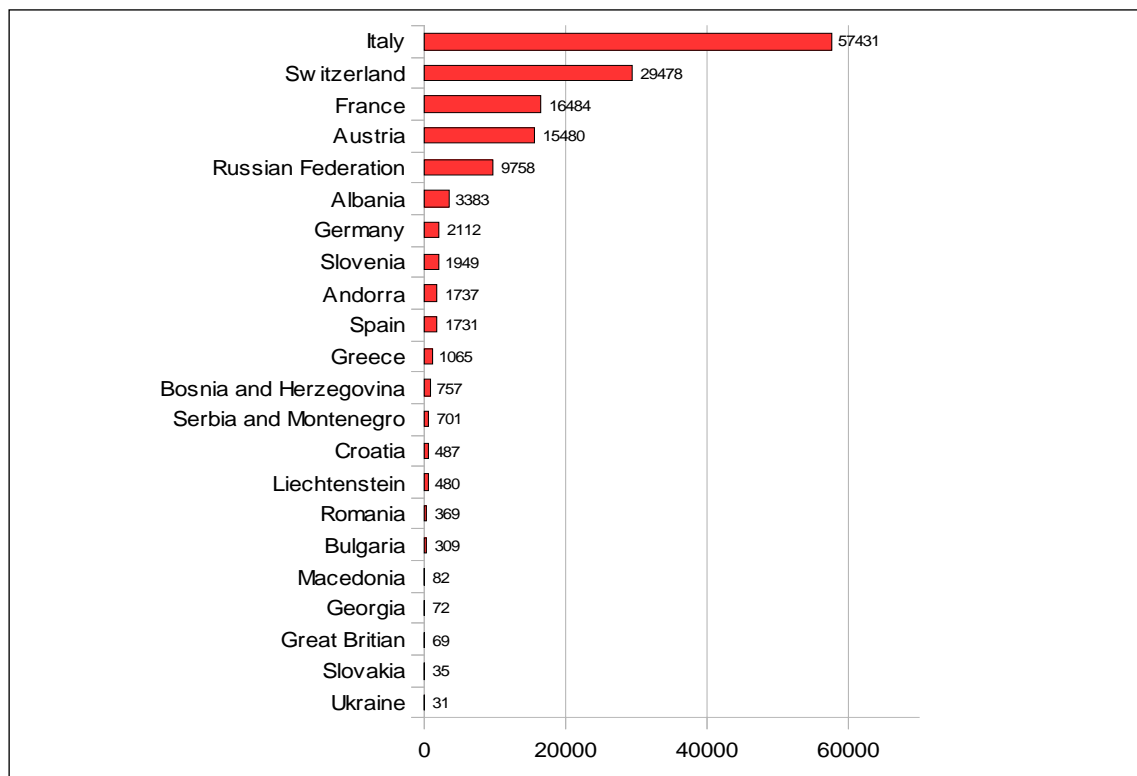


Figure 5-16: Number of people potentially affected by rock falls by country.

This contribution has to be considered as a pilot-study to test the feasibility of risk assessment over very large regions, using a simple physical model to define the areas potentially affected by rock falls. Each of the three steps of the procedure can be strongly improved: (1) the susceptibility maps used here are limited to rock falls. They should be extended to debris-flows and shallow landslides; (2) the slope activity index used is somehow a poor substitute for the probability of rock fall occurrence. Ongoing works aim to bridge the gap between such geomorphic indexes and a real hazard estimator; (3) the present risk estimations are very crude and address only the number of people potentially affected. Other social and economic indicators should be used too.

This study shows that it is feasible to use physical models to draw susceptibility and risk maps over very large areas. Both, necessary datasets and physical models are available. This method does not depend of any inventory of events. Presently there is yet a large potential of technical development to improve the products.

6 DISCUSSION

6.1 INPUT DATA

The available input data was the same for all three models. The datasets are in many respects improvable. The biggest challenge is to find a suitable dataset for the estimation of the precipitation trigger. Here, we were forced to apply a monthly dataset of global data. Other datasets are under development, but not available so far. It is our impression that the performance of the models can improve significantly by using more detailed precipitation datasets that also quantify the likelihood of extreme precipitation events.

Geological and lithological maps usually give no estimate of the thickness of soils and geological deposits. This is a major disadvantage in the estimation of landslide hazard with the applied methods. It may lead to an underestimation of landslide hazard especially in less steep terrain, where the models' terrain factor does not indicate a hazard to exist.

The results of the models now depend mainly on the terrain steepness, focusing the hotspots to the mountainous areas in Europe. Better data on both extreme precipitation and lithological setting would allow putting more weight on these factors in the hope to include also areas where slow moving landslides in gentle terrain occur. Probably, the use of remote sensing data could here help the further development of the models. On the other hand, one has always to remember that the datasets need to be homogenous and available for all over Europe. This is probably the biggest challenge for an analysis like this.

6.2 APPLIED METHODS

Three models were tested in this study. The ICG and JRC models applied different weights to gridded data and combined the resulting layers to susceptibility and hazard maps. The largest uncertainty in the model development is the weight of each of the input grids to the total landslide hazard. More and detailed research should investigate automated Monte Carlo methods to improve the choice of weights in the models. This would also give a better estimation on the uncertainties in the models.

To allow a better comparison of the models, exposed area, population and infrastructure were computed using the same methods for both the JRC and the ICG model. Unfortunately, this analysis could not be extended to the UNIL model. The method counts the number of pixels of exposed area and population using the polygons for the European countries as a mask. The infrastructure was resampled into a grid and then counted in the same manner. The approach was tested by controlling the total values per country against national UN data from 2007.

6.3 MODEL VALIDATION

The results from the models were tested and validated in Italy, Romania, UK and Norway. It is always possible to find both areas where the models cover the observed situation well and other areas where the agreement is poor.

For precipitation-induced slides, responsible project partners from all four countries reported good agreement between the model results and observed landslide events on a national scale. More detailed studies on regional and local scale show however discrepancies between modelled and observed landslide hazard. In both Norway and Romania, this is found in areas with less steep terrain and geological settings that are not represented by the available geological map. Torrents and shallow landslides seem to be well represented in all areas. Also rock falls are reproduced reasonable well by the models. Here the topography is the most important factor. The SRTM topography dataset is probably the most accurate dataset in the analysis compared to rough/coarse scale estimations such as is the case for the precipitation dataset.

The areas exposed to hazard from earthquake-induced landslides are generally well represented by the ICG and JRC models. Romania reports a decreasing fit in less steep areas with complex geology. In steep mountain areas the results fit well.

In Italy, both maps for precipitation and seismic-induced landslides give good results on a national scale and the results are adequate for a European study. Problems arise on a local scale, where complex geological sedimentary settings are causing landslide hazard in more gentle terrain.

6.4 RISK ASSESSMENT

The risk assessment of landslide hazard was not very successful due to a poor loss dataset. The CRED dataset only covers fatalities from 17 European countries and the numbers are vastly underestimated (Table 10-12). A serious attempt to create a better dataset should be done within the SafeLand project.

The only alternative left to achieve a picture of the risk hotspots in Europe is to calculate the exposure for each country and for Europe as a whole. The results clearly point out Italy and Spain with the largest number of people exposed. But relative to the total population, small alpine countries score highest. It is suggested from experience that areas with a higher risk also have a higher resilience and have well established risk mitigation strategies in place. However, areas in the middle of the risk scale are often the areas that are less frequently affected by landslides and where the consequences due to lacking mitigation are most severe.

A rough estimate of affected infrastructure shows that a large number of roads and railways are situated in areas with considerable landslide hazard. This is an important issue, which needs to be addressed with regard to society's access to affected areas providing emergency relief and reconstruction. Economic consequences may be higher due to breakdown in transport systems than due to the physical damages caused by the original event.

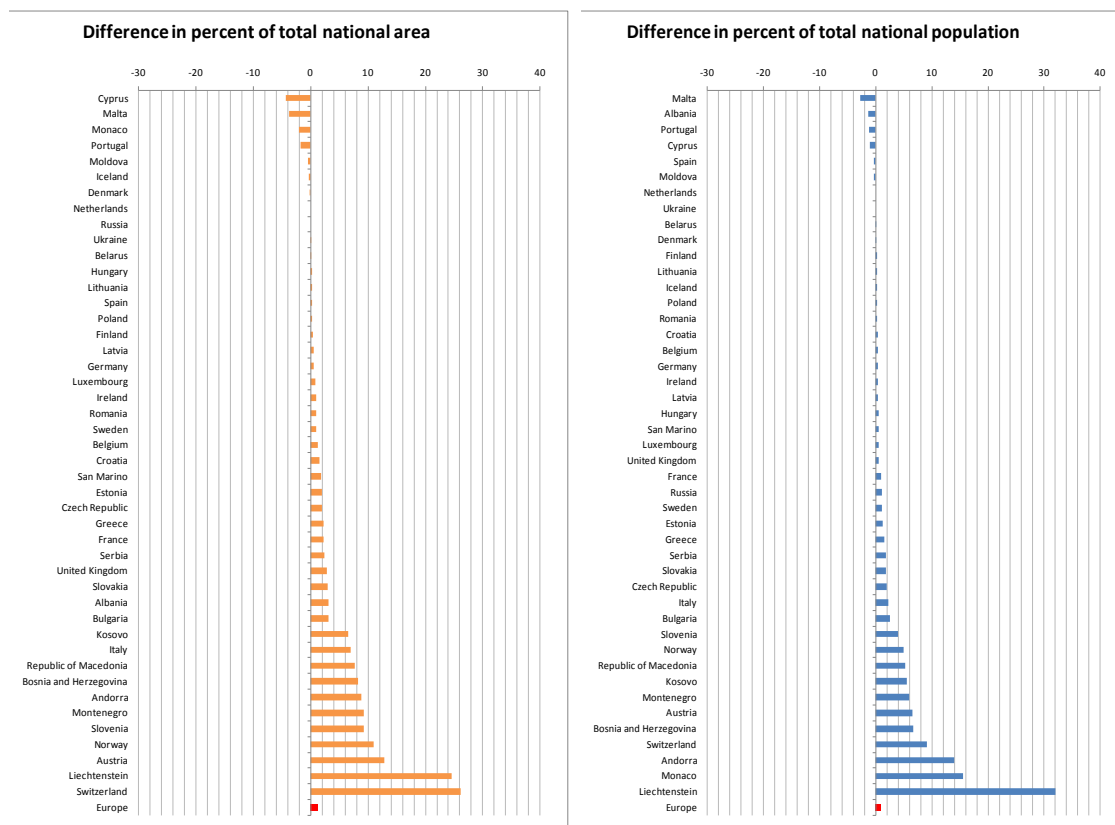


Figure 6-1: Country-wise comparison of the ICG and JRC results for percentage of total exposed area and population.

The comparison of the ICG and JRC models shows that the differences between the models are not too large. They range mostly within 5-10% of the total area or population in a country. For the roughness of the analysis, this is a promising trend. Nevertheless, it should be mentioned that the differences are largest in the mountainous countries such as Norway, Switzerland and Slovenia (Figure 6-1 and Figure 6-2). Here, the different weighting of terrain may play a role. This difference also shows that countries with a general high exposure need to assess the hazard and risk in more detail on a national level.

The ranking of the most exposed countries both in total and relative numbers is very similar from the two models. The first five countries agree well between the models, such that the selection of hotspots is possible. Italy plays an important role in both models. Here, the combination of high population density and large areas with moderate landslide hazard yields large numbers of exposed people and infrastructure.

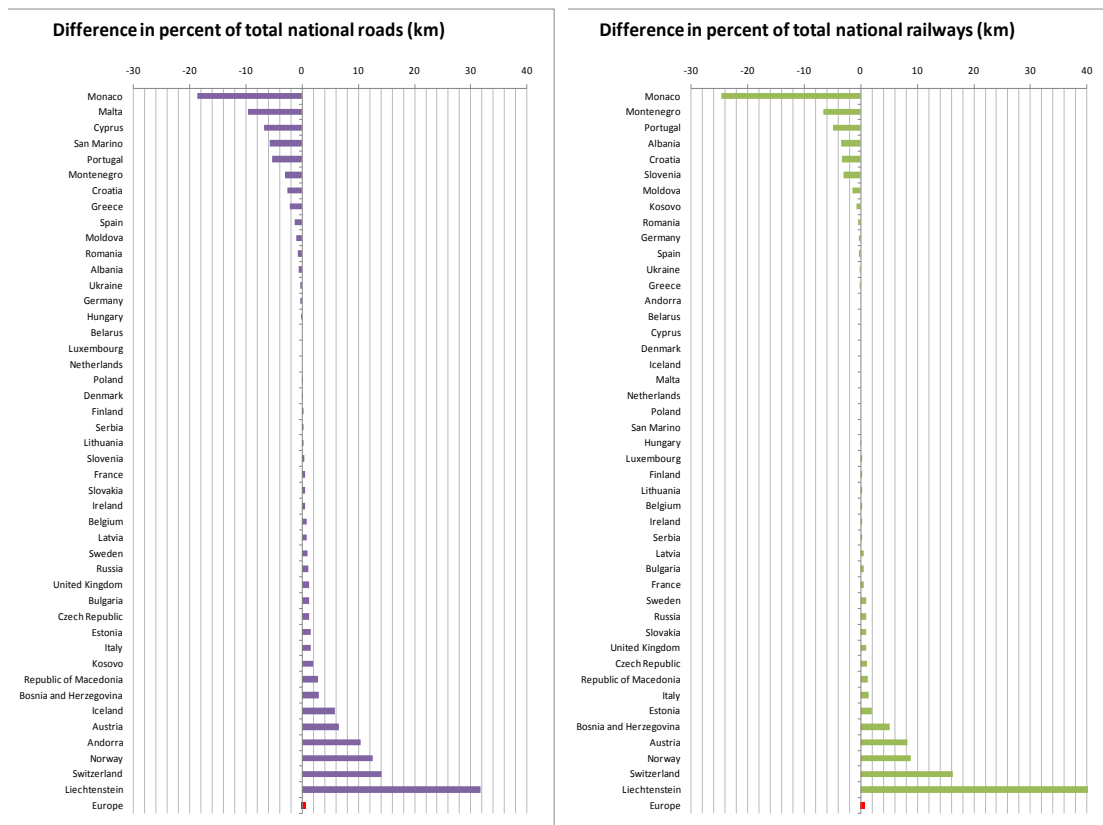


Figure 6-2: Country-wise comparison of the ICG and JRC results for percentage of total exposed roads and railways.

7 CONCLUSIONS

Landslide risk in Europe was estimated using a method based on gridded map data for Europe. The results show that hazard and exposure related to landslides is widely distributed. Some European countries are mostly unaffected by this natural phenomena, while landslides seriously affect daily life in many other countries. Italy has the highest number of people exposed to landslide hazard. On the other hand, Italy is a country well experienced in mitigating landslide risk. In other countries such as Romania, where the majority of the exposed people live in low or medium hazard areas, landslides are less common and therefore catch local people and authorities unprepared, thereby causing larger damage.

It is estimated that in the range of 1.3 to 3.6 million Europeans live in areas with high landslide hazard. In addition to the people directly threatened in their homes, 8 000 - 20 000 km of roads and railways are highly exposed causing additional direct threats to life and economic assets as well as problems for emergency response and recovery operations.

The applied methods yield only rough estimates and can easily be improved by acquiring new and better datasets. Especially for the precipitation trigger and soil cover, new datasets with a higher resolution would improve the models significantly. On the other hand, the validation in four countries shows good results on a national scale. Therefore, one can conclude that in total, the results represent the landslide hazard and risk in Europe reasonably well.

The lack of good loss data is a major problem for a quantitative risk analysis on a European scale. The involvement of the SafeLand partners should make it feasible to provide such a dataset for the involved countries.

8 REFERENCES

- Allison, P.D., 2001. Logistic Regression Using the SAS System: Theory and Application. Wiley Interscience, New York. 288 pp.
- Beguería S., 2006. Validation and evaluation of predictive models in hazard assessment and risk management. *Natural Hazards*, 37(3): 315-329.
- Dilley M, Chen RS, Deichmann U, Lerner-Lam AL, Arnold M, et al., 2005. Natural Disaster Hotspots – A Global Risk Analysis. Report International Bank for Reconstruction and Development/The World Bank and Columbia University: 132
- EM-DAT, 2003. The OFDA/CRED International Disaster Database - www.em-dat.net - Université Catholique de Louvain - Brussels -Belgium
- Giardini D, Grünthal G, Shedlock K, Zhang P., 2003. The GSHAP Global Seismic Hazard Map. In Lee W, Kanamori H, Jennings P (eds.), 2003. *International Handbook of Earthquake and Engineering Seismology*. IASPEI.
- Hosmer and Lemeshow, 2000. Applied logistic regression, John Wiley & Sons, New York.
- Laguardia, G. and Niemeyer, S., 2008. On the comparison between the LISFLOOD modelled and the ERS/SCAT derived soil moisture estimates. *Hydrol. Earth Syst. Sci. Discuss.*, 5, 1227–1265.
- Nadim, F., Kjekstad, O., Peduzzi, P., Herold, C. and Jaedicke, C., 2006. *Global landslide and avalanche hotspots*. *Landslides*, Vol. 3, No. 2, 159-174
- Peduzzi P., Dao H., Herold C., Mouton F., 2002. Global Risk And Vulnerability Index Trends per Year (GRAVITY), phase II: Development, analysis and results. 56 p. http://www.grid.unep.ch/product/publication/download/ew_gravity2.pdf
- SafeLand deliverable D8.1: Project handbook, p14 (<https://extranet.safeland-fp7.eu/WP8/D8.1/Deliverable%20documents/D8.1-Final.pdf>)
- UN/ISDR , 2009. *Global Assessment Report on Disaster Risk Reduction. Risk and Poverty in a Changing Climate*. United Nations, Geneva, Switzerland.
- Van Den Eeckhaut, M., Vanwalleghe, T., Poesen, J., Govers, G., Verstraeten, G., Vandekerckhove, L., 2006. Prediction of landslide susceptibility using rare events logistic regression: a case-study in the Flemish Ardennes, Belgium, *Geomorphology*, 76, 392-410.
- Jaboyedoff, M. and Labiouse V., 2003. Preliminary assessment of rockfall hazard based on GIS data. ISRM 2003–Technology roadmap for rock mechanics, South African Institute of Mining and Metallurgy
- Foster, C., Gibson, A., and Wildman, G., 2008. The new National Landslide Database and Landslide Hazard Assessment of Great Britain. In: *Proceedings, The First World Landslide Forum, Parallel Session Volume*, pp 203-206. International Consortium on Landslides/United Nations University, Tokyo, Japan.
- Winter M.G., Macgregor, F., and Shackman, L. eds., 2008. *Scottish Road Network Landslides Study: Implementation*. Edinburgh, Transport Scotland.

9 APPENDIX A – DATA INPUT

The following datasets were collected by the ICG GIS team and prepared for the modelling groups. The datasets were the best available maps with data that covered all of the project area (as defined in 9.7). Better and more detailed datasets can be found for some countries, but no better homogeneous datasets were available for Europe. However, ongoing research constantly produces new European or global datasets that will improve this type of analysis in the future. The data was made available on a FTP service and will also be accessible for other work packages in the project.

9.1 DIGITAL ELEVATION MODEL

Dataset: SRTM 3arcsec - Slope

Source: <http://srtm.csi.cgiar.org/>

Resolution: 3arcsec

Restrictions: Only to be used in the SafeLand project

Description: The sloperaster is derived from the SRTM DEM using ArcGIS Slope function. This is an updated version, as the previous version contained errors for the Azores.

Link to the data: ftp://ftp.ngi.no/Data/Slope_S60_SRTM_v2.gdb.zip

Dataset: GTopo - Slope

Source: http://eros.usgs.gov/#/Find_Data/Products_and_Data_Available/gtopo30_info

Resolution: 3 arcsec but only resampled from 30 arcsec to get a dataset with same resolution (but not same quality) as SRTM 3 arcsec

Projection: WGS84

Restrictions: Only to be used in the SafeLand project

Description: Slope derived from the DEM model.

Link to the data: ftp://ftp.ngi.no/Data/Slope_N60.gdb.zip

Dataset: Slope Norway

Source: Norwegian Mapping Agency

Resolution: 3 arcsec

Projection: WGS84

Restrictions: Only to be used in the SafeLand project

Description: The dataset is resampled from a 15m DEM which is based on 20m contour lines. To make the “Slope Norway” dataset the original 15m DEM was resampled to 60m and the slope was calculated. The slopemap was then projected to geographical coordinates with a resolution of 3 arcsec.

Link to the data: ftp://ftp.ngi.no/Data/Slope_Norway.gdb.zip

9.2 GEOLOGY

Dataset: IGME5000

Source: Bundesanstalt für Geowissenschaften und Rohstoffe, <http://www.bgr.bund.de/>

Data format: Vector

Projection: WGS84

Restrictions: This data has been released to the SafeLand project members on the conditions that it should **only be used in the SafeLand project**. Make sure copies of this data are deleted after project end.

Description: Data from 1:5M geological map. <http://www.bgr.de/karten/igme5000/igme5000.htm>

Link to the data: ftp://ftp.ngi.no/Data/geology_bgr.zip

Dataset: Geological Map of the World

Source: Commission for the Geological Map of the World, <http://ccgm.free.fr/>

Data format: Raster

Resolution: 30 arcsec

Projection: WGS84

Restrictions: Only to be used in the SafeLand project

Description: The global dataset is clipped to the borders of Europe

Link to the data: <ftp://ftp.ngi.no/Data/geology.gdb.zip>

9.3 GLACIERS

Dataset: Global Land Ice Measurements from Space (GLIMS)

Source: National Snow and Ice Data Center

Data format: Vector

Projection: WGS84

Restrictions: Only to be used in the SafeLand project

More information: <http://www.glims.org/About/>

Description: The global dataset is clipped to the borders of Europe

Link to the data: <ftp://ftp.ngi.no/Data/glacier.gdb.zip>

9.4 LAKES AND RIVERS

Dataset: Rivers from ESRI Maps and Data

Source: ESRI, <http://www.esri.com/>

Data format: Vector

Restrictions:

More information: <http://www.esri.com/data/data-maps/index.html>

Description:

Link to the data: <ftp://ftp.ngi.no/Data/river.gdb.zip> (esri_rivers)

Dataset: Rivers from Catchment Characterisation and Modelling (CCM2)

Source: European Commission Joint Research Centre (JRC), <http://ec.europa.eu/dgs/jrc/>

Data format: Vector

Restrictions: Only to be used in the SafeLand project

More information: <http://ccm.jrc.ec.europa.eu/php/index.php?action=view&id=24>

Description:

Link to the data: <ftp://ftp.ngi.no/Data/river.gdb.zip> (jrc_rivers)

Dataset: Lakes from Catchment Characterisation and Modelling (CCM2)

Source: European Commission Joint Research Centre (JRC), <http://ec.europa.eu/dgs/jrc/>

Data format: Vector

Restrictions: Only to be used in the SafeLand project

More information: <http://ccm.jrc.ec.europa.eu/php/index.php?action=view&id=24>

Description:

Link to the data: <ftp://ftp.ngi.no/Data/river.gdb.zip> (jrc_lakes)

Dataset: Coastline from Catchment Characterisation and Modelling (CCM2)

Source: European Commission Joint Research Centre (JRC), <http://ec.europa.eu/dgs/jrc/>

Data format: Vector

Restrictions: Only to be used in the SafeLand project

More information: <http://ccm.jrc.ec.europa.eu/php/index.php?action=view&id=24>

Description: This defines the outer boundary of the project data. The polygon has been used to clip the project data.

Link to the data: <ftp://ftp.ngi.no/Data/river.gdb.zip> (jrc_coast)

Dataset: River basins from Catchment Characterisation and Modelling (CCM2)

Source: European Commission Joint Research Centre (JRC), <http://ec.europa.eu/dgs/jrc/>

Data format: Vector

Restrictions: Only to be used in the SafeLand project

More information: <http://ccm.jrc.ec.europa.eu/php/index.php?action=view&id=24>

Description: This defines the outer boundary of the project data. The polygon has been used to clip the project data.

Link to the data: <ftp://ftp.ngi.no/Data/river.gdb.zip> (jrc_seaoutlets)

9.5 LAND USE

Dataset: Global Land Cover 2000 (GLC 2000)

Source: Institute for Environment and Sustainability's (IES; European Commission Joint Research Centre, JRC), <http://ies.jrc.ec.europa.eu/>

Data format: Raster

Resolution: 30 arcsec

Projection: WGS84

Restrictions: Only to be used in the SafeLand project

More information: <http://geoserver.isciences.com:8080/geonetwork/srv/en/metadata.show?id=55>

Description:

Link to the data: <ftp://ftp.ngi.no/Data/landcover.gdb.zip> (glc_2000)

Dataset: GLOBCOVER (GLC 2004-2006)

Source: European Space Agency, <http://www.esa.int/>

Data format: Raster

Resolution: 10 arcsec

Projection: WGS84

Restrictions: Only to be used in the SafeLand project

More information: <http://ionia1.esrin.esa.int/>

Description: The global dataset is clipped to the borders of Europe. Description of raster values is given in a excel file which is included in the zip-file.

Link to the data: <ftp://ftp.ngi.no/Data/landcover.gdb.zip> (glc_2004)

9.6 LANDSLIDE EVENTS

Dataset: Landslide inventories from Barcelonnette (France), Campania (Italy) and Norway

Data format: Vector (points)

Restrictions: Only to be used in the SafeLand project

Description: Landslide inventories from Barcelonnette (France), Campania (Italy) and Norway. The dataset comprises one dataset per region and a combined dataset for all three regions. The attribute SAFELAND_TARGET specifies whether a point is either to be used as model input (SAFELAND_TARGET = MODEL) or for verification of results (SAFELAND_TARGET = VERIFICATION).

Link to the data: ftp://ftp.ngi.no/Data/Landslide_inventories.gdb.zip

Data was provided from:

Data set	Contact person	Organisation
Barcelonnette	Jean-Philippe Malet	University of Strasbourg (www.unistra.fr)
Campania	Tonino Santo	AMRA (www.amrcenter.com)
Norway	Kari Sletten	Norwegian Geological Survey (www.ngu.no)

9.7 PRECIPITATION

Dataset:

- 100 year extreme monthly Precipitation (Precip_100_year_max)
- Mean monthly yearly maximum (Precipt_Mean_MonthlyMax)
- Stddev of monthly yearly maximum (Precip_Stddev_MonthlyMax)

Source: Global Precipitation Climatology Centre, Deutscher Wetterdienst, Offenbach, Germany

Data format: Raster

Resolution: 0.5 degrees

Projection: WGS84

Restrictions: Only to be used in the SafeLand project

More information: <http://gpcc.dwd.de>

Description:

The source of the precipitation data is the monthly precipitation time series (1951 - 2004) from Global Precipitation Climatology Centre (GPCC) run by Germany's National Meteorological Service, DWD (Rudolf et al, 2005). The dataset is based on quality-controlled data from a larger number of stations (up to 43,000) with irregular coverage in time. This product is optimized for best spatial coverage and use for water budget studies. The products contain precipitation totals, anomalies, number of gauges and systematic error and correction factors.

The datasource has a series of 54 years, from 1951 to 2004. The maximum registered values per annum were used to calculate the expected 100-year monthly precipitation for every grid point assuming a Gumbel distribution.

This is done by:

1. Choosing the highest monthly rainfall in the dataset for each year in each pixel.
2. Evaluating the mean, μ , and the standard deviation, σ , of the annual.
3. maximums.

4. Fitting a Gumbel distribution to the data using the mean and standard deviation computed in Step 2.
5. Finding the 1% fractile of the Gumbel distribution, which corresponds to the 100-year extreme monthly rainfall.

There are three datasets provided in the geodatabase

- The extreme monthly maximum rainfall
- The mean monthly yearly maximum
- The stddev of monthly yearly maximum

Link to data: <ftp://ftp.ngi.no/Data/Precipitation.gdb.zip>

9.8 SEISMICITY

Dataset: The Global Seismic Hazard Assessment Program (GSHAP)

Source: UN/IDNDR

Data format: Raster

Resolution: 6 arcminutes

Projection: WGS84

Restrictions: Only to be used in the SafeLand project

More information: <http://www.seismo.ethz.ch/GSHAP/global/>

Description: The global dataset is clipped to the borders of Europe. The data set used for the classification of the seismic trigger factor was the expected Peak Ground Acceleration (PGA) with 475-year return period (10% probability of exceedance in 50 years) from the Global Seismic Hazard Program, GSHAP (Giardini et al, 2003). GSHAP was launched in 1992 by the International Lithosphere Program (ILP) with the support of the International Council of Scientific Unions (ICSU) and in the framework of the United Nations International Decade for Natural Disaster Reduction (UN/IDNDR). The primary goal of GSHAP was to create a global seismic hazard map in a harmonized and regionally coordinated fashion, based on advanced methods in probabilistic seismic hazard assessments (PSHA). Modern PSHA are made of four basic elements: earthquake catalogue, earthquake source characterization, strong seismic ground motion and computation of seismic hazard.

Link to the data: <ftp://ftp.ngi.no/Data/seismic.gdb.zip>

9.9 SNOW COVER

Dataset: MODIS/Terra Snow Cover Monthly L3 Global 0.05Deg CMG, Version 5

Source: [National Snow and Ice Data Center \(NSIDC\)](http://nsidc.org/)

Data format: Raster

Resolution: 3 arcminutes

Projection: WGS84

Restrictions: Only to be used in the SafeLand project

More information: <http://www.seismo.ethz.ch/GSHAP/global/>

Description: The global dataset is clipped to the borders of Europe. Each dataset is given the name of the first date of the month (i.e. March 2003 is named “2003-03-01”).

Link to the data: ftp://ftp.ngi.no/Data/snowcover_monthly_2000-2009.zip

Dataset: Monthly medians from MODIS/Terra snow cover

Source: [National Snow and Ice Data Center \(NSIDC\)](http://www.nsidc.org/)

Data format: Raster

Resolution: 3 arcminutes

Projection: WGS84

Restrictions: Only to be used in the SafeLand project

More information: <http://www.seismo.ethz.ch/GSHAP/global/>

Description: The global dataset is clipped to the borders of Europe. The dataset is generated by calculating medians of the MODIS/Terra Snow Cover Monthly dataset for years 2001-2009.

Link to the data: <ftp://ftp.ngi.no/Data/snowcover.gdb.zip>

9.10 SOIL COVER

Dataset: Map of World Soil Resource

Source: FAO

Data format: Vector

Restrictions: Only to be used in the SafeLand project

More information: <http://www.fao.org/ag/agl/agll/wrb/soilres.stm>

Description: The global dataset is clipped to the borders of Europe.

Link to the data: <ftp://ftp.ngi.no/Data/soildata.gdb.zip> (FAO_soil_map)

Dataset: ISRIC-WISE derived soil properties

Source: ISRIC, <http://www.isric.org/>

Data format: Raster

Resolution: 5 arcminutes

Projection: WGS84

Restrictions: Only to be used in the SafeLand project

More information:

<http://www.isric.org/UK/About+Soils/Soil+data/Geographic+data/Global/WISE5by5minutes.htm>

Description: The global dataset is clipped to the borders of Europe.

Link to the data: <ftp://ftp.ngi.no/Data/soildata.gdb.zip> (isric_wise)

9.11 SOIL MOISTURE

Dataset: Average Top Soil Moisture Conditions in Europe

Source: Institute for Environment and Sustainability's (IES; European Commission Joint Research Centre, JRC), <http://edo.jrc.ec.europa.eu>

Data format: Raster

Resolution: 5 km

Projection: WGS84

Restrictions: Only to be used in the SafeLand project

More information: <http://edo.jrc.ec.europa.eu/php/index.php?action=view&id=20>

Description: Average Top Soil Moisture Conditions in Europe, Unit: pF values (soil suction), baseline period: 1/1958 - 12/2001, underlying hydrological model: LISFLOOD, underlying soil data: European Soil Map, adapted (Languardía and Niemeyer, 2008).

Link to the data: <ftp://ftp.ngi.no/Data/Moisture.gdb.zip>

9.12 INFRASTRUCTURE

Dataset: Major roads from OpenStreetMap

Source: OpenStreetMap, <http://www.openstreetmap.org/>

Data format: Vector

Restrictions: Only to be used in the SafeLand project

More information: <http://www.openstreetmap.org/>

Description: The dataset is extracted of minor roads from OpenStreetMap database by Cloudmade (<http://www.cloudmade.com/>). The dataset is a merger of the datasets “Europe”, “Cyprus”, “Canary Islands” and roads at Madeira from the “Portugal” dataset. The data provided is of “motorway”, “motorway_link”, “trunk”, “trunk_link”, “primary”, “primary_link”, “secondary” and “secondary_link”, as defined by OpenStreetmap highway type (cf. http://wiki.openstreetmap.org/wiki/Map_Features#Highway) (using the selection “TYPE” = ‘motorway’ OR “TYPE” = ‘motorway_link’ OR “TYPE” = ‘trunk’ OR “TYPE” = ‘trunk_link’ OR “TYPE” = ‘primary’ OR “TYPE” = ‘primary_link’ OR “TYPE” = ‘secondary’ OR “TYPE” = ‘secondary_link’ in ArcGIS). The data has been merged for all countries.

Link to the data: <ftp://ftp.ngi.no/Data/roadsandrailways.gdb.zip> (osm_majorroads)

Dataset: Minor roads from OpenStreetMap

Source: OpenStreetMap (<http://www.openstreetmap.org/>) / Cloudmade (<http://www.cloudmade.com/>)

Data format: Vector

Restrictions: Only to be used in the SafeLand project

More information: <http://www.openstreetmap.org/>

Description: The dataset is extracted of minor roads from OpenStreetMap database by Cloudmade (<http://www.cloudmade.com/>). The dataset is a merger of the datasets “Europe”, “Cyprus”, “Canary Islands” and roads at Madeira from the “Portugal” dataset. The data provided is of “tertiary”, “unclassified”, “road” and “residential”, as defined by OpenStreetmap highway type (cf. http://wiki.openstreetmap.org/wiki/Map_Features#Highway) (using the selection “TYPE” = ‘tertiary’ OR “TYPE” = ‘unclassified’ OR “TYPE” = ‘road’ OR “TYPE” = ‘residential’ in ArcGIS). The data has been merged for all countries.

Link to the data: <ftp://ftp.ngi.no/Data/minorroads.gdb.zip>

Dataset: Roads from ESRI map and data

Source: ESRI, <http://www.esri.com/>

Data format: Vector

Restrictions: Only to be used in the SafeLand project by ArcGIS users.

More information: <http://www.esri.com/data/data-maps/index.html>

Description: The global dataset is clipped to the borders of Europe.

Link to the data: <ftp://ftp.ngi.no/Data/roadsandrailways.gdb.zip> (esri_roads)

Dataset: Railways from OpenStreetmap

Source: OpenStreetMap, <http://www.openstreetmap.org/>

Data format: Vector

Restrictions: Only to be used in the SafeLand project.

More information: <http://www.esri.com/data/data-maps/index.html>

Description: Railways for Europe by OpenStreetMap. Railways from ESRI Data and Maps recommended instead of this, because of its completeness.

Link to the data: <ftp://ftp.ngi.no/Data/roadsandrailways.gdb.zip> (osm_railways)

Dataset: Railways from ESRI Data and Maps DVD

Source: ESRI, <http://www.esri.com/>

Data format: Vector

Restrictions: Only to be used in the SafeLand project by ArcGIS users.

More information: <http://www.esri.com/data/data-maps/index.html>

Description: From ESRI Data and Maps DVD.

Link to the data: <ftp://ftp.ngi.no/Data/roadsandrailways.gdb.zip> (esri_railways)

9.13 POPULATION

Dataset: Global Rural-Urban Mapping Project (GRUMP)

Source: Center for International Earth Science Information Network (CIESIN)

<http://sedac.ciesin.columbia.edu/gpw/>

Resolution: 30 arcsec

Projection: WGS84

Restrictions: Only to be used in the SafeLand project

Description: The global dataset is clipped to the borders of Europe. The data is provided as an integer dataset. To get the real population density per 30 arcsec numbers must be divided by 100. The GRUMP population surfaces and urban-rural extents have been developed based on three inputs: administrative boundary data sets and associated population estimates used in the preparation of Gridded Population of the World, version 3 (GPWv3); Night-time Lights of the World from the National Geophysical Data Center, the world stable lights data for 1994-1995; and a collection of population place locations and population estimates put together at CIESIN based on a number of public sources.

Link to the data: <ftp://ftp.ngi.no/Data/population.gdb.zip>

9.14 PROJECT EXTENT

Dataset: Project extent

Source: SafeLand

Data format: Vector

Restrictions: Only to be used in the SafeLand project

More information:

Description: This defines the outer boundary of the project data. The polygon has been used to clip the project data.

Link to the data: <ftp://ftp.ngi.no/Data/projectextent.gdb.zip>

10 APPENDIX B – MODEL DESCRIPTIONS

10.1 ICG MODEL

The ICG model is based on the experience gained in the HOTSPOT study from 2006. This type of analysis is based on expert judged reclassification and weighting of different factors that are assumed to be important for landslide susceptibility and hazard. Once the hazard is established, risk is estimated by considering exposure and vulnerability.

The analysis is a simple pixel based multiplication of the important factors to achieve a hazard index. This is done independently for two triggers, rainfall and seismicity.

10.1.1 Model for Landslide Hazard Evaluation

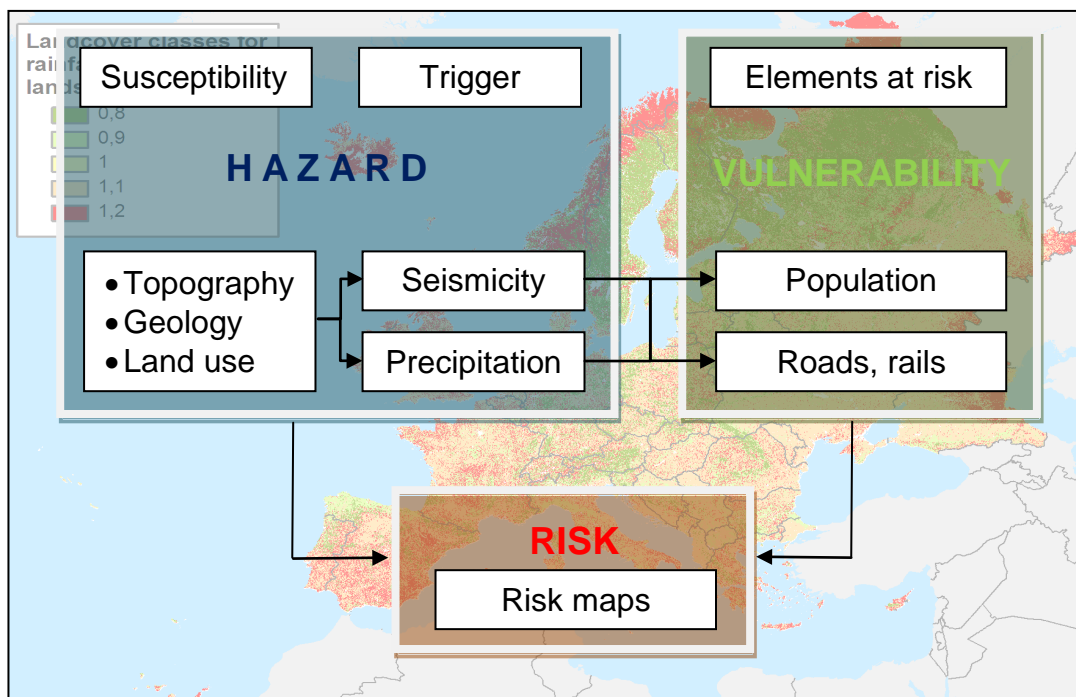


Figure 10-1: Schematic approach for landslide hazard and risk evaluation.

The term “landslide” in this study focuses on events involving gravity-driven rapid mass movement down-slope, like rockslides, debris flows, and rainfall- and earthquake-induced slides; which pose a threat to human life. Slow moving slides have significant economic consequences for constructions and infrastructure, but rarely cause any fatalities.

To identify the global landslide hazard and risk "hotspots", Nadim et al. (2006) adopted a simplified first-pass analysis method. The scale of their analysis was a grid of roughly 1km x 1km pixels where landslide hazard, defined as the annual probability of occurrence of a potentially destructive landslide event, was estimated by an appropriate combination of the triggering factors (mainly extreme precipitation and seismicity) and susceptibility factors (slope, lithology, vegetation and landuse). The principles of the method are depicted in Figure 10-1.

The weights of different triggering and susceptibility factors were calibrated to the information available in landslide inventories and physical processes. The general approach used in the present study is a modified and improved version of the approach used by Nadim et al. (2006).

One of the key improvements in the present model is the increased resolution on the DEM and consequently the slope data. In previous studies a 30 arc second resolution was used, whereas the present study uses the 3 arc seconds SRTM dataset.

The hazard maps are divided in precipitation-induced landslide hazard and earthquake-induced landslide hazard. The landslide hazard indices were estimated using the following equations:

$$H_r = (S_r \times S_l \times S_v) \times T_p \quad (1)$$

$$H_e = (S_r \times S_l \times S_v) \times T_s \quad (2)$$

where H_r and H_e are landslide hazard indices for rainfall and earthquake-induced landslides respectively, S_r is the slope factor within a selected grid, S_l is lithological (or geological) conditions factor, S_v is the vegetation cover factor T_p is the precipitation factor and T_s describes the seismic conditions.

The population exposure maps were calculated using the following equations

where POP is population and $H_{r,ref}$ and $H_{e,ref}$ are normalization factors allowing categorization of the exposure data as shown in Figures A10 to A13.

10.1.2 Data preparation

Most of the available input data needs a thorough preparation before it can be used in a GIS analysis. The method calculates hazard and risk pixel by pixel and all data has to be regridded to the available grid size of the underlying digital elevation model. In the case of this analysis, south of 60° north, the resolution is 3 arc seconds, north of 60° another dataset had to be used that yields only 30 arc seconds resolution.

10.1.3 Slope factor S_r

The slope factor represents the natural landscape ruggedness within a grid unit. In February 2000, NASA collected elevation data for much of the world using a radar instrument aboard

the Space Shuttle. The raw data collected on the mission were processed over three years. NASA has now released a global elevation dataset called SRTM3, referring to the name of the mission and the resolution of the data, which is 3 arc-seconds, or approximately 90 by 90 m per data sample near the equator. The SRTM3 data set covers the globe from 60 degrees south latitude to 60 degrees north latitude. The vertical accuracy is estimated such that 90% of posts are within 16m tolerance of the actual position.

North of 60 degrees a different dataset had to be used. We chose the GTOPO dataset with a resolution of roughly 1 x 1 km.

The SRTM and N50 slope angle data are classified into hazard classes as shown in columns 1 through 3 in Table 1 below. In order to make a corresponding hazard classification for the GTOPO slope angle data (which have a pixel area of 100 times the SRTM and N50 data), two test areas have been identified where SRTM/N50 slope angle data are compared to GTOPO slope angle data:

1. Norway (N50 data compared to GTOPO data)
2. Southern Europe: Mainly Alps and Balkans (SRTM data compared to GTOPO data)

In Figure 10-2 and Figure 10-3 are shown histograms for each of these two test areas comparing GTOPO slope angle data to N50 data (Norway) and SRTM data (Southern Europe).

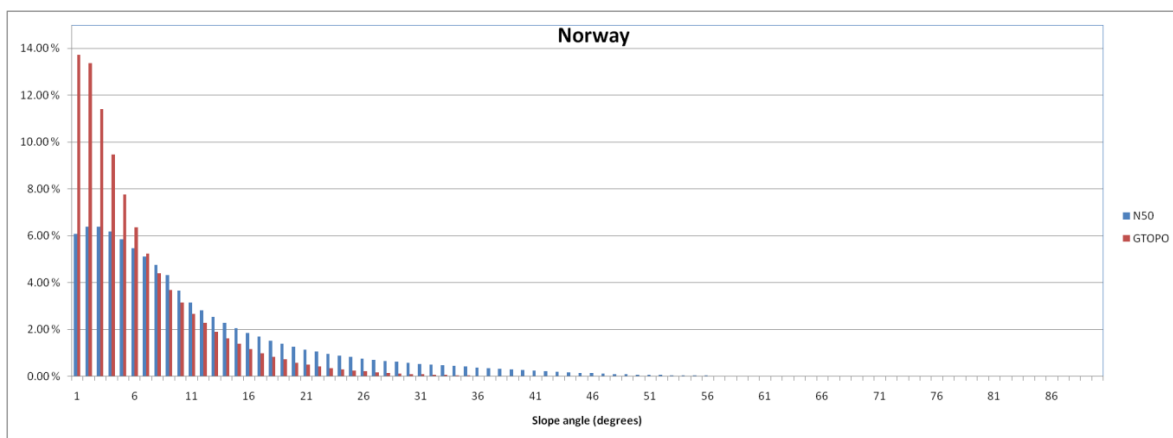


Figure 10-2: Histogram showing the percentage of land area having certain slope angle for test area 1: Norway. Comparison of GTOPO slope angle data to N50 slope angle data

Both curves show that the fine resolution data (N50 and SRTM) on average show higher slope angle than the coarser GTOPO data. The histogram data have then been used to establish slope angle ranges for each hazard class for GTOPO data (corresponding to the SRTM/N50 slope angle ranges in columns 2 and 3 in Figure 1). The criteria used is that for any given hazard class, the fraction of the land area belonging to this hazard class should be independent of whether SRTM/N50 or GTOPO data is used.

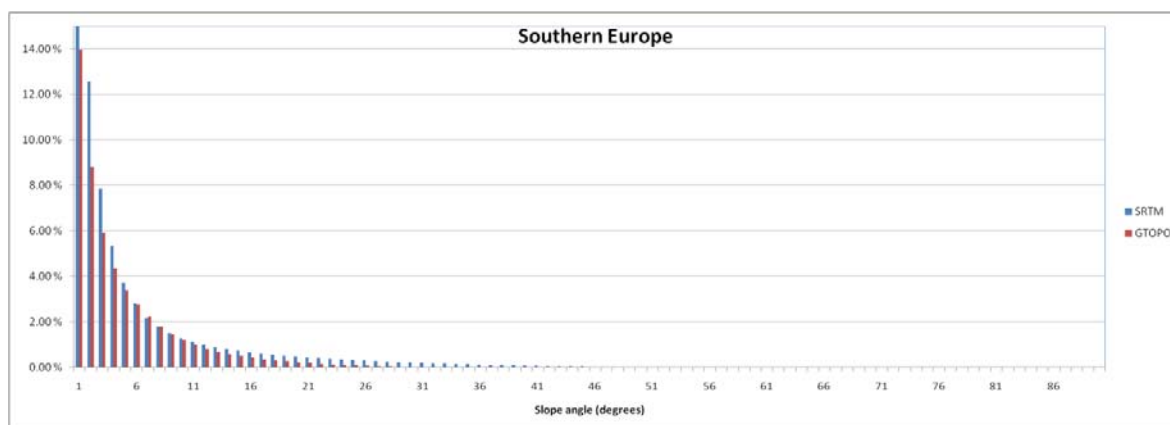


Figure 10-3: Histogram showing the percentage of land area having certain slope angle for test area 1: Southern Europe. Comparison of GTOPO slope angle data to SRTM slope angle data

The result of the analysis is shown in Table 10-1. The resulting slope angles for each of the hazard classes for GTOPO data are given in columns 4 and 5.

Columns 6 and 7 are results for test area 1 Norway.

Column 6 shows the fraction of land area belonging to each hazard class based on the N50 angle ranges from column 2 and 3.

Column 7 shows the fraction of land area belonging to each hazard class based on the GTOPO angle ranges from column 4 and 5.

Column 6 and 7 are in reasonable agreement indicating a good recalibration.

Columns 8 and 9 are results for test area 2 Southern Europe.

Column 8 shows the fraction of land area belonging to each hazard class based on the SRTM angle ranges from column 2 and 3.

Column 9 shows the fraction of land area belonging to each hazard class based on the GTOPO angle ranges from column 4 and 5.

Column 8 and 9 are in reasonable agreement, except for rows one and two. This discrepancy is believed to be of minor importance as hazard classes 0 and 1 represent low hazard levels.

Table 10-1: Slope angle ranges for each hazard class for SRTM and N50 data

S _r	Angle N50 / SRTM		Angle GTOPO		N50 Norway	GTOPO Norway	SRTM S Europe	GTOPO S Europe
	From	To	From	To	Fraction	Fraction	Fraction	Fraction
0	0	1	0	0	11.20 %	4.27 %	28.48 %	48.07 %
1	1	6	1	3	30.88 %	38.52 %	49.68 %	28.66 %
2	6	12	4	7	26.45 %	28.83 %	10.64 %	12.71 %
3	12	18	8	10	13.23 %	11.25 %	4.69 %	4.44 %
4	18	24	11	13	7.33 %	6.84 %	2.78 %	2.51 %
5	24	40	14	22	8.76 %	8.23 %	3.19 %	3.02 %
3	40	45	23	26	1.07 %	1.10 %	0.30 %	0.39 %
3	45	90	27	90	1.07 %	0.96 %	0.23 %	0.20 %

Note: for slopes which angle is less than 1° (i.e. for flat or nearly flat areas), S_r is set equal to zero because the resulting landslide hazard is zero even if the other factors are favourable.

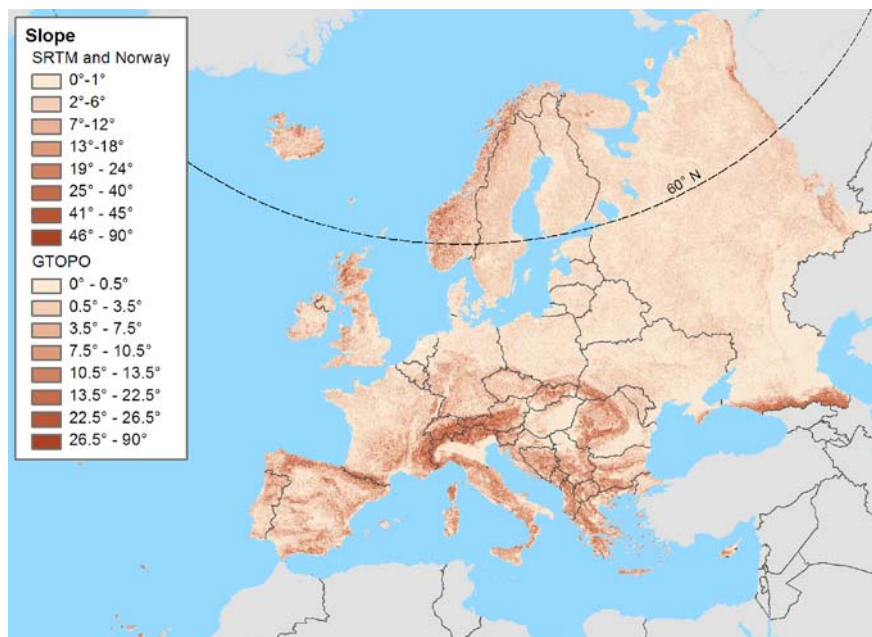


Figure 10-4: Slope factor S_r for the study area.

10.1.4 Lithology factor S_l

This is probably the most difficult parameter to assess. Ideally, detailed geotechnical information should be used but, at the global scale, only a general geological description is available. Rock strength and fracturing are the most important factors to evaluate lithological characteristics, and these characteristics can vary greatly over short distances.

The dataset used in the study was the Geological map of Europe at 1/5,000,000 scale published by Bundesanstalt für Geowissenschaften und Rohstoffe. The map is available on request from the institution. This map is the best geological dataset compiled at a European scale showing the geology of the whole continent, including land areas and oceans. In the map, three main types of rocks are identified: sedimentary rocks, extrusive volcanic rocks and endogenous rocks (plutonic or strongly metamorphosed).

Table 10-2: Classification of the lithology based on the European geological map.

Lithology and stratigraphy	Susceptibility	S_l
<ul style="list-style-type: none"> Extrusive volcanic rocks - Precambrian, Proterozoic, Paleozoic and Archean. Endogenous rocks (plutonic and/or metamorphic) - Precambrian, Proterozoic, Paleozoic and Archean. 	Low	1
<ul style="list-style-type: none"> Old sedimentary rocks - Precambrian, Archean, Proterozoic, Paleozoic. Extrusive volcanic rocks – Paleozoic, Mesozoic. Endogenous rocks - Paleozoic, Mesozoic, Triassic, Jurassic, Cretaceous. 	Moderate	1
<ul style="list-style-type: none"> Sedimentary rocks - Paleozoic, Mesozoic, Triassic, Jurassic, Cretaceous. Extrusive volcanic rocks – Mesozoic, Triassic, Jurassic, Cretaceous. Endogenous rocks – Meso-Cenozoic, Cenozoic. 	Medium	2
<ul style="list-style-type: none"> Sedimentary rocks – Cenozoic, Quaternary. Extrusive volcanic rocks – Meso-Cenozoic. 	High	3
<ul style="list-style-type: none"> Extrusive volcanic rocks – Cenozoic. 	Very high	3

Three susceptibility classes were used in the analyses, as shown in Table 10-2. Usually old rocks are stronger than young rocks. Plutonic rocks are usually strong and represent low susceptibility. Strength of metamorphic rocks is variable, but these rocks often have planar structures such as foliation and therefore may represent higher susceptibility than plutonic rocks. Lava rocks will usually be strong, but may be associated with tuff (weak material). Therefore, areas with recent volcanism are classified as highly susceptible. Sedimentary rocks are often weak, especially young ones.

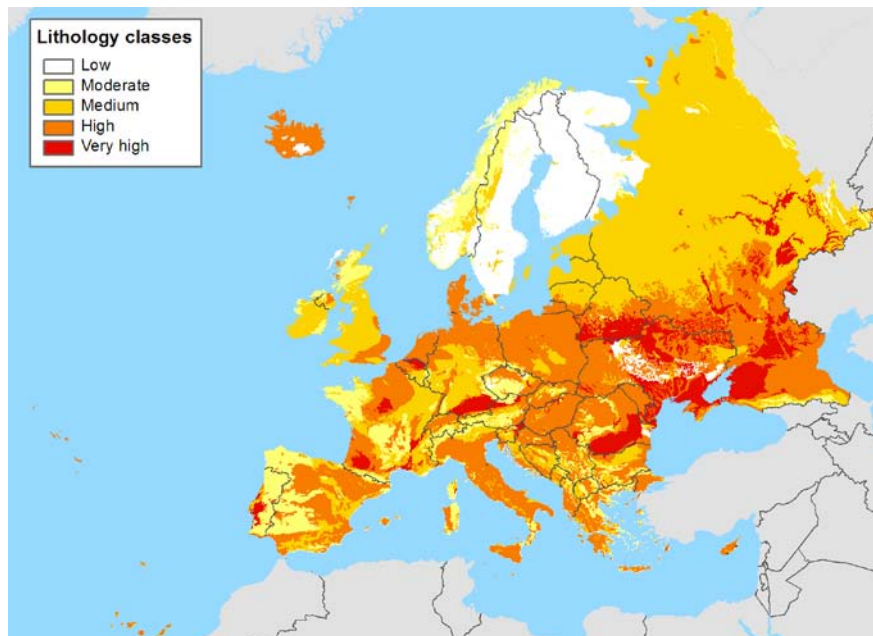


Figure 10-5: Lithology factor S_l for the study area.

10.1.5 Land cover index S_v

The GLOBECOVER v2.2 database has 22 different classes of land use, which have been translated into 5 categories (scale 1 to 5) with respect to resistance to landslides. Table 10-3 shows the range of S_v for these 5 categories.

Table 10-3: Classification of land cover for the hazard analysis

Category of land cover w.r.t. resistance to landslides	Vegetation cover index S_v for rainfall-induced slides	Vegetation cover index S_v for earthquake-induced slides
5	0.8	0.9
4	0.9	0.95
3	1.0	1.0
2	1.1	1.05
1	1.2	1.1

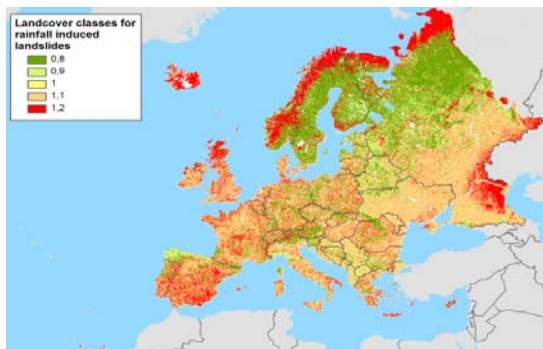


Figure 10-6: Vegetation cover index S_v for precipitation-induced landslides

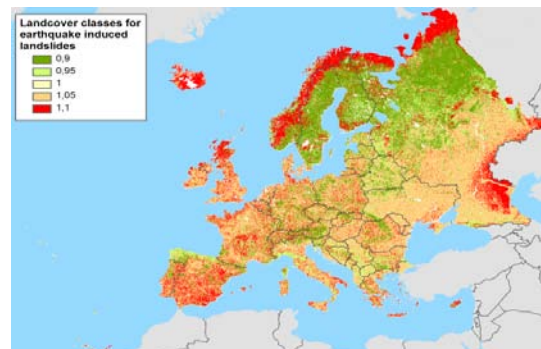


Figure 10-7: Vegetation cover index S_v for earthquake-induced landslides

10.1.6 Precipitation trigger factor T_p

The categorisation of T_p was based on the estimate of the 100-year extreme monthly rainfall (i.e. extreme monthly rainfall with 100 years return period). The data processing procedure is described in chapter 9.7.

On the basis of the estimated 100-year extreme monthly rainfall, a precipitation index T_{p1} was assigned as listed in Table 10-4.

Table 10-4: Classification of the estimated monthly extreme rainfall

100-year extreme monthly rainfall (mm)	Susceptibility	T_{p1}
0000 – 0330	Low	1
0331 – 0625	Moderate	2
0626 – 1000	Medium	3
1001 – 1500	High	4
> 1500	Very high	5

The precipitation index used by Nadim et al. (2006) in the Global Hotspots study was identical to T_{p1} . Recent research has shown that it is the extreme precipitation events that trigger slides, and the definition of “extreme” depends on what is “normal” at a particular location. In other words, the geometry of natural slopes is adapted to the normal precipitation events at a given location. In order to trigger a slide, anomalously high precipitation is required. In the present study, an anomaly factor is included in the precipitation trigger index. The potential for anomaly was quantified by considering the coefficient of variation (mean divided by standard deviation) of the data obtained in Step 2 of estimation of the 100-year extreme monthly rainfall. The following range for anomaly factor is suggested (Table 10-5) “a” denotes the smallest value of $CoV = \sigma/\mu$ obtained for the whole globe, and “b” denotes the largest value of CoV . The values of “a” and “b” obtained from the calculations were respectively 0.11 and 3.60):

Table 10-5: Classification of coefficient of variation of highest monthly annual rainfall

Coefficient of variation of highest monthly annual rainfall, $CoV = \sigma/\mu$	Anomaly factor T_a
$a \rightarrow a + 0.2 \cdot (b - a)$	0.8
$a + 0.2 \cdot (b - a) \rightarrow a + 0.4 \cdot (b - a)$	0.9
$a + 0.4 \cdot (b - a) \rightarrow a + 0.6 \cdot (b - a)$	1.0
$a + 0.6 \cdot (b - a) \rightarrow a + 0.8 \cdot (b - a)$	1.1
$a + 0.8 \cdot (b - a) \rightarrow b$	1.2

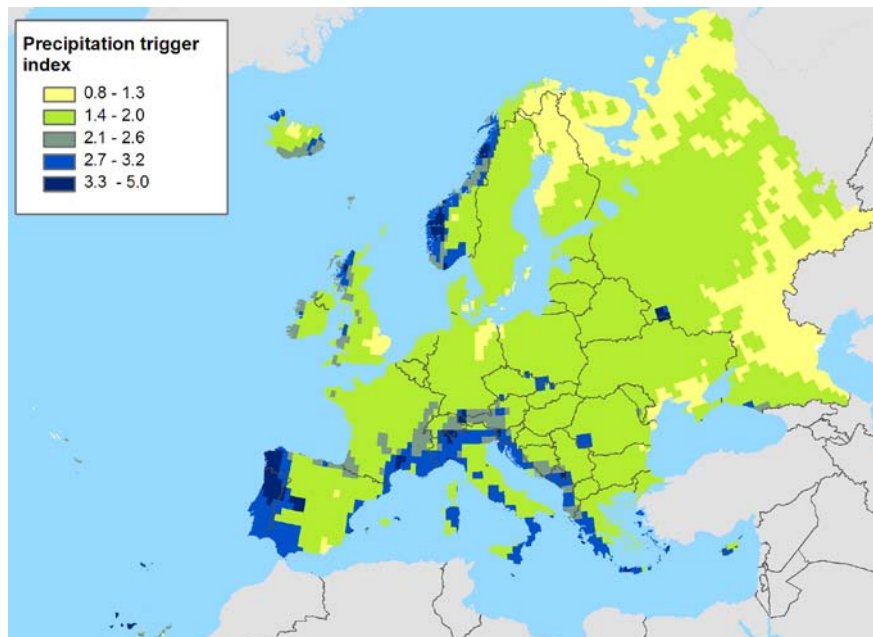


Figure 10-8: Precipitation index T_{p1} for the study area.

The precipitation trigger index, T_p , was obtained by the equation below:

$$T_p = T_{p1} \times T_a \quad (3)$$

The variation range for T_p is therefore 0.8 – 5.0.

10.1.7 Seismic trigger factor T_s

The data set used for the classification of the seismic trigger factor was the expected Peak Ground Acceleration (PGA) from the Global Seismic Hazard Program, GSHAP (Giardini et al, 2003). For the study, the Peak Ground Acceleration (PGA) with 475-year return period was used as the representative triggering parameter for seismically-induced landslides.

The seismic trigger index, T_s , was evaluated from the GSHAP PGA_{475} data according to Table 10-6.

Table 10-6: Classification of the maximum estimated ground acceleration into seismic trigger index

GSHAP PGA_{475} (m/s^2)	T_s
0.00 – 0.50	0.1
0.51 – 1.00	0.4
1.01 – 1.50	0.8
1.51 – 2.00	1.5
2.01 – 2.50	2.5
2.51 – 3.00	3.5
3.01 – 3.50	5
3.51 – 4.00	6
4.01 – 4.50	7.5
Greater than 4.50	10

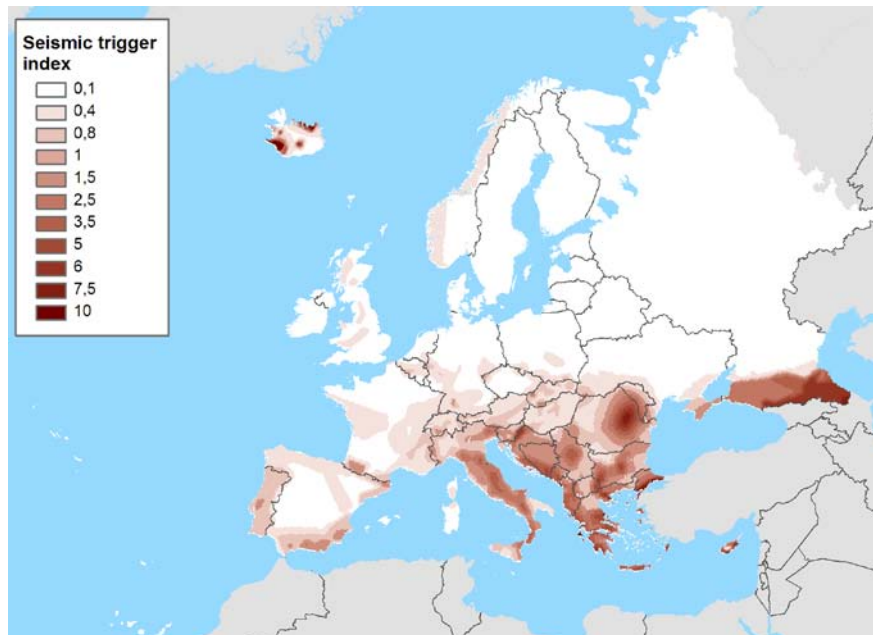


Figure 10-9: Seismic trigger factor T_s for the study area.

10.1.8 Categorisation of landslide hazard

The obtained landslide hazard indices were calibrated against the databases of landslide events in selected (mostly European) countries to obtain the frequency of the events. On the basis of this calibration, the following landslide hazard classifications were established:

Table 10-7: Classification of the landslide hazard due to precipitation and seismicity

Values for $H_{\text{landslide, rainfall}}$	Values for $H_{\text{landslide, earthquake}}$	Class	Classification of landslide hazard potential	Representative annual frequency in 1 km ² grid cell
≤ 2	≤ 7	0	Negligible	~ 0.00 %
3 – 9	8 – 24	1	Very low	~ 0.00 %
10 – 20	25 – 47	2	Low	0.01 %
21 – 36	48 – 74	3	Low to moderate	0.03 %
37 – 54	75 – 108	4	Moderate	0.10 %
55 – 74	109 – 152	5	Medium	0.30 %
75 – 99	153 – 205	6	Medium to high	1.00 %
100 – 134	206 – 270	7	High	3.00 %
> 134	> 270	8	Very high	10.00 %

10.2 JRC MODEL

10.2.1 Introduction

This section contains a concise description of the methodology for landslide hazard assessment in Europe used by JRC. In a first step, landslide susceptibility was estimated using the statistical model logistic regression. Then, the obtained classified landslide susceptibility map was confronted with precipitation and seismic data respectively to obtain two qualitative hazard maps, one for hydrologically-triggered landslides and one for seismically-triggered landslides.

10.2.2 Data preparation

10.2.2.1 Exploratory or independent variables

For assessing landslide susceptibility with ordinary logistic regression (OLR), seven independent variables were extracted from the maps made available for D2.10 by ICG (Table 10-8; see Appendix A for detailed information and references). Given that the provided maps did not have a uniform resolution, the maps were rescaled to a cell size of 30 arcsec (ca. 930 m). Maps with categorical variables such as the lithological, soil and land cover maps had a high number of classes and were reclassified.

Table 10-8: Independent variables used in logistic regression (See Appendix A for detailed information and references of the base maps from which these variables were obtained).

Variable	Reference	Numerical/categorical
Slope	SRTM; GTOPO	Numerical
Standard deviation of Slope	SRTM; GTOPO	Numerical
Lithology – type	IGME5000	Categorical (12 Classes)
Lithology – age	IGME5000	Categorical (9 Classes)
Soil type	FAO	Categorical (8 Classes)
Land cover	GLC 2004-2006	Categorical (7 Classes)
Soil moisture	JRC	Numerical

10.2.2.2 Response or dependent variable

The binary dependent variable used in the OLR is the presence (1) or absence (0) of a landslide. We mainly focused on landslides of the slide and flow type and therefore rock falls were not included in our selected sample. Within the timeframe of the deliverable we tried to obtain a representative sample of landslide-affected and landslide-free grid cells.

From the databases provided by ICG (Annex A) we extracted a random sample of 100 landslides in Norway, 100 landslides in Campania (Italy) and 50 landslides in the Barcelonnette Basin (France). We further used a landslide inventory created by JRC, containing 972 landslides in March 2010. This inventory is produced in Google Earth. Mapped landslides are indicated as point features and obtained from visual inspection of the Google Earth images in combination with consultation of scientific publications on landslides inventory maps from all over Europe. With regard to our own landslide inventory we realize that the ca. 1000 landslides mapped are only a very small proportion of the true number of landslides in Europe. However, the time for the preparation of the map was limited. So we chose to put more time in collecting landslide data from all over Europe instead of having a more complete coverage of the Alps, Apennines and Pyrenees (i.e. the regions in which

landslides are generally visible on Google Earth) and hence a higher total number of landslides in the database. Overall, we had therefore 1222 landslides.

The selection of ‘landslide-free’ grid cells was not straightforward. First of all, due to the lack of a complete landslide inventory map of Europe, we are not able to select grid cells that are definitely landslide-free. A specific selection procedure was set up to select a representative sample. It was decided for example not to extract the sample of landslide-free grid cells uniformly over the selected study area, because otherwise more than 80% of the selected grid cells would be located in flat areas.

10.2.3 Model for Landslide Susceptibility Evaluation

10.2.3.1 Methodology

Ordinary logistic regression (OLR) describes the relationship between a dichotomous response variable (Y , i.e., the presence or absence of a landslide) and a set of independent variables (x_1, x_2, \dots, x_n). The independent variables may be continuous or discrete (with dummy variables) and do not need a normal frequency distribution. The logistic response function can be written as (Hosmer and Lemeshow, 2000; Allison, 2001):

$$P(Y = 1) = p = \frac{1}{1 + e^{-\left(\alpha + \sum_{i=1}^n \beta_i x_i\right)}} \quad \text{Eq. (1)}$$

where p is the probability of occurrence of a landslide, α is the intercept and β_i is the coefficient for the independent variable x_i estimated by maximum likelihood. Eq. (1) can be linearized with the following transformation in which the natural logarithm of the odds, $\log(p/1-p)$, called the logit, is linearly related with the independent variables:

$$\log\left(\frac{p}{1-p}\right) = \alpha + \beta_1 x_1 + \beta_2 x_2 + \dots + \beta_n x_n \quad \text{Eq. (2)}$$

During the last decade OLR has been increasingly used for landslide susceptibility assessment and attention has been paid to objective evaluation and validation of the calibrated models (e.g. Begueria, 2006; Van Den Eeckhaut et al., 2006). Also in this study the obtained logistic regression model was evaluated and validated (with data not used for model calibration) prior to proceeding to the landslide hazard assessment. Confusion matrices and Receiver Operation Characteristic (ROC) curves were produced and analyzed (Hosmer and Lemeshow, 2000). Analysis of confusion matrices and ROC curves were further useful for the selection of the boundaries of the ten classes in which the final landslide susceptibility map was reclassified. The objective here was to classify a large proportion of the known landslides without classifying a too large proportion of the European territory as highly susceptible.

10.2.3.2 Results

Several models were calibrated and evaluated. For the finally selected logistic regression model the area under the ROC curve (AUC) is 0.888, which indicates excellent discrimination

of the landslide-affected and landslide-free grid cells in our sample. Hence, the model was able to correctly classify a high proportion of the landslide sample without incorrectly classifying a high proportion of the landslide-free sample.

The stability of the model was further tested by producing 10 logistic regression models using each time 75% of the sample for calibration and the remaining 25% for validation.

10.2.4 Model for Landslide Hazard Evaluation

10.2.4.1 Model for rainfall-induced landslides

The rainfall information used for hydrologically-triggered landslide hazard assessment is extracted from the “Precip_100_year_max.map” provided by ICG (Annex A). This map displays 100-year extreme monthly precipitation. The continuous rainfall depths were first classified in six categories (Table 10-9) and then confronted with the classified landslide susceptibility map. The confrontation map contained $10 \times 6 = 60$ different hazard classes, which were reclassified in seven hazard classes showing increasing landslide hazard from 1 to 7 (Figure 10-10; Table 10-10). In this final rainfall-induced landslide hazard maps class 0 represents lakes.

Table 10-9: Classification of 100-year extreme monthly precipitation (Global Precipitation Climatology Centre, Deutscher Wetterdienst) in six classes.

Class	Numerical/categorical
1	< 200
2	200 – 249
3	250 – 299
4	300 – 349
5	350 – 399
6	≥ 400

Table 10-10: Distribution of the selected study area over the seven hazard classes of the rainfall- and earthquake- induced landslide hazard map produced by JRC.

Hazard Level	Description	% Study area		% Study area (cumulative)	
		Precipitation trigger	Seismic trigger	Precipitation trigger	Seismic trigger
1	Very low	61.48	59.31	100.00	100.00
2	Low	20.89	22.52	38.52	40.69
3	Low to moderate	10.15	10.61	17.64	18.18
4	Moderate	3.80	3.80	7.49	7.57
5	Moderate to high	1.49	1.70	3.68	3.77
6	High	1.40	1.47	2.20	2.07
7	Very high	0.79	0.60	0.79	0.60
		100.00	100.00		

Figure 10-10: Classified rainfall-induced landslide hazard map produced by JRC.

10.2.4.2 Model for earthquake-induced landslides

The seismic information used for the earthquake-induced landslide hazard assessment is extracted from the “Classified Global Seismic Hazard Assessment Program (GSHAP) map” (Annex A). This map displays the peak ground acceleration (PGA; m/s^2) with a 10% probability of exceedance in 50 years, 475-year return period. The continuous PGA were first classified in nine categories (Table 10-11). These class boundaries are corresponding with those used by UN/IDNDR who produced the map. Then, the classified GSHAP map was confronted with the classified landslide susceptibility map. The confrontation map contained $9 \times 10 = 90$ different hazard classes that were reclassified in seven hazard classes showing increasing landslide hazard from 1 to 7 (Figure 10-11). In this final earthquake-induced landslide hazard maps class 0 represents lakes.

Table 10-11: Classification of the Classified Global Seismic Hazard Assessment Program (GSHAP) map (<http://www.seismo.ethz.ch/GSHAP>) in nine classes.

Class	Numerical/categorical
1	< 0.20
2	0.20 – 0.39
3	0.40 – 0.79
4	0.80 – 1.59
5	1.60 – 2.39
6	2.40 – 3.19
7	3.20 – 3.99
8	4.00 – 4.79
9	≥ 4.80

Figure 10-11: Classified earthquake-induced landslide hazard map produced by JRC.

10.3 UNIL MODEL

10.3.1 Introduction

Hotspots detection has for goals to provide an overview of areas where the susceptibility, hazard or risk to a phenomenon is higher than normal. Such results are used by international or governmental agencies and development banks as support to prioritize the allocation of resources to exposed regions. At global scale examples of hotspots detection for landslide and avalanche were already produced by Nadim et al (2006) and UNISDR (2009).

The aims of the present contribution are: (1) to provide a first map of rock fall susceptibility for Europe at a scale that can be used for regional planning (cell size: ~100x100 m), (2) to identify transport corridors of European importance that can be affected by rock falls, (3) to provide a simplified risk map with the number of people exposed to rock fall over Europe (cell size: ~10x10 km).

10.3.2 Data and Methods

The datasets used are: (1) the SRTM DEM, 3 arc-second cell size grid reprojected in UTM zones with a cell size of 100m. This DEM is only available for latitude up to 60° North and then limits the northern extend of the area considered; (2) the ESRI transportation (roads and railways) dataset for Europe; (3) the LandScan 2008™ High Resolution Global Population Data Set (cell size: 30 arc-second), copyrighted by UT Battelle (US-Department of Energy).

The procedure is composed of three main steps (Figure 10-12).

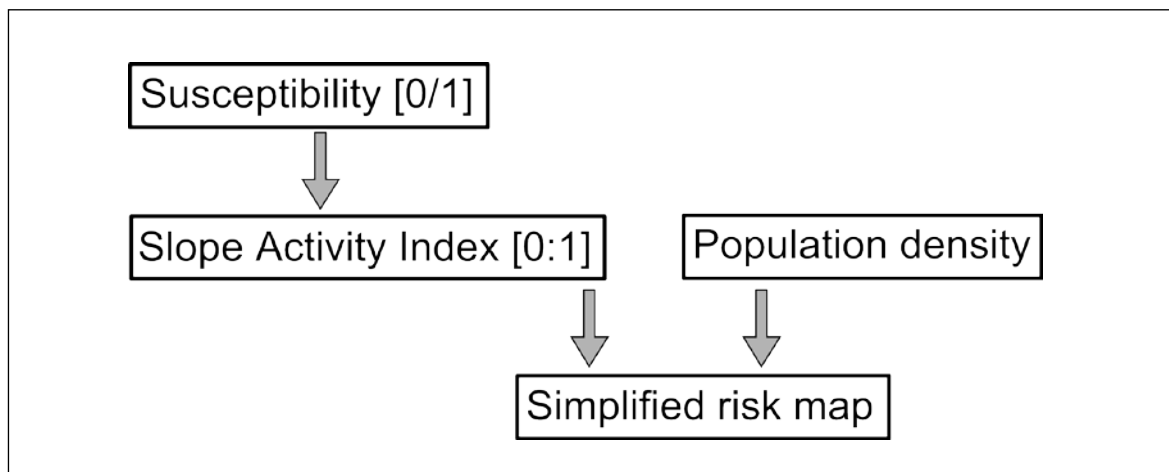


Figure 10-12: Steps of the procedure : 1) susceptibility mapping, 2) Slope activity index calculation, 3) risk mapping

- (a) Rock fall susceptibility mapping using a simple physical model. The potential release areas of blocks are defined as the locations where the slope angle is over 30°. The 100 m cell size DEM is used to estimate the slope angle. The propagation is estimated from each cell of the release areas with a cone propagation model (Jaboyedoff & Labiouse 2003). The angle of propagation (Fahrböschung) is 30° (Figure 10-13).

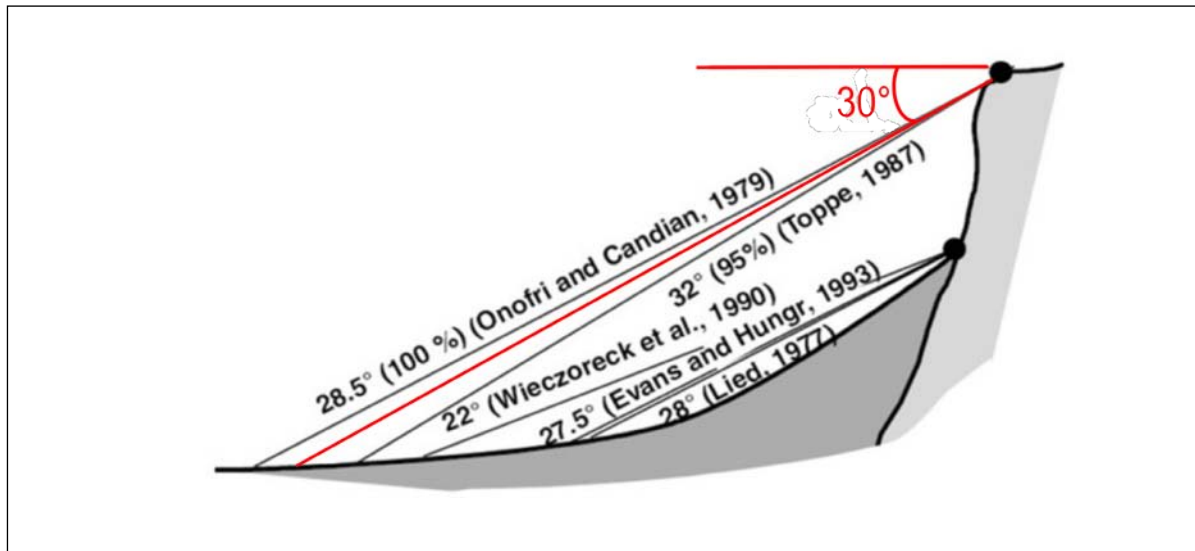


Figure 10-13: Review of rock fall propagation angles proposed by different authors (from Jaboyedoff and Labiouse 2003). A 30° angle is used in this project.

- (b) The whole processing was achieved with the software RAS (Institute of Geomatics and Risk Analysis, University of Lausanne), which is able to handle large datasets. The product of this step is a binary map indicating if a cell of the DEM is inside or outside a zone that can be affected by rock falls (Figure 10-14).

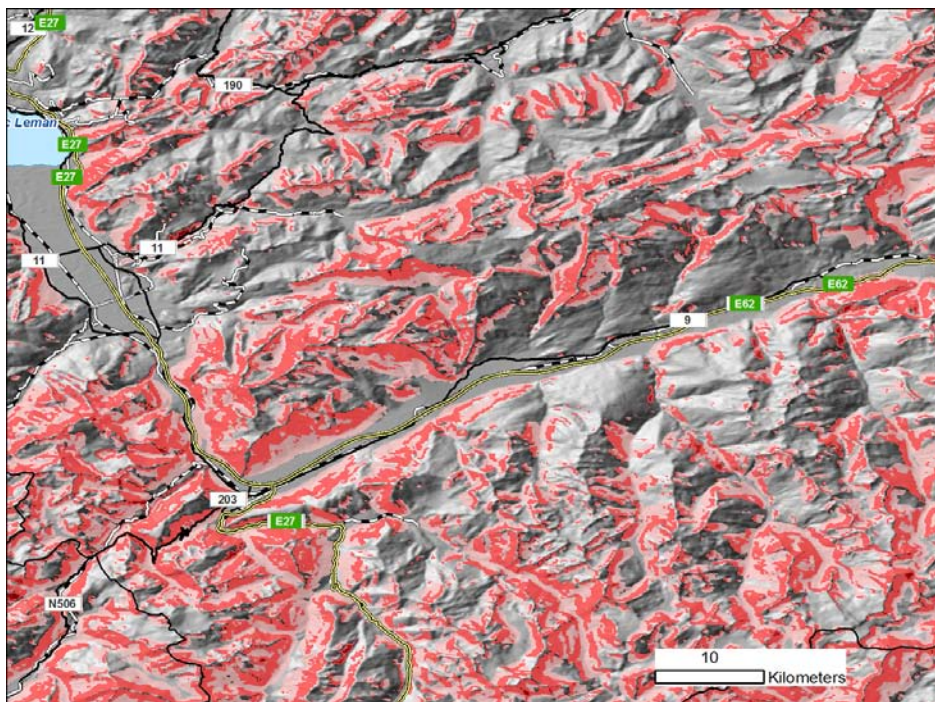


Figure 10-14: Detail of the rock fall susceptibility map drawn for Europe. In red: potential release areas, in pink: propagation zones

- (c) Definition of an index of rock fall activity. The susceptibility maps drawn during the 1st step do not include any information on rock fall activity, production or probability. As the goal of this project is hotspot detection, an index was developed to assess qualitatively the potential activity of a region. This slope activity index (SAI) is calculated using a moving window of 21x21 cells (=2.1x2.1 km), such as SAI increases with (i) the angle of the steepest slope in the window, and (ii) the proportion of slope over 30° in the window (Figure 10-15).

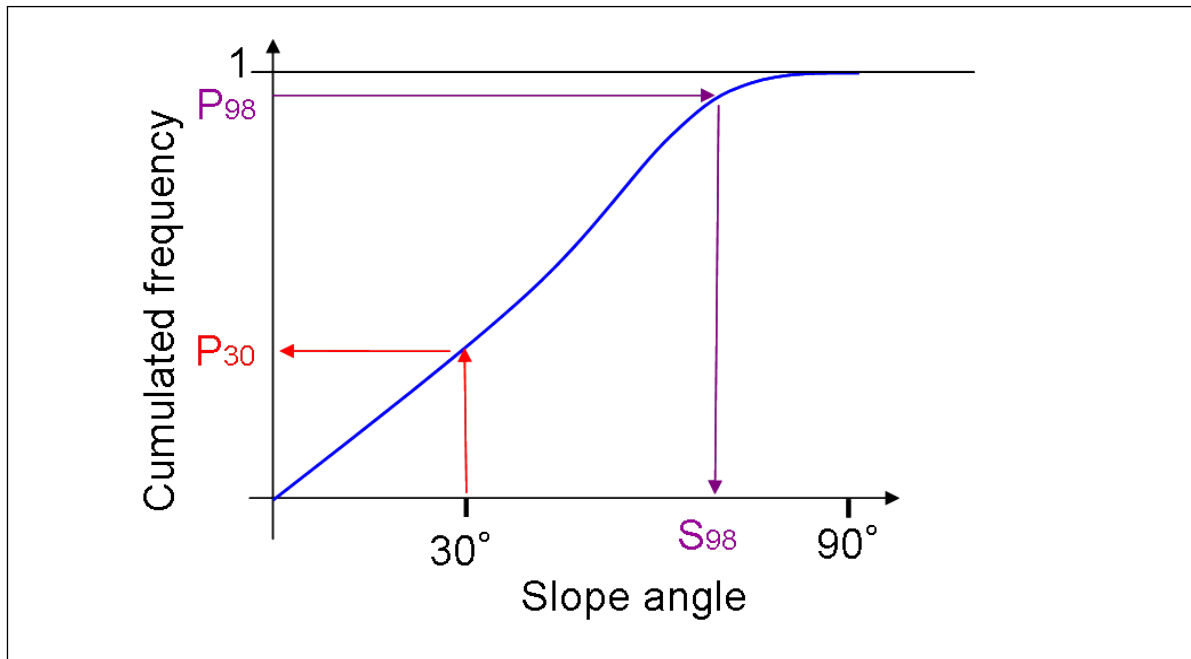


Figure 10-15: Example of cumulated frequency of the slope angle distribution, in a window of 21x21 cells.

$$SAI = (S_{98} - 30^\circ) / 60^\circ * (1 - P_{30})$$

With SAI = slope activity index

S_{98} = steepest slope angle in the window (measured at percentile 98%)

P_{30} = percentile of cells of the window with a slope angle less than 30°.

Values for SAI can range from 0 to 1, with 1 as maximum of activity (Figure 10-16) when all the cells of the window are steeper than 30° and the maximum slope angle in the window is vertical. Then the SAI is actually a weighting factor that moderates the susceptibility.

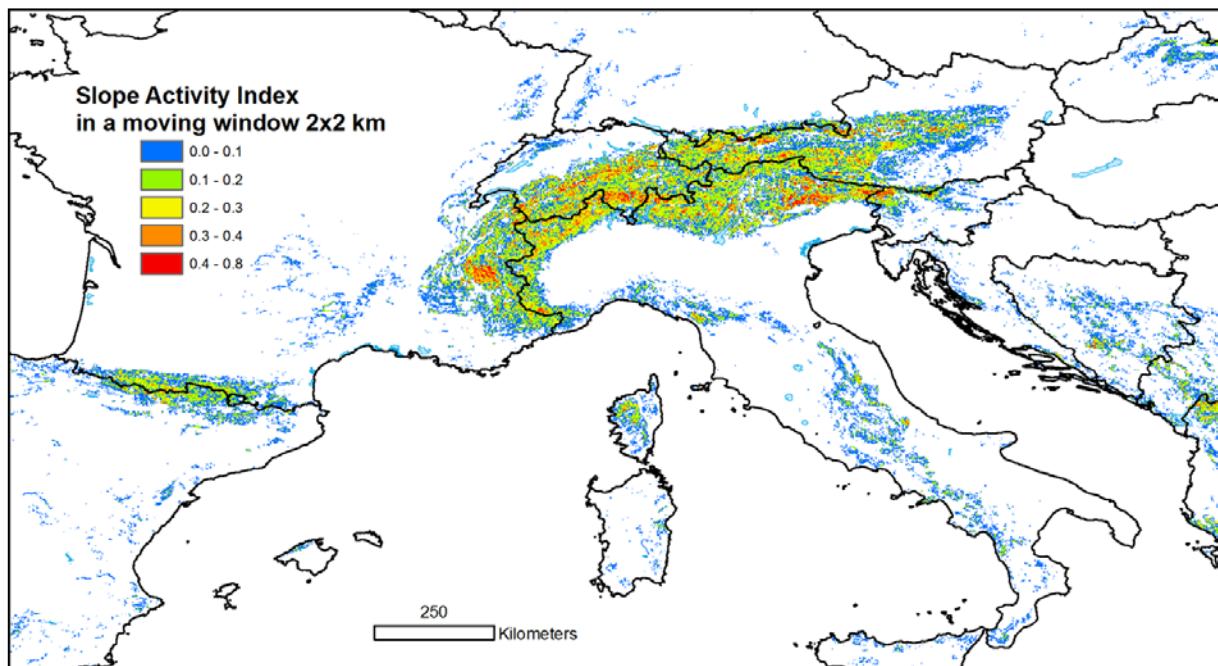


Figure 10-16: Subset of the slope activity index (SAI) map

- (d) Finally a low resolution (10x10 km) map of population at risk is computed by grid multiplication (Figure 10-17). The multiplication is done at the cell size of the highest resolution, i.e. 100m, and then the results are aggregated (sum) in a 10x10 km cell. The final map gives then the number of people potentially exposed to rock fall in 100 km².

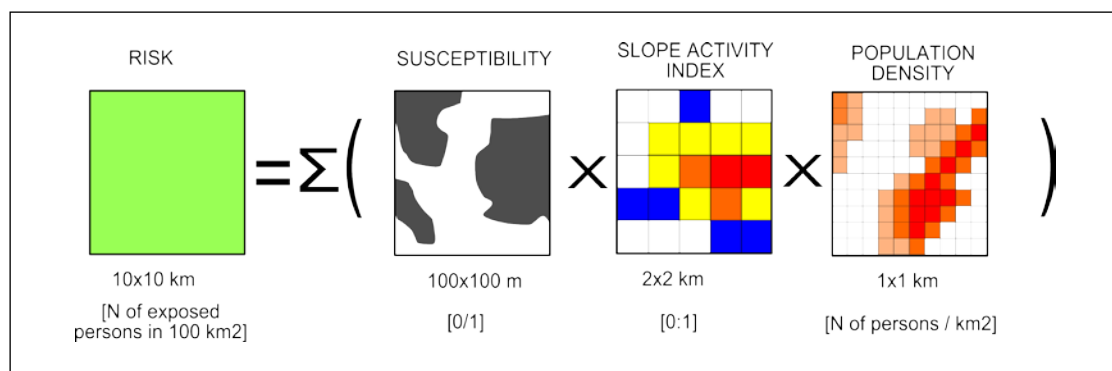


Figure 10-17: Calculation principle of the simplified risk map. Cell sizes and units of the datasets are indicated under the pictures.

10.4 RISK ASSESSMENT

An attempt was made to assess landslide risk at national level based on a methodology adapted from “Natural Disaster Hotspots – A Global Risk Analysis” (Dilley et. al, 2005) which concluded that at global level, landslide risk was represented well by a weighted aggregation of four factors: physical exposure, Human Development Index, arable land and forest cover percentages.

The landslide model developed during the Hotspots study is based on loss data from the CRED database (EM-DAT, 2003). As no other publicly available database covering the whole of Europe is available, it was decided to try to calibrate the European model based on CRED data for this study as well. The focus was set on data from the period 1950-2010. For this period, the CRED database has recorded losses for 17 European countries (Table 10-12). No events with mortality are reported for the other 28 countries included in this study.

Table 10-12: Landslide loss data from the CRED database focused on the period 1950-2010.

Country	Average annual number of people killed by mass movements
Italy	41.00
Russia	11.28
Austria	5.96
Switzerland	4.91
France	2.96
United Kingdom	2.33
Spain	1.40
Norway	1.21
Albania	0.95
Iceland	0.83
Portugal	0.48
Slovakia	0.30
Sweden	0.21
Bulgaria	0.18
Bosnia & Herzegovina	0.10
Czech Republic	0.10
Germany	0.08

The CRED database reports only landslide events that either have killed more than 10 people, or have affected more than 100 people. This fact, on top of the possibility of large events being unreported or being registered as caused by flooding or earthquakes instead of landslides, has resulted in landslide loss numbers being too low and consequently possibly ill distributed between the European countries.

For example, the national mass movement database (including snow avalanches) for Norway has registered a total of approximately 33 000 events, whereof 28 000 since year 1900. The total number of people killed is roughly 5300, 1100 since year 1900. In comparison, CRED has registered only one mass movement event in Norway, with 73 people killed. An idea of how the CRED criteria of including only event killing 10 people or more influences mortality numbers can be obtained from Table 10-13, which compares mortality in all events to mortality for large events for Norway, Sri Lanka and Nepal. The data indicates that more than half of the mortality occurs in events killing less than 10 people. This not only results in severe underreporting, but also leads to unpredictable relative errors between countries. Some countries probably have a larger share or mortalities in smaller events (for example 77% for Norway after 1900), as opposed to Sri Lanka (44%).

Table 10-13: The portion of people killed in large events (killing 10 or more people) compared to total mortality numbers (Data source: Norwegian mass movement database and the Desinventar database)

Country	Period	Number of people killed in events killing 10 or more people	Total number of people killed by mass movements	Fraction of people killed by large events
Norway	All historic events	2295	5319	43.1 %
Norway	1900 - 2009	247	1087	22.7 %
Sri Lanka	1974 - 2009	456	807	56.5 %
Nepal	1971 - 2007	1774	3953	44.9 %

Based on the investigation above it is believed that the quality of the CRED data for Europe is too low to obtain a reasonably reliable risk model for Europe. It is therefore decided to adopt physical exposure as a risk proxy, until better loss data becomes available.

The intersection of the landslide hazard "hotspots" with population density and infrastructure density maps provides a first-pass estimate of landslide risk "hotspots". The risk computations in the Natural Disaster Hotspots project were calibrated according to past human losses recorded by various natural disaster impact databases. The estimation of expected losses was achieved by first combining frequency and population exposed, in order to provide the physical exposure, and then performing a regression analysis using different sets of uncorrelated socio-economical parameters in order to identify the best indicators that were the best proxy for approaching human vulnerability to landslides in a given country (Peduzzi et al., 2002; Nadim et al., 2006).

Since landslides are highly correlated with other natural disasters, one may overestimate the total risk from all natural hazards if one simply adds the individual risks. This is particularly significant for earthquake-induced landslides, where the fatalities due to the earthquake event reported in various databases are inclusive of those caused by landslides. In the new analyses, the landslide hazard due to earthquakes and rainfall are differentiated. This should make it possible to correct for some of the correlations among the risks associated with different natural hazards when the total risk is estimated.

10.4.1 Discussion

Regarding the new vegetation cover index that was used in the ICG model, a relatively small variation range was assigned to the index. This was due to the contradictory opinions of different experts regarding the effects of vegetation cover on slope stability. It is also in agreement with the results obtained by JRC, as land cover had only a relatively low importance in the logistic regression model.

The lithology factor is probably the weakest link of the model. The IGME5000 dataset features a much better resolution than the Geological Map of the World. Still, an index that could better describe the soil conditions would improve the model results. However, we are not aware of any global database of soil conditions (or Quaternary sediment thickness for that matter). It should, however, be noted that great efforts were made to translate the map into different classes of material (rock and soil) that, from a geological and engineering point of view, are considered susceptible to landslides.

10.4.2 Evaluation of physical exposure

The Global Rural Urban Mapping Project (GRUMP) dataset prepared by the Center for International Earth Science Information Network (CIESIN) at Columbia University was used for estimating the population exposed to landslides.

The GRUMP population surfaces consist of raster grids of population counts (people) and densities at 30 arc-second resolution. The GRUMP population distribution in 2007 for the study region is shown on Figure 10-20.

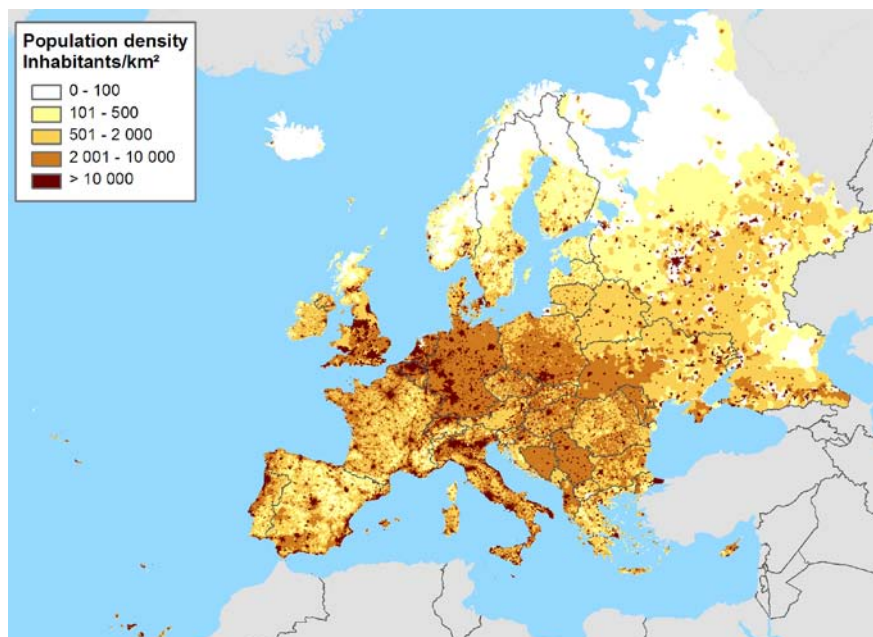


Figure 10-18: GRUMP – Population density (per pixel of 30 arc_sec × 30 arc_sec) in the study area in 2007.

Physical exposure was computed by weighting the landslide hazard maps with respect to the population density in each pixel (see Sec. 2 of this appendix). The results obtained for physical exposure are shown in Figure 10-21 and Figure 10-22.

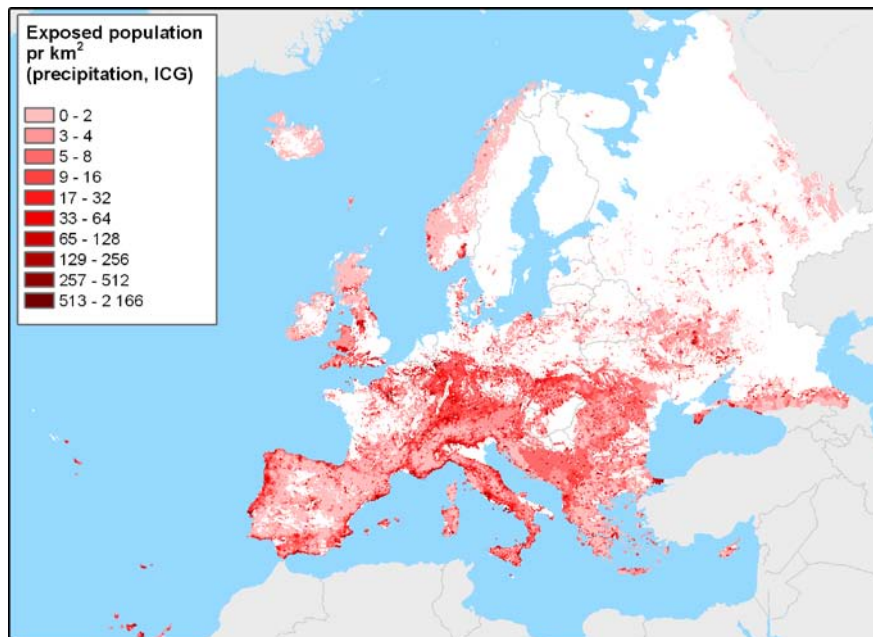


Figure 10-19: Population exposure to precipitation-induced landslides in the study area.

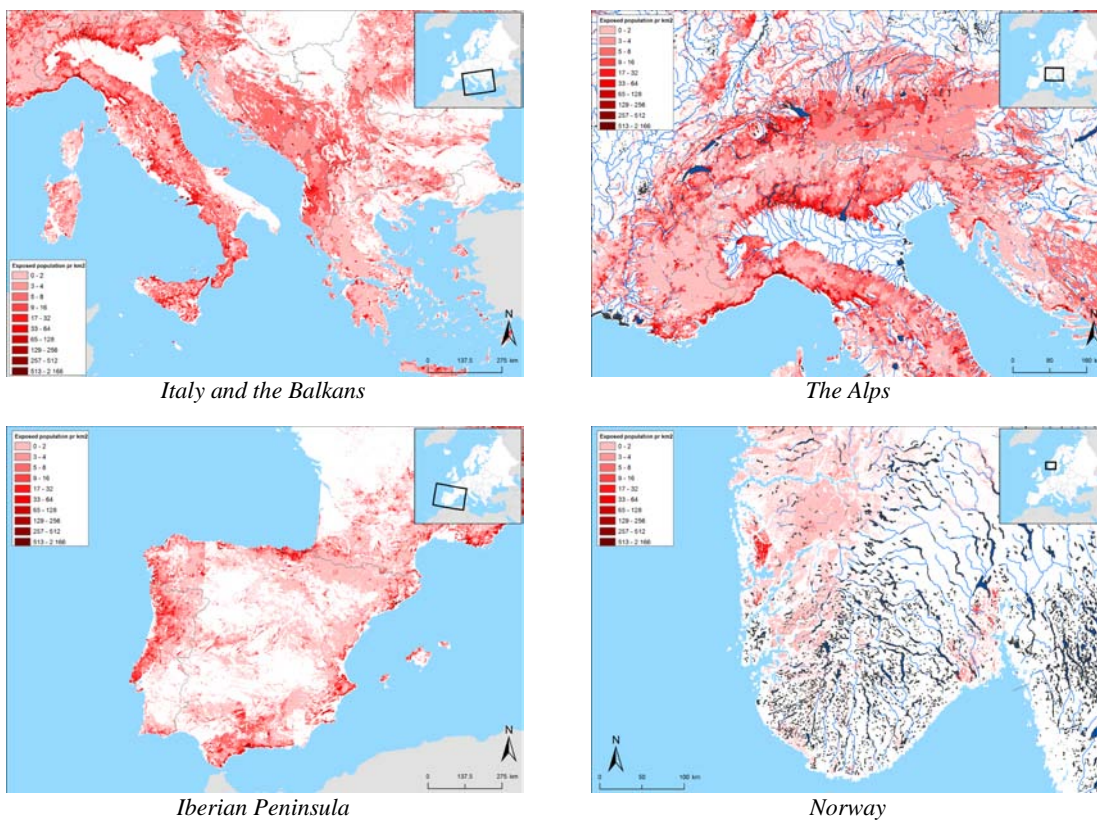


Figure 10-20: Population exposure to precipitation-induced landslides in selected regions of the study area.

11 APPENDIX C – MODEL VALIDATION

The model results were validated by SafeLand partners that have access to national or local datasets of landslide hazard or even inventories of landslide events. The task was to compare the results from the modelled hazard maps with local registrations and experience. A short questionnaire with eight questions was sent to the project partners in Italy (UNIFI, AMRA), Scotland (TRL), Romania (GIR) and Norway (ICG).

The following eight questions were addressed:

No	Question
1	Does the hazard map show reasonable hazard levels in the areas where you experience significant/high landslide hazard?
2	Find examples for good fit and for areas where the results are bad. Please send us the geographical information for those areas (a shapefile with polygons covering “good areas” and a file with “bad area” polygons)
3	Do you have any explanation or suggestions why the results are different from your experience?
4	Where are typical areas that show good results (any special geology, water ways, land cover, etc.)?
5	Where are typical areas that show poor results (any special geology, water ways, land cover, etc.)?
6	In total, is too much land covered by high hazard or too little? Does this even out on a national basis?
7	Do you have special hotspots in your country? Is the hazard map reasonably correct for these areas?
8	What is your overall impression? Are the results applicable on a European scale?

11.1 ANSWERS FROM ROMANIA (GIR)

The Geological institute of Romania (Raluca Maftai) has performed a short validation of the results both from ICG and JRC. There are significant problems with correctly classifying zones prone to precipitation-induced landslide while zones prone to earthquake-induced landslides are well represented in both models (Figure 11-1). Detailed answers are given in Table 11-1.

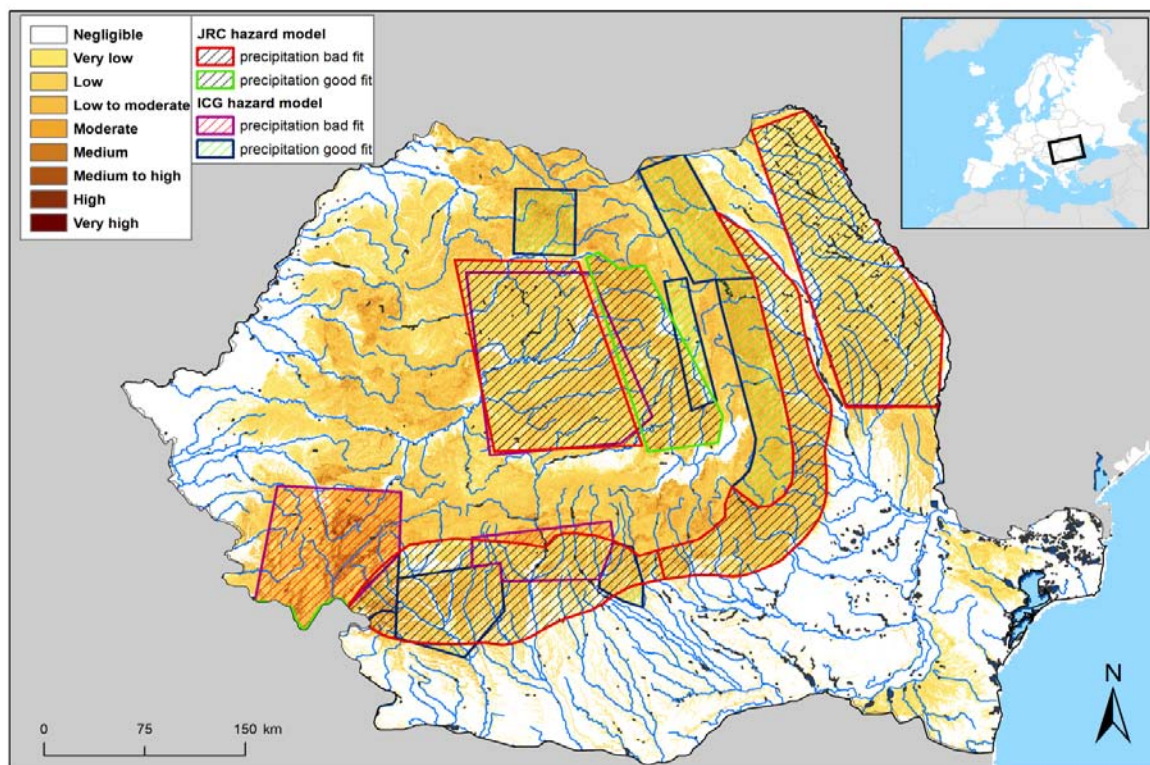


Figure 11-1: Map showing the areas of good and bad fit of the hazard model results in Romania

Table 11-1: Answers on the questionnaire from Romania

No	Question	ICG (precipitation)	ICG (earthquake)	JRC (precipitation)	JRC (earthquake)
1	Does the hazard map show reasonable hazard levels in the areas where you experience significant/high landslide hazard?	<ul style="list-style-type: none"> On a national scale, the significant/high landslide hazard is poorly represented; the most affected areas are: the central-eastern part (Eastern Carpathians, Subcarpathians); north-east (Moldavian Plateau); intra-Carpathian area (Transylvanian Plateau); the southern part of the Meridional Carpathians (Getic Plateau) 	<ul style="list-style-type: none"> On a national scale, the results of the analysis look very good 	<ul style="list-style-type: none"> Some significant/high landslide hazard areas are not/insufficiently represented. 	<ul style="list-style-type: none"> The hazard levels are reasonably represented.
2	Find examples for good fit and for areas where the results are bad. Please send us the geographical information for those areas (a shapefile with polygons covering “good areas” and a file with “bad area” polygons)	<ul style="list-style-type: none"> In the south-west all types of slides are overestimated (except along the Danube River); Bad fit for deep-seated landslides in the intra-Carpathian area; Bad fit for all slides in molasse deposits; Good fit for shallow landslides, earth flows and debris flows affecting the Northern part of Transylvanian Plateau 	<ul style="list-style-type: none"> Good fit for all types of landslides triggered by earthquakes generated in the Vrancea seismic area. 	<ul style="list-style-type: none"> Bad fit for the Carpathian chain (Eastern Carpathians, Southern Carpathians, Western Carpathians) – the hazard level is overestimated; Bad fit for Moldavian Plateau, Transylvanian Plateau, Getic Plateau – underestimated. These areas have medium to medium-high hazard levels; up to high and very high landslide hazard in the Subcarpathians; Good fit for the eastern part of the Transylvanian Plateau and SW, along the Danube River. 	<ul style="list-style-type: none"> Good fit for the mountainous, less good for the hilly curvature area; Bad fit for the rest of the Carpathian area;
3	Do you have any explanation or suggestions why the results are different from your experience?	<ul style="list-style-type: none"> No national landslide inventory as input data for the model, only studies at regional scale or local experience 	<ul style="list-style-type: none"> 	<ul style="list-style-type: none"> No national landslide inventory as input data for the model, only studies at regional scale or local experience. Landslides in soils not in rocks prevail, due to soil and weather characteristics. 	<ul style="list-style-type: none"> Landslide hazard is higher in soils (Subcarpathians) than in rocks (Carpathians)
4	Where are typical areas that show good results (any special geology, water ways, land cover etc.)?	<ul style="list-style-type: none"> Quaternary deposits, deforested areas, steep terrains 	<ul style="list-style-type: none"> Molasse, Paleogene and Cretaceous flysch deposits, mainly steep terrains 	<ul style="list-style-type: none"> Deforested areas, steep terrains 	<ul style="list-style-type: none"> Molasse, Paleogene and Cretaceous flysch deposits, mainly steep terrains
5	Where are typical areas that show poor results (any special geology, water ways, land cover etc.)?	<ul style="list-style-type: none"> Molasse deposits, less steep terrains 	<ul style="list-style-type: none"> 	<ul style="list-style-type: none"> Molasse deposits, less steep terrains 	<ul style="list-style-type: none"> Generally, the Carpathian chain
6	In total, is too much land covered by high hazard or too little? Does this even out on a national basis?	<ul style="list-style-type: none"> Insufficiently coverage for moderate – medium landslide hazard; the negligible level is very well represented; generally, the lower scales cover the lower to medium areas (exception: the mountainous areas where the hazard is low or very low) 	<ul style="list-style-type: none"> The lower as well as the higher scales of hazard are well covered 	<ul style="list-style-type: none"> The north-east (Moldavian Plateau), central (Transylvanian Plateau) and southern (Getic Plateau) areas are not sufficiently covered; the same for the Subcarpathians. The hazard is too high for the Carpathians 	<ul style="list-style-type: none"> At national scale, the high hazard levels cover too much territory, the only significant area for this level being the Curvature Carpathians and Subcarpathians
7	Do you have special hotspots in your country? Is the hazard map reasonably correct for these areas?	<ul style="list-style-type: none"> Central-eastern part: Eastern Carpathians - good fit, Subcarpathians - less good; north-east: Moldavian Plateau, less good; intra-Carpathian area: Transylvanian Plateau, good fit in the northern part, less good for the rest; the northern part of the Meridional Carpathians: Getic Plateau, bad fit for the lower scale of hazard. 	<ul style="list-style-type: none"> The Curvature Subcarpathians, very good fit 	<ul style="list-style-type: none"> The hazard map does not emphasize the main landslide prone areas. 	<ul style="list-style-type: none"> Curvature Subcarpathians – good fit
8	What is your overall impression? Are the results applicable on a European scale?	<ul style="list-style-type: none"> The model is “soft” for the most landslide prone areas (probably, due to no landslide inventory input), but generally good. 	<ul style="list-style-type: none"> The model is applicable on a national scale 	<ul style="list-style-type: none"> On a national scale, the model is too “coarse”; no agreement in the higher scale of hazard 	<ul style="list-style-type: none"> The model shows too much land covered by medium-high hazard.

11.2 ANSWERS FROM ITALY (UNIFI)

The validation of hotspot maps in Italy was done by Veronica Tofani & Ascanio Rosi, Department of Earth Sciences, University of Firenze (UNIFI)

11.2.1 Introduction

The Hotspot maps produced by ICG and JRC have been validated in Italy at two different scales:

- At a national scale making use of a national database of the most hazardous landslides in Italy. This database has been prepared by the Italian Ministry of Environment and counts around 40000 landslides. The database is partially incomplete.
- At the river basin scale using the susceptibility map of the Arno River Basin, located in the Northern Apennines. The Arno river has an extension of around 9100 km². The susceptibility map produced through a statistical approach classifies the territory of the river basin into 4 classes of susceptibility (S1, S2, S3, S4).

The description of the results of the validation process are reported below. For each Hotspot map (NGI precipitation, NGI earthquake, JRC precipitation and JRC earthquake) brief answers of proposed questions are reported.

11.2.2 ICG Precipitation Model

11.2.2.1 National scale

Question 1: Does the hazard map show reasonable hazard levels in the areas where you experience significant/high landslide hazard?

As reported in Figure 11-2 landslides are correctly identified by the hazard map, since the majority of the landslides are in the higher classes of hazard. Only the 15 % of the landslides are classified in lowest classes (0, 1, 2).

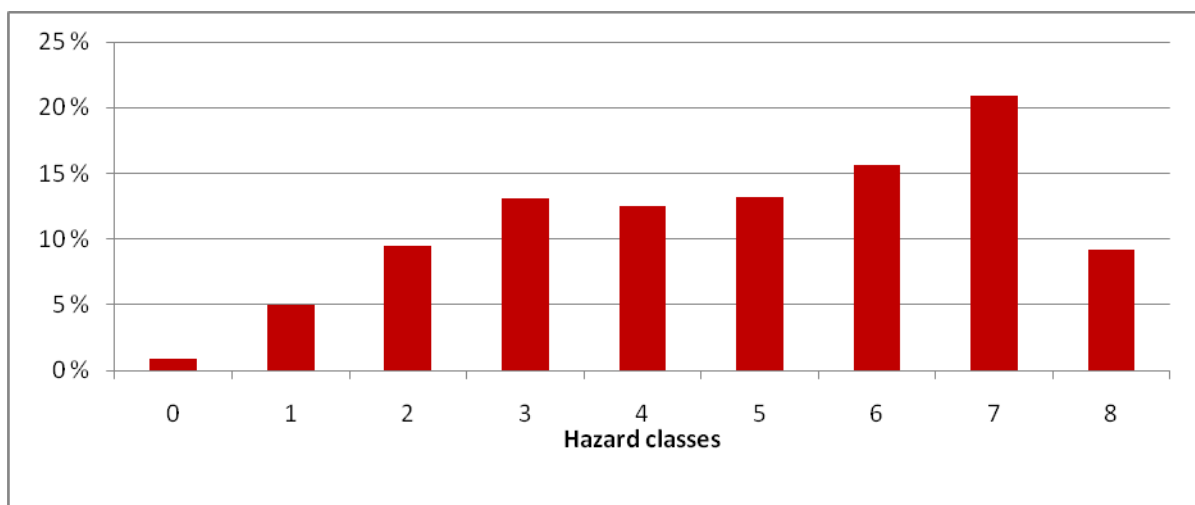


Figure 11-2: Number of landslides (percentage) classified in each class of normalized hazard to the areal extension of each class.

Question 2: Find examples for good fit and for areas where the results are bad. Please send us the geographical information for those areas (a shapefile with polygons covering “good areas” and a file with “bad area” polygons)

Since the landslide map at the national scale is largely incomplete, the identification of good and bad fitting areas is quite difficult. Anyway we can observe that from a national point of view there is a good fit in the eastern Alps and a general bad fit in the Arno river basin, Northern Apennines (Figure 11-3).

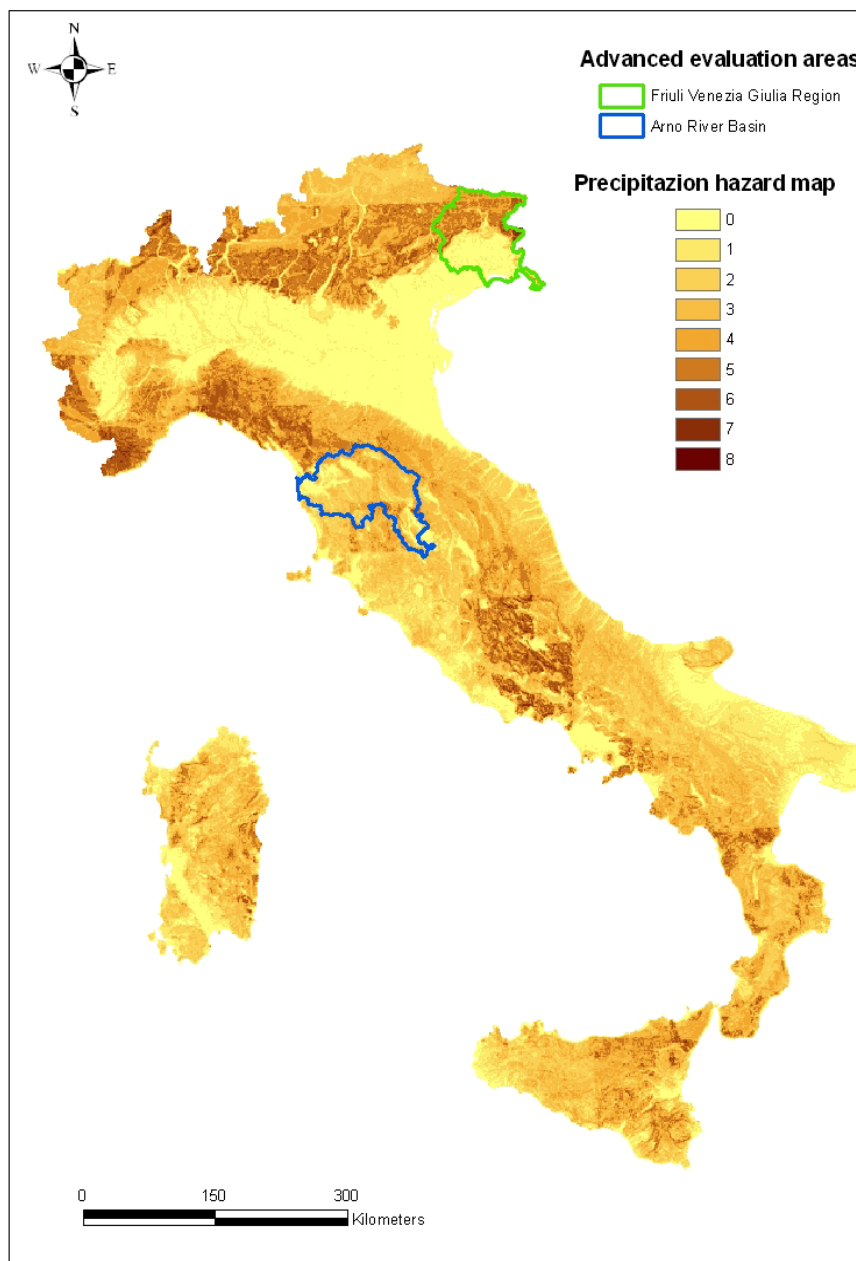


Figure 11-3: Good fit (in green) and bad fit (in blue) between the landslide map and the hazard map.

Question 4: *Where are typical areas that show good results (any special geology, water ways, land cover etc.)?*

At national level it has not been observed any special geology, water ways or land cover which show better results than others.

Question 5: *Where are typical areas that show poor results (any special geology, water ways, land cover etc.)?*

At the national level has not been observed any special geology, water ways or land cover which show worse results than others.

Question 6: *In total, is too much land covered by high hazard or too little? Does this even out on a national basis?’*

In general there is a good balance between high and low hazard. Anyway, sometimes there are few problems maybe related to the goodness of the input data or to computational issues. These problems can be observed along the two main mountain chains in Italy, Alps and Apennines where in some cases there are strong differences in terms of hazard and within areas with the same geological and physiographic features.

Question 7: *Do you have special hotspots in your country? Is the hazard map reasonably correct for these areas?*

In Italy, at the national level, the most hazardous areas are in the Alps and in the Apennines although subjected to different types of landslides. As explained above the hazard map is usually reasonably correct for the areas with some problems as above explained.

Question 8: *What is your overall impression? Are the results applicable on a European scale?*

The results can be applied at European scale.

11.2.2.2 Basin scale (Arno River Basin, Central Italy (Error! Reference source not found.))

Question 1: Does the hazard map show reasonable hazard levels in the areas where you experience significant/high landslide hazard?

In Figure 11-4 is reported the distribution of hazard levels from the hotspot map for each class of susceptibility within the Arno river basin. In general, it can be observed an increase of the highest classes of hazard from the lowest class of susceptibility (S1) to the highest one (S4).

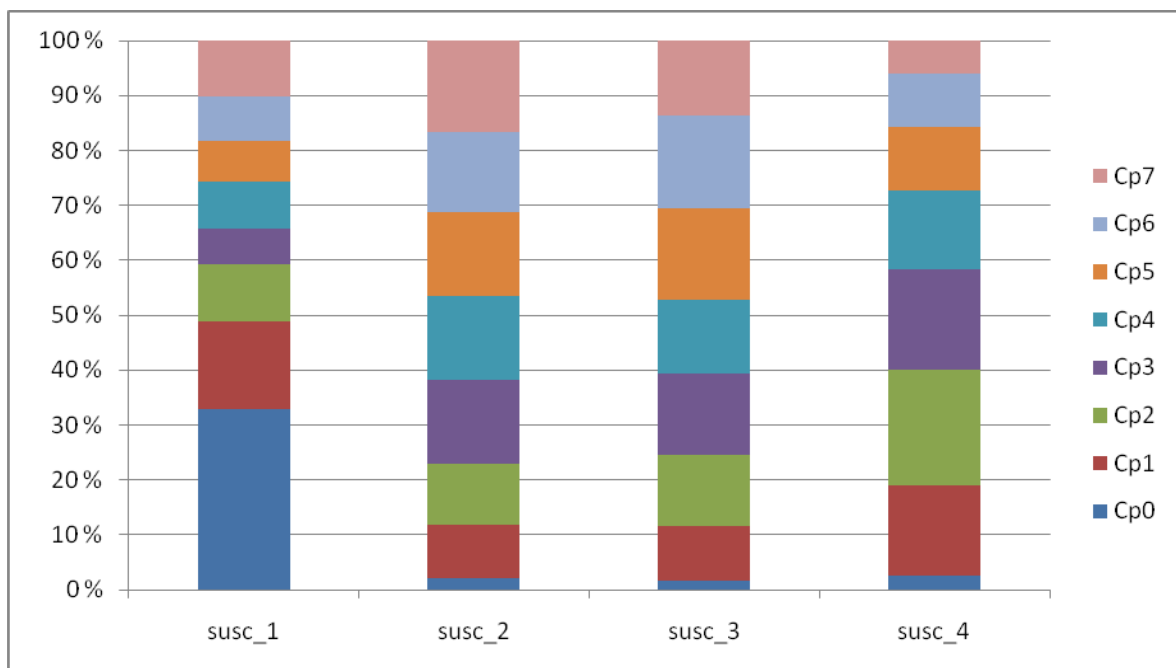


Figure 11-4: Distribution of hazard levels from the hotspot map for each class of susceptibility within the Arno river basin.

Question 2: Find examples for good fit and for areas where results are bad. Please send us the geographical information for those areas (a shapefile with polygons covering “good areas” and a file with “bad area” polygons)

Prefacing that at this scale is more evident the non homogeneous results may be related to the input data, it is possible to find areas with a good fit such as a region in the northern part of the basin and areas with bad fit such as a central and south portion of the basin (Figure 11-5).

Question 3: Do you have any explanation or suggestions why the results are different from your experience?

The areas of “bad fit” are characterized by a complex geology, with different lithologies and a strong local variability.

Question 6: In total, is too much land covered by high hazard or too little? Does this even out on a national basis

There is generally a good balance between high and low hazard also at the basin scale.

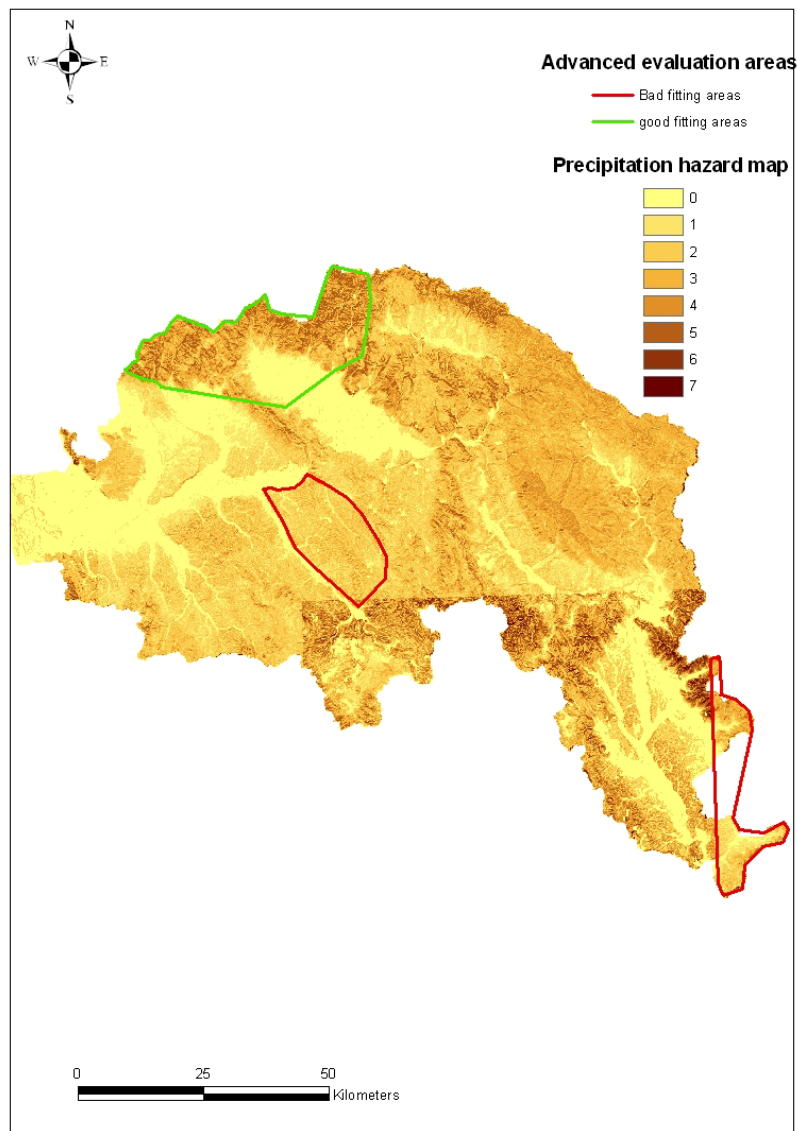


Figure 11-5: Good fit (in green) and bad fit (in red) between the susceptibility map of the Arno river basin and the hazard map.

Question 7: Do you have special hotspots in your country? Is the hazard map reasonably correct for these areas?

In the Arno river basin the most hazardous areas are along the Apennines and in central zones where some geological features, like pliocenic deposits (sands and clays) are the main cause of landsliding despite low slope degrees. The hazard map is generally correct in the Apennines, less correct in the central part of the basin where this type of soil outcrops.

Question 8: What is your overall impression? Are results applicable on a European scale?

The achieved results can be applied at a European scale more focusing on the input data.

11.2.3 ICG Seismic Model

11.2.3.1 National scale

Question 1: Does the hazard map show reasonable hazard levels in the areas where you experience significant/high landslide hazard?

As reported in Figure 11-6 the highest level of earthquake-induced hazard reached in Italy is level 6. Landslides are correctly identified by the hazard map since the majority of the landslides are in the higher classes of hazard (4, 5, 6).

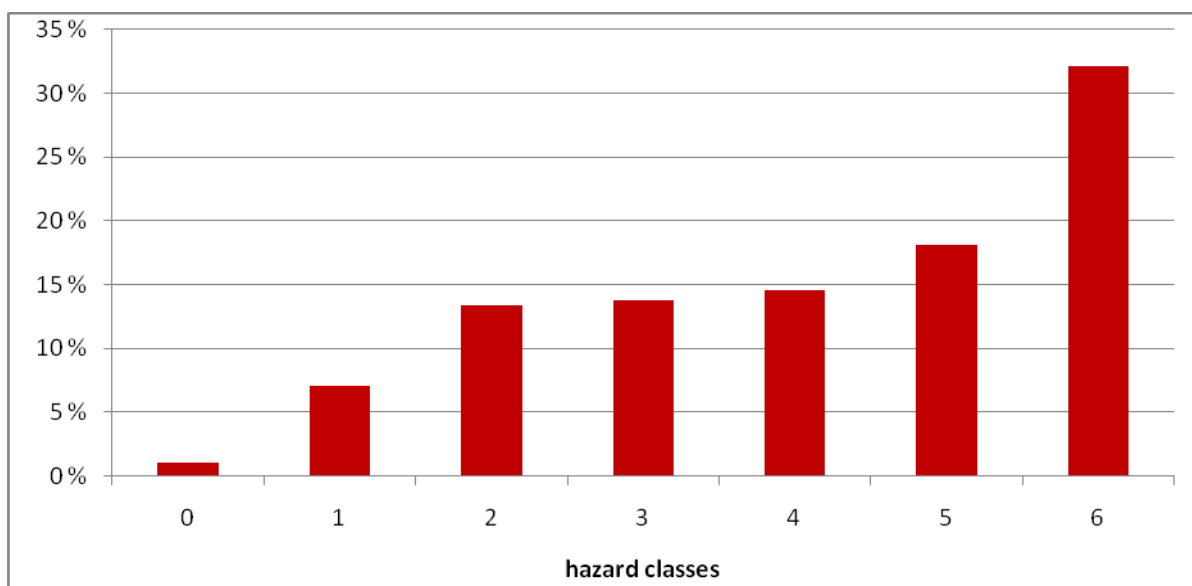


Figure 11-6: Number of landslides (expressed as a percentage) classified in each class of hazard normalized to the areal extension of each class.

Question 2: Find examples for good fit and for areas where results are bad. Please send us the geographical information for those areas (a shapefile with polygons covering “good areas” and a file with “bad area” polygons)

The general impression is that landslides induced by earthquake are correctly identified.

Question 8: What is your overall impression? Are the results applicable on a European scale?

The results can be applied at a European scale.

11.2.3.2 Basin scale (Arno River Basin, Central Italy)

Question 1: Does the hazard map show reasonable hazard levels in the areas where you experience significant/high landslide hazard?

In Figure 11-7 is reported the distribution of hazard levels-related to earthquakes - from the hotspot map. Each class of susceptibility within the Arno river basin is outlined here below. At this scale of analysis results seem worse than at a national level. As reported the distribution of the hazard classes is almost the same for the three highest classes of susceptibility (S2, S3, S4). Since the seismic hazard is not very high (except the areas located along the Apennines chain) the major triggering factor of landslides in the Arno river basin is the precipitation.

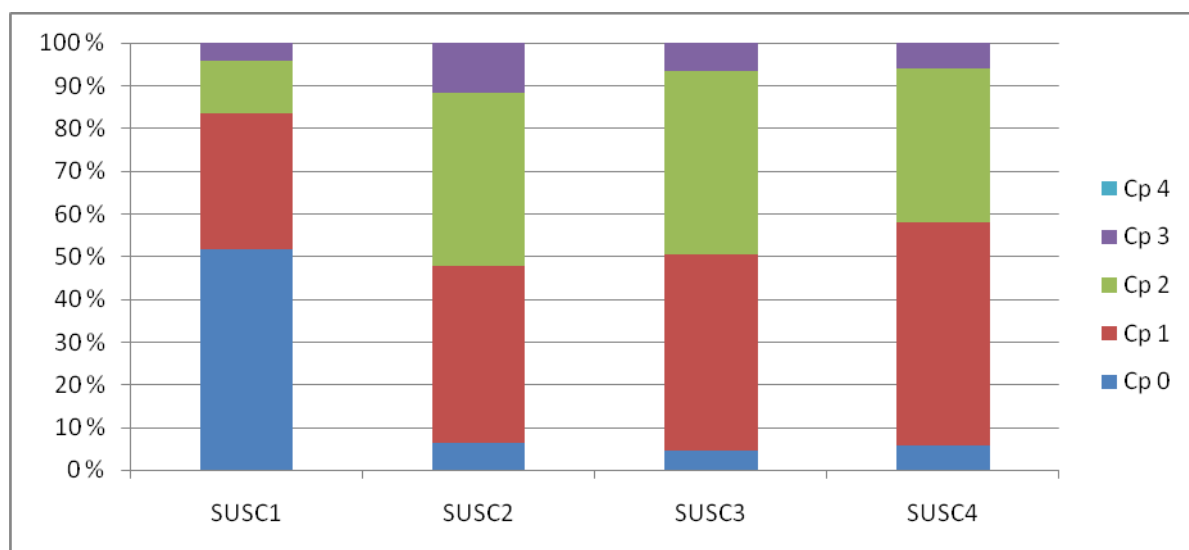


Figure 11-7: Distribution of hazard levels from the hotspot map for each class of susceptibility within the Arno river basin.

Question 2: Find examples for good fit and for areas where the results are bad. Please send us the geographical information for those areas (a shapefile with polygons covering “good areas” and a file with “bad area” polygons)

The Mugello area in the north-east part of the river basin has a good fit since it is the most seismic region in the basin and presents the highest level of hazard (Figure 11-8).

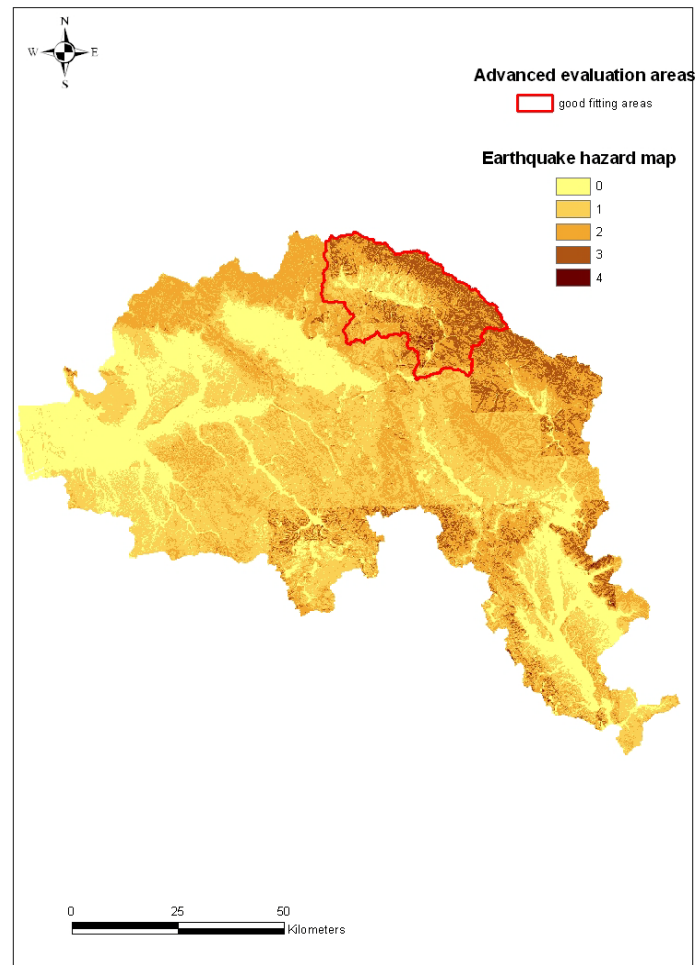


Figure 11-8: Example of good fit of the earthquake hazard map with the Arno river basin susceptibility map.

Question 4: *Where are typical areas that show good results (any special geology, water ways, land cover etc.)?*

At the river basin scale it has not been observed any special geology, water ways or land cover which show better results than others.

Question 5: *Where are typical areas that show poor results (any special geology, water ways, land cover etc.)?*

At river basin scale is not been observed any special geology, water ways or land cover which show worst results than others.

Question 6: *In total, is too much land covered by high hazard or too little? Does this even out on a national basis?'*

There is a good balance between the high and low hazard. The higher values are located along the Apennines chain where the seismic hazard is higher while the lower values are located in the central part of the basin where the seismic hazard is lower.

Question 7: *Do you have special hotspots in your country? Is the hazard map reasonably correct for these areas?*

Within the Arno river basin, the Mugello basin (Figure 11-8) has instability factors, such as geology and topography and a high level of seismic hazard. The combination of these two factors can cause general instability conditions. The hazard map is correct for this area.

Question 8: *What is your overall impression? Are the results applicable on a European scale?*

The results can be applied at European scale with special attention to the selection of input data. For instance, in some areas there are strong differences between close areas with the same geological and physiographic features.

11.2.4 JRC Precipitation Model

The JRC precipitation hotspot map has been validated only with the national landslide inventory map.

Question 1: *Does the hazard map show reasonable hazard levels in the areas where you experience significant/high landslide hazard?*

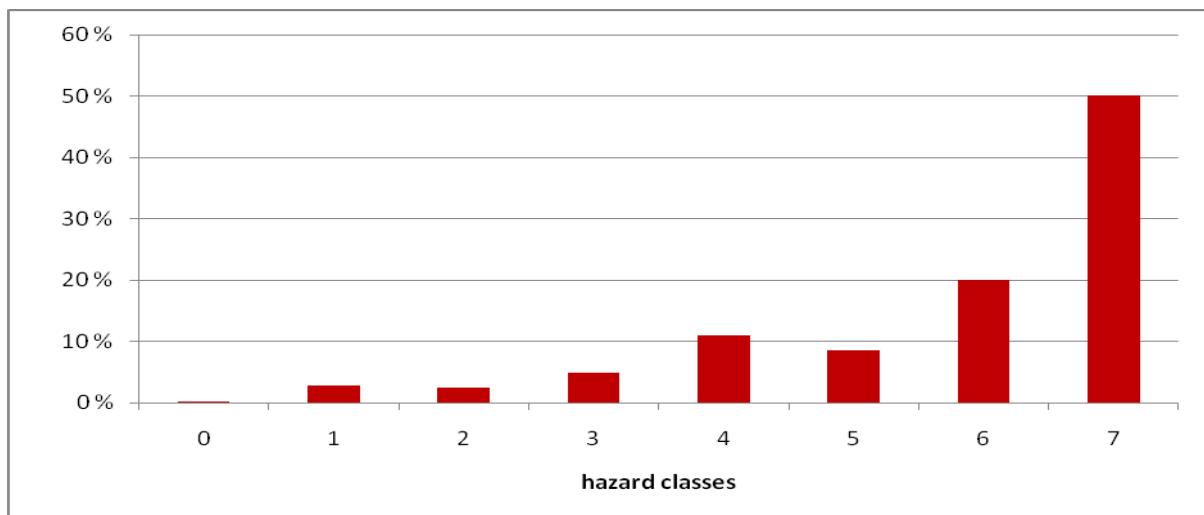


Figure 11-9 shows the distribution of the number of landslides classified in each class of hazard. This result of the validation shows that the 50% of the landslides are classified in the highest class of hazard.

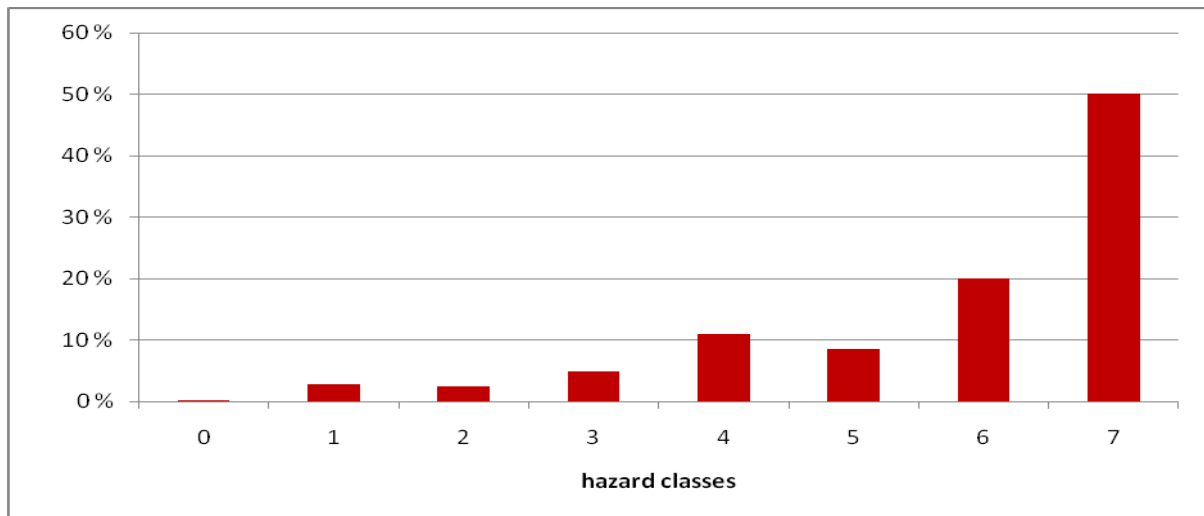


Figure 11-9: Number of landslides (expressed as a percentage) classified in each class of hazard normalized to the areal extension of each class.

11.2.5 JRC Seismic Model

The JRC earthquake hotspot map has been validated only with the national landslide inventory map.

Question 1: Does the hazard map show reasonable hazard levels in the areas where you experience significant/high landslide hazard?

Figure 11-10 shows the distribution of the number of landslides classified in each class of hazard. This result of the validation shows that more than 60% of the landslides are classified into the highest class of hazard.

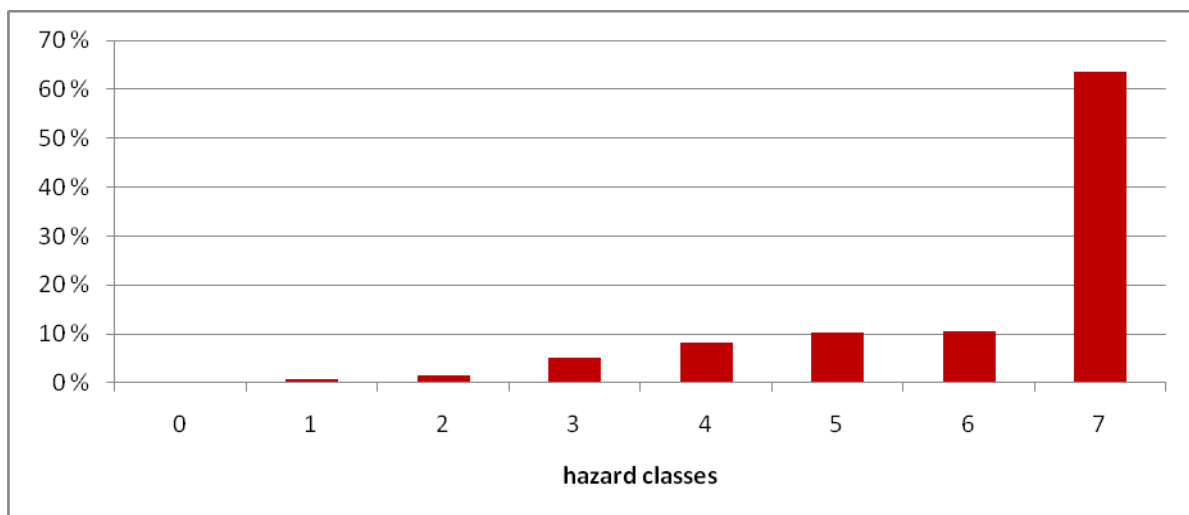


Figure 11-10: Number of landslides (expressed as a percentage) classified in each class of hazard normalized to the areal extension of each class.

11.3 ANSWERS FROM SCOTLAND (TRL)

11.3.1 Imagery Examined

The following Landslide Hazard GIS models have been developed in SafeLand:

International Centre for Geohazards (ICG) model which is based on the combination and weighting of different gridded layers which are then classified according judgment on their effect on slope instability. Precipitation and seismic-induced landslide triggers were modeled.

Joint Research Council (JRC) model which was developed utilizing the same basic principles as, but independent of the ICG model and using a statistical model to calculate landslide hazard and risk. Precipitation and seismic-induced landslide triggers were modeled.

Université de Lausanne (UNIL) model which estimates rock fall susceptibility by identifying possible rock fall source areas, then calculating the estimated run-out length for each source pixel. The susceptibility is independent of any trigger or event likelihood.

11.3.1.1 Data for Comparative Purposes

The following sources were used to validate the GIS models in Scotland:

Extracts from the *National Landslide Database for Great Britain* which is maintained by the British Geological Survey (BGS) (Foster *et al.* 2008).

Extracts from *GeoSure*, a GIS-based assessment of landslide and other hazards in Great Britain maintained by the BGS (Foster *et al.* 2008).

Scottish Road Network Landslides Study (SRNLS), a detailed study of debris flow susceptibility (on a 25m grid) for the whole of Scotland (Winter *et al.* 2008).

Various forms of mapping to provide positional referencing, this included but was not limited to Ordnance Survey mapping at various scales and other Ordnance Survey data issued under the OpenData™ scheme.

The experience of the authors of landslides in Scotland, the rest of the UK and Europe was also used to make the observations set out in the following sections; this experience totals more than 25 years.

11.3.2 Areas Examined

For the purposes of validating the models three case study areas were selected in Scotland. These areas were chosen as they have a known history of landslide hazard, most notably debris flow, and represent varied geological and geomorphological settings.

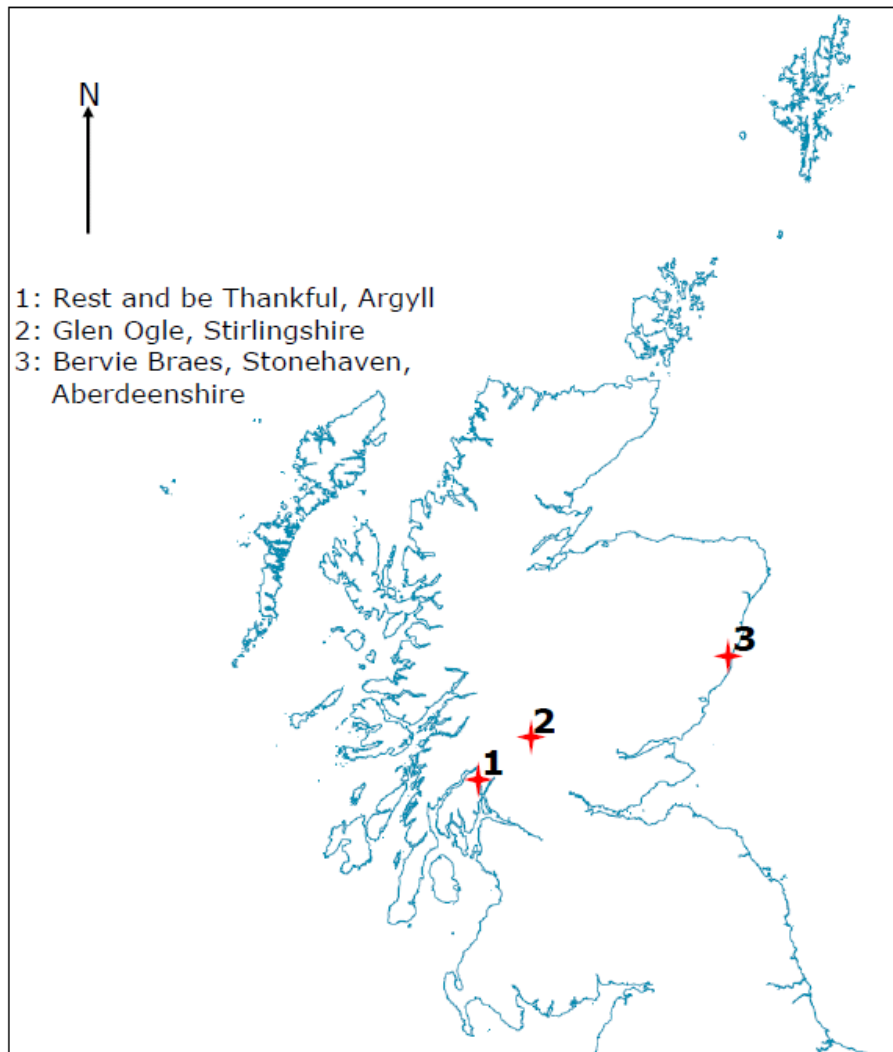


Figure 1. Case Study Location Plan.

In addition areas of England with known and limited landslide hazards were examined in a less formal sense/ more observational along with the imagery for Europe as a whole.

11.3.2.1 Rest and be Thankful, Argyll

The Rest and be Thankful is situated in the mountainous SW Highlands of Scotland (Figure 1 & 2). The GeoSure extract provided by the BGS centers on approximately NN 23000 07000 and covers an area of approximately 121 km².

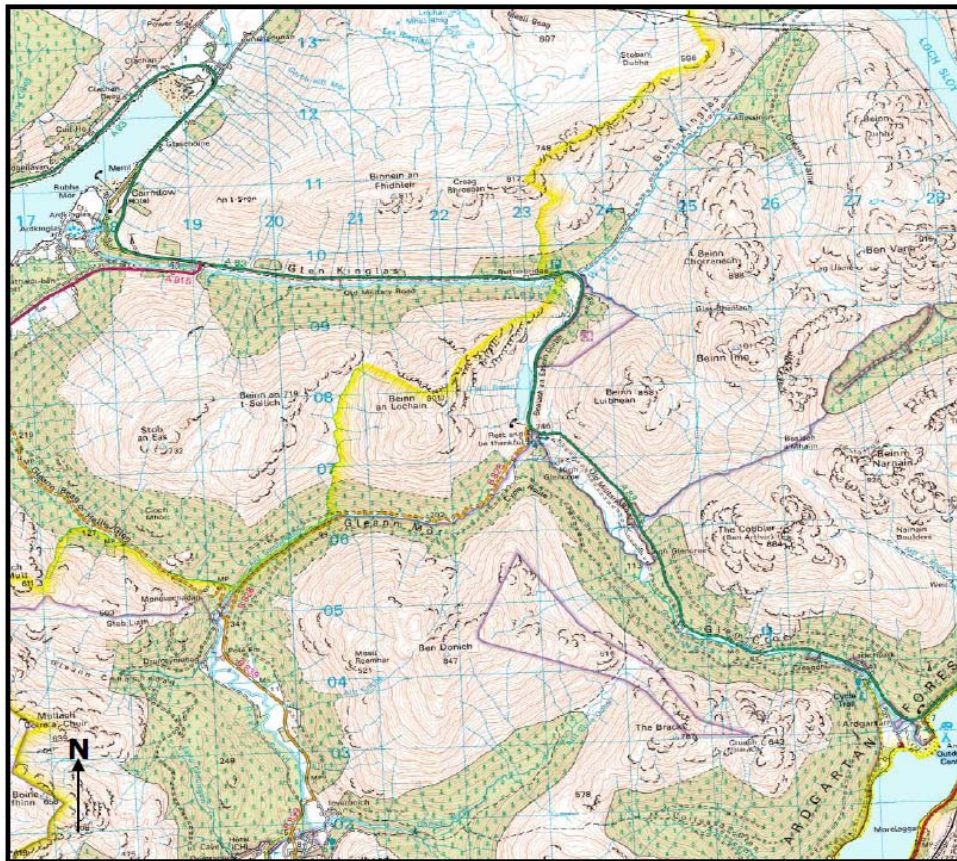


Figure 2. Rest and be Thankful study area (OS Data ©Crown Copyright. All rights reserved. Transport Scotland 100046668, 2010).

Hillsides in this area are incised by frequent stream channels (Figure 2). Lower slopes are commonly utilized for forestry, while upper slopes are typically vegetated with heather and other scrubby plants. Rock outcrops become more frequent on the upper reaches of hillsides, forming crags in places. While population density is low, high numbers of tourists pass through the region.

Bedrock across this part of the SW Highlands comprises metamorphic units of all grades from pelites to schist. Slopes are generally covered by thin glacial deposits. The National Landslide Database holds a number of entries for the Rest and be Thankful and surrounds.

11.3.2.2 Glen Ogle, Stirlingshire

The SE to NW oriented valley that is known as Glen Ogle is also situated within the SW Highlands (Figure 1 & 3). The slopes are predominantly vegetated by heather and bracken with some crags. The GeoSure extract centers on approximately NN 57000 26000. The NW corner of the extract is at NN 54000 31000 while the SE corner is at NN 61000 22000, with an approximate areal coverage of 63 km².



Figure 4. Bervie Braes study area (OS Data ©Crown Copyright. All rights reserved. Transport Scotland 100046668, 2010).

The setting of Bervie Braes varies significantly from that of the Rest and be Thankful and Glen Ogle in terms of its coastal location, geomorphology, and geology. Furthermore, a number of residential properties are situated at the foot of the slope at Bervie Braes (Figure 4).

Bedrock at this location typically comprises sandstones and conglomerates. The superficial deposits include glacial tills, sands and gravels, and raised beach deposits, and are relatively widespread across the area.

11.3.4 ICG Precipitation Model

In the *Rest and be Thankful* area, the model (Figure 5) broadly reflects the areas and regions of hillsides that correspond with known landslide hazard, particularly debris flow hazard. Compared to the SRNLS (Figure 6), there are some interesting points of difference and commonality.

Unsurprisingly, while the SRNLS tends to highlight specific locations the ICG model tends to highlight, or otherwise, entire hillsides. Areas in which this is successful include:

- The hillsides along the NE shore of Loch Fyne between NN 18600 12500 and NN 11400 08800.
- The higher slopes above Glen Kinglas (NN 19000 10000 to NN 23000 10000) which reflects the tendency of debris flow to be initiated at or about the streamline on this hillside, although the medium level of hazard indicated on the lower slopes appears to be potentially spurious.

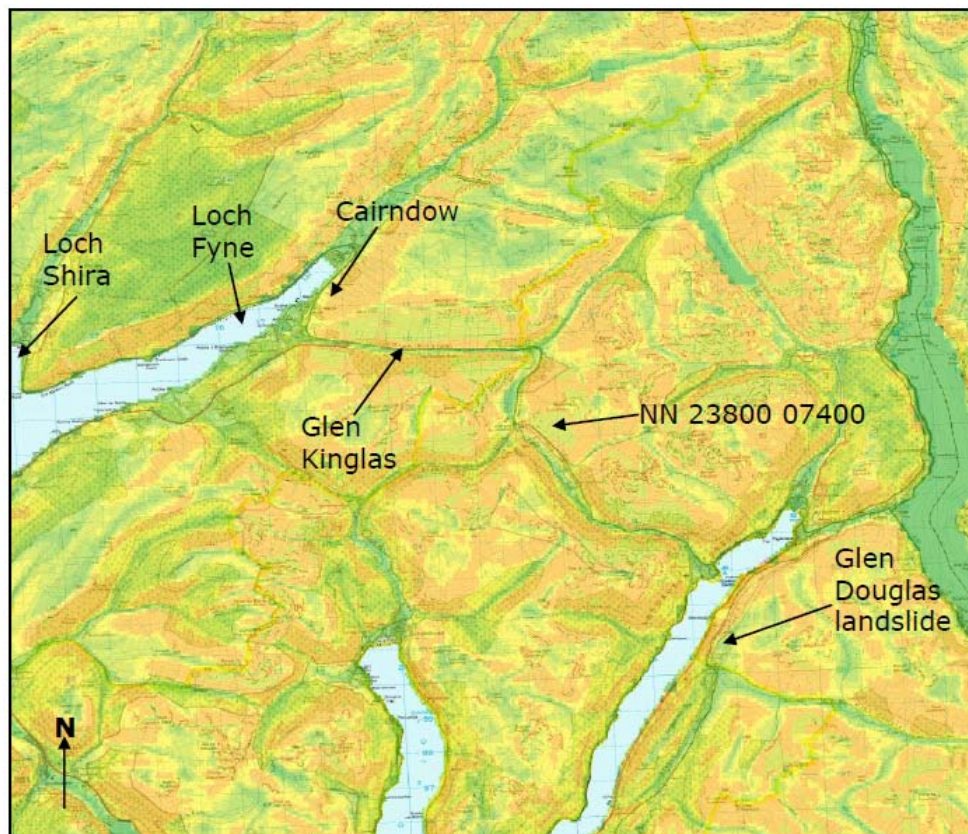


Figure 5. ICG Precipitation Model for the *Rest and be Thankful* (OS Data ©Crown Copyright. All rights reserved. Transport Scotland 100046668, 2010).

Key: Green: Negligible to low hazard
Yellow/orange: Moderate hazard
Red: High hazard

Areas where this is less successful include:

- The slope roughly centered upon NN 23800 07400, which is known to be one of the highest hazard (and risk) sites in Scotland for debris flow particularly when the proximity of the strategic A83 road is taken into account. The BGS landslide inventory records four events on this slope (Figure 7), although experience indicates that events on this slope have been frequent over the last 20 years – generally between annual and bi-annual.
- The hazards indicated in the region of the Glen Douglas landslide (approximately NN 28000 01000) appear to be low in this area where there has been a long history of reactivation.
- Similarly, the E shore of Loch Shira (NN 11500 09500) which is again an area well-known for its translational slide. Landslides are also shown on the geological map for the area.

Interestingly, the ICG model does highlight elevated hazards in the Cairndow area (NN 19000 11000) which both the SRNLS and GeoSure (Figure 7) models highlight less well.

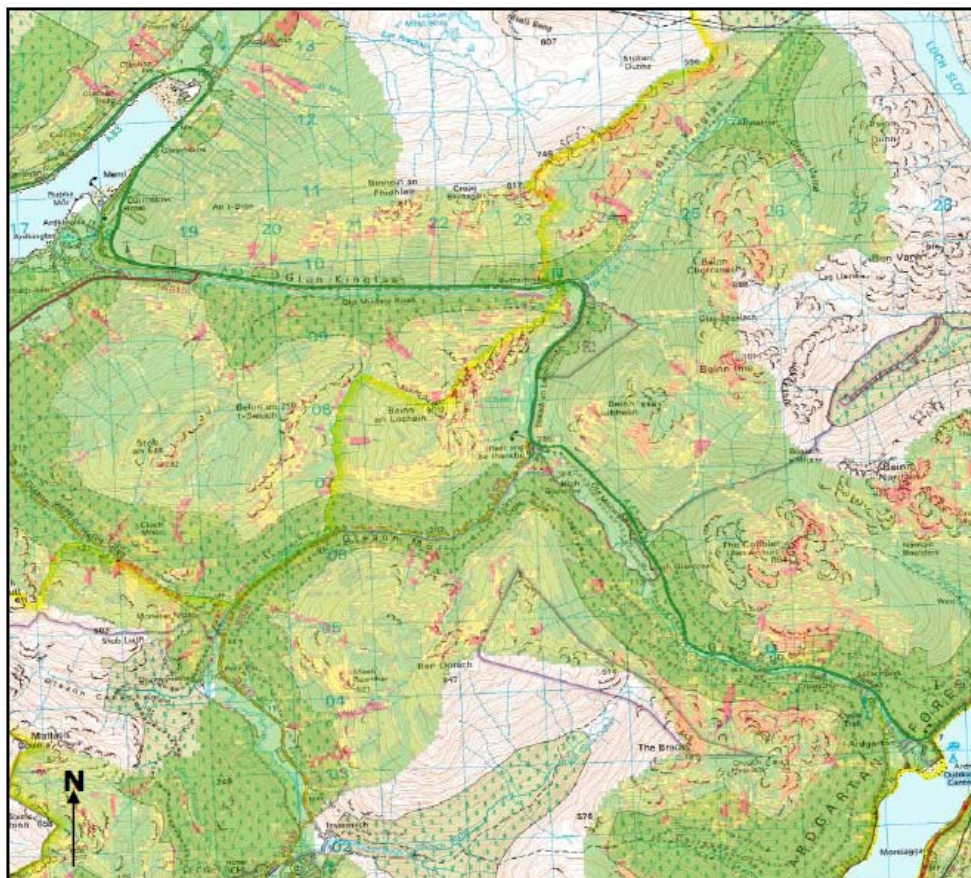


Figure 6. SRNLS GIS Model for the Rest and be Thankful (OS Data ©Crown Copyright. All rights reserved. Transport Scotland 100046668, 2010).

Key: Green: Negligible to low hazard
Yellow/orange: Moderate hazard

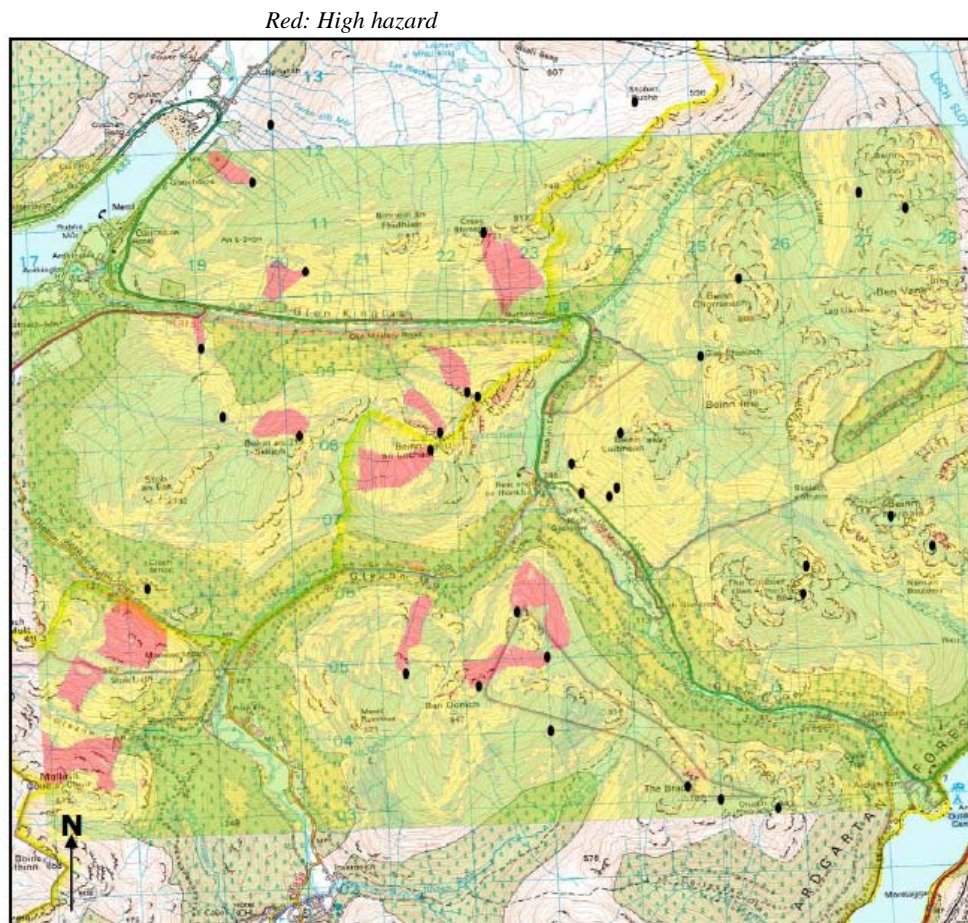


Figure 7. GeoSure extract for the Rest and be Thankful with landslide events recorded in BGS landslide inventory (OS Data ©Crown Copyright. All rights reserved. Transport Scotland 100046668, 2010) (BGS data reproduced with the permission of the British Geological Survey ©NERC. All rights Reserved).

Key: Green: Negligible to low hazard
 Yellow/orange: Moderate hazard
 Red: High hazard
Landslide inventory record

The ICG model (Figure 8) shows relatively slight hazards in the *Glen Ogle* area. Experience and the SRNLS model (Figure 9) contradict this – specifically the two debris flow events of August 2004 that occurred on the eastern slope of the glen and the rock fall events that occurred on the western side of the glen and affected the railway line until it was closed in 1965, in large part due to the risks posed by rock fall. While the BGS inventory shows specific landslides rating to both of the aforementioned GeoSure (Figure 10) follows the ICG model in not specifically highlighting this area as being of high hazard.

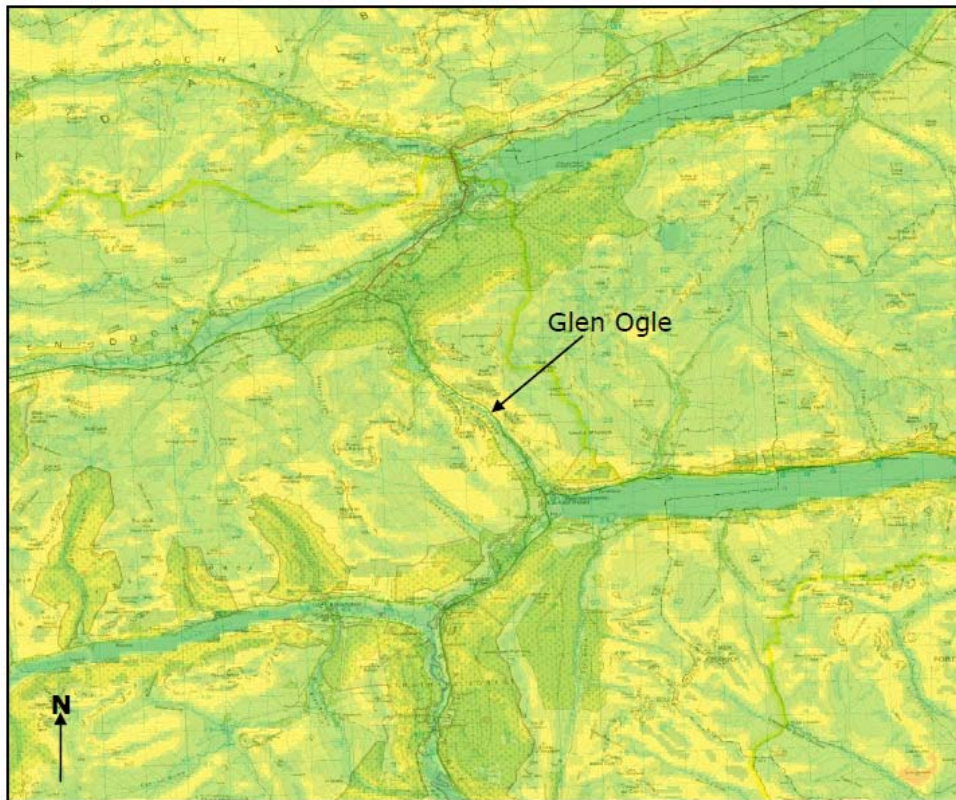


Figure 8. ICG Precipitation Model for Glen Ogle (OS Data ©Crown Copyright. All rights reserved. Transport Scotland 100046668, 2010).

Key: Green: Negligible to low hazard
Yellow/orange: Moderate hazard
Red: High hazard

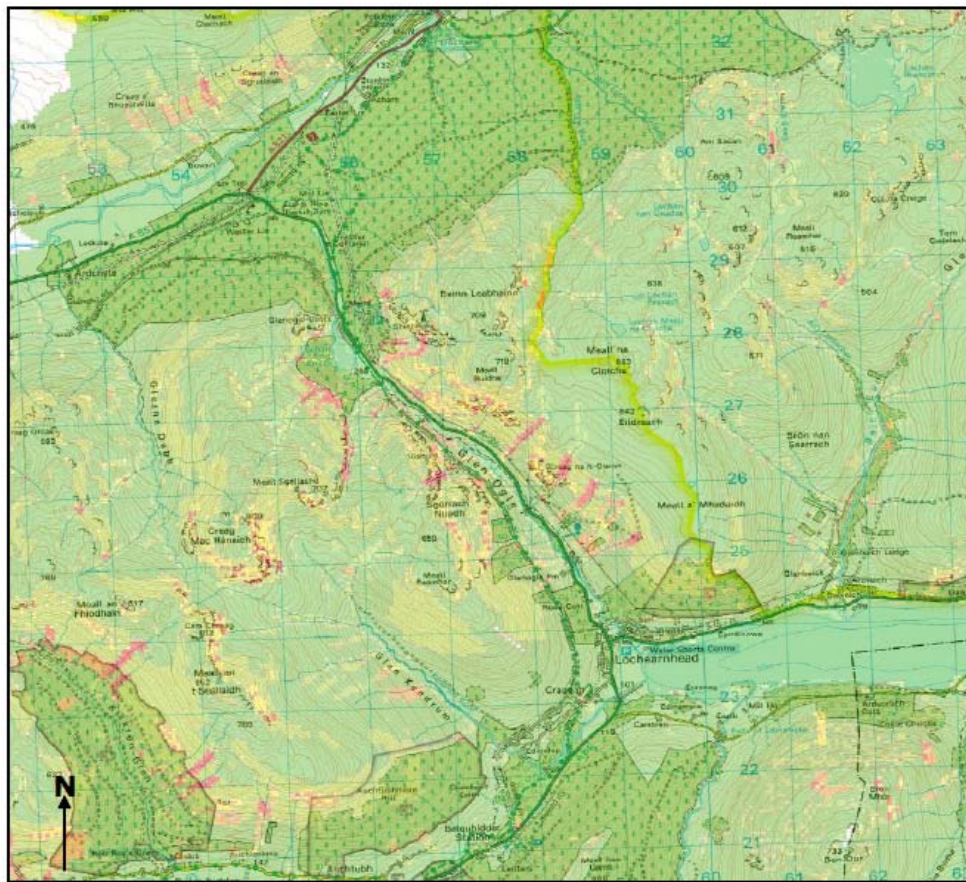


Figure 9. SRNLS GIS Model for Glen Ogle (OS Data ©Crown Copyright. All rights reserved.
Transport Scotland 100046668, 2010).

Key: Green: Negligible to low hazard
Yellow/orange: Moderate hazard
Red: High hazard

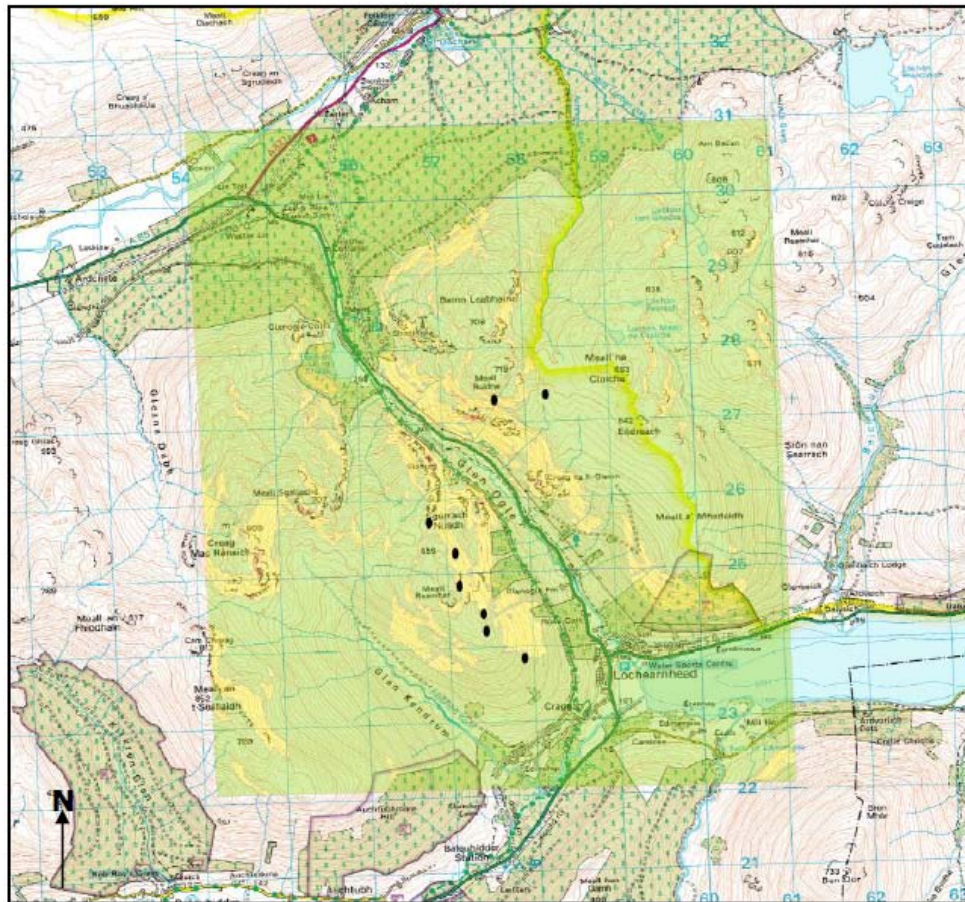


Figure 10. GeoSure extract for Glen Ogle with landslide events recorded in BGS landslide inventory (OS Data ©Crown Copyright. All rights reserved. Transport Scotland 100046668, 2010) (BGS data reproduced with the permission of the British Geological Survey ©NERC. All rights Reserved).

Key: Green: Negligible to low hazard
Yellow/orange: Moderate hazard
Red: High hazard
Landslide inventory record

Unsurprisingly, the ICG (Figure 11) model does not pick-up any form of hazard at the small area of *Bervie Braes* in Stonehaven. This is a very small area with significant hazards and risks relevant to a residential area. Despite its much higher resolution, even the SRNLS (Figure 12) only hints at a hazard in one very small zone at the edge of the high hazard area. Unsurprisingly the GeoSure model (Figure 13) mirrors the ICG model. It is worth-noting that GeoSure is widely recognized as not covering coastal hazards effectively.



Figure 11. ICG Precipitation Model for Bervie Braes (OS Data ©Crown Copyright. All rights reserved. Transport Scotland 100046668, 2010).

Key: Green: Negligible to low hazard
Yellow/orange: Moderate hazard
Red: High hazard



Figure 12. SRNLS GIS Model for Glen Ogle (OS Data ©Crown Copyright. All rights reserved. Transport Scotland 100046668, 2010).

Key: Green: Negligible to low hazard
Yellow/orange: Moderate hazard
Red: High hazard



Figure 13. GeoSure extract for Bervie Braes with landslide events recorded in BGS landslide inventory (OS Data ©Crown Copyright. All rights reserved. Transport Scotland 100046668, 2010) (BGS data reproduced with the permission of the British Geological Survey ©NERC. All rights Reserved).

Key: Green: Negligible to low hazard
Yellow/orange: Moderate hazard
Red: High hazard
Landslide inventory record

11.3.4.1 Discrepancies and Commonalities

We are mindful that we have used relatively small areas to make our assessments. This, in turn, makes it difficult to make generalized statements as to the underlying reasons for discrepancies and commonalities. However, there are no obvious or outstanding reasons relating to *inter alia* geology, geomorphology, water and land cover for these discrepancies and commonalities.

11.3.4.2 Coverage

In general it does seem that approximately the right amount of land is covered by high hazard and the model does seem to broadly highlight the correct regions. However, some obvious and well known features such as the Mam Tor (deep-seated) landslide are omitted and the Isle of Wight Undercliff area and S Wales are somewhat underplayed. Indeed, coastal landslides are not generally well-represented, although we recognize the difficulties inherent in doing so.

The assessment has been undertaken using known hotspots and a visual examination of the model at the national (UK) scale. We also note that there are some unusual artefacts in the imagery that appear to be data led. These manifest as vertical boundaries in N Wales, N Scotland and S England, the latter of which also exhibits a ‘box’. While they appear to be less clear-cut we also noted similar boundaries in the Alpine region.

Similarly, the results appear to give a broadly correct regional distribution at the European scale.

11.3.5 JRC Precipitation Model

While the ICG precipitation model seems to produce a resolution approximating to 100m pixels the resolution of the JRC precipitation model appears to approximate to 500m pixels. This presents particular problems in coastal areas where, for example, entire 1km grid squares have no data assigned.

Given the rather coarse scale of the JRC model it is difficult to make any form of valid comparison in an area such as the *Rest and be Thankful* (Figure 14). While it is fully accepted that the model is intended to be used at a continental scale, some pixels appear entirely within the area of Loch Lomond. Other pixels appear within sea lochs (i.e. offshore) while other pixels forming part of the land mass are not assigned any form of assessment (see NN 14000 08000 for example).

Similarly, in the *Glen Ogle* area high hazard areas are defined within the area of Lochs Earn, Tay and Voil (Figure 15).

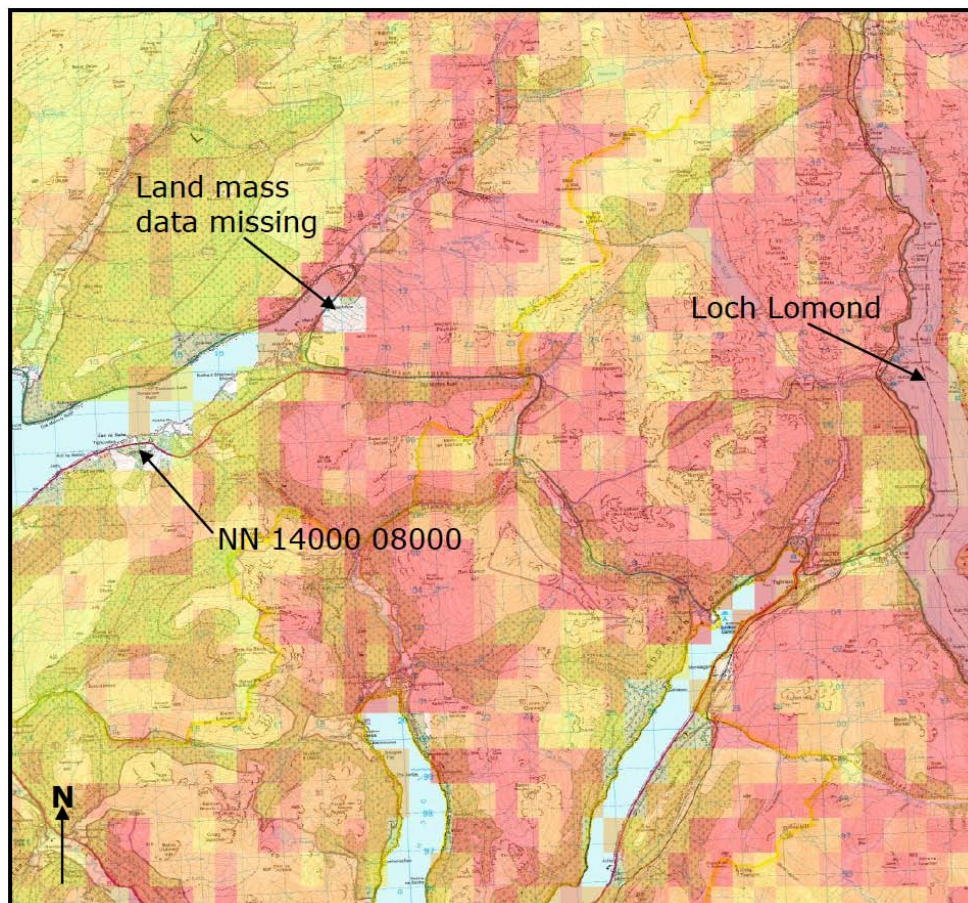


Figure 14. JRC Precipitation Model for *Rest and be Thankful* (OS Data ©Crown Copyright. All rights reserved. Transport Scotland 100046668, 2010).

Key: Green: Negligible to low hazard
Yellow/orange: Moderate hazard
Red: High hazard

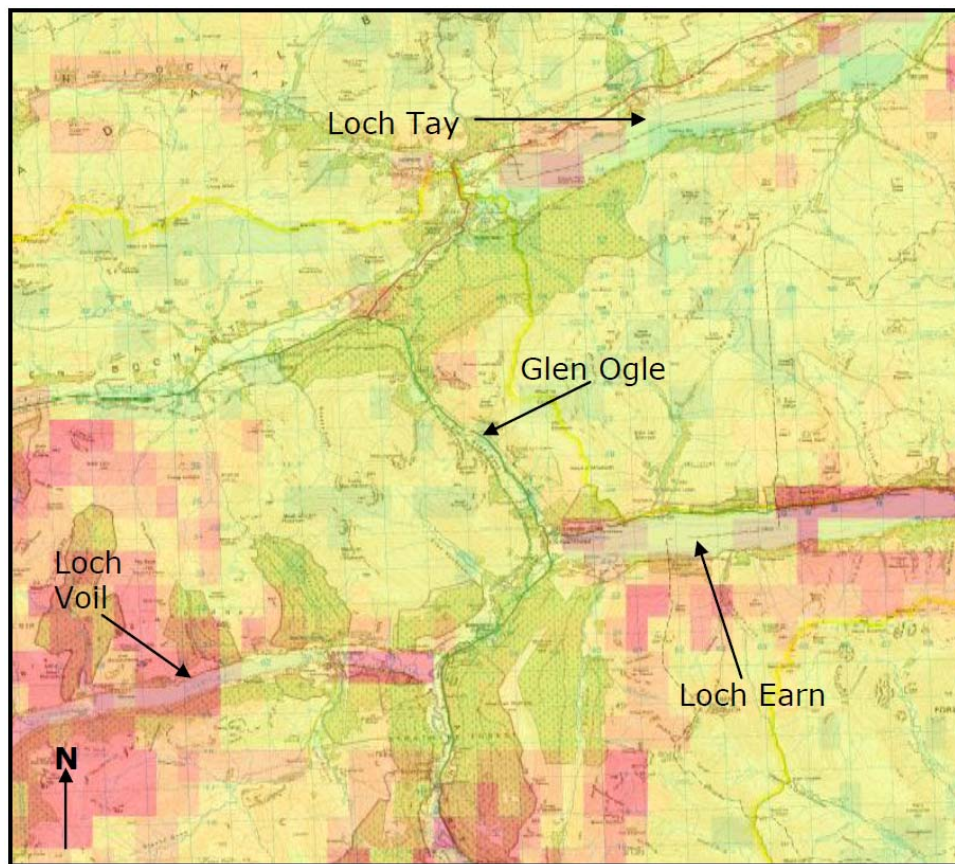


Figure 15. JRC Precipitation Model for Glen Ogle (OS Data ©Crown Copyright. All rights reserved. Transport Scotland 100046668, 2010).

Key: Green: Negligible to low hazard
Yellow/orange: Moderate hazard
Red: High hazard

Setting-aside the issues, raised in the opening paragraph, the JRC model does appear to assign a ‘slight’ hazard to the 1km grid square containing Bervie Braes (Figure 16). This may imply that a high hazard at the specific location has been averaged out across the entire grid square.

11.3.5.1 Discrepancies and Commonalities

The discrepancies noted above seem to be a function of the pixel size/resolution used as much as for any physical reason.

11.3.5.2 Coverage

In general it does seem that too much of parts of the land are covered by high hazards and that others are not expressed in terms of the appropriate hazards. Indeed, the model seems to take a rather ‘all-or-nothing’ approach to the representation of hazards. This does then rather beg the question as to how the model should be used at a national, regional or continental scale.



Figure 16. JRC Precipitation Model for Bervie Braes (OS Data ©Crown Copyright. All rights reserved. Transport Scotland 100046668, 2010).

Key: Green: Negligible to low hazard
Yellow/orange: Moderate hazard
Red: High hazard

Notwithstanding this, the model does seem to broadly highlight the correct regions. However, some obvious and well known features such as the Mam Tor (deep-seated) landslide are not highlighted although an area to the north is highlighted, this could be an area with a high susceptibility to peat slides but it is not entirely clear. Again, setting-aside the issues related to resolution at the coast the model does seem to pick-up on some areas of hazard along the coastal margins of the UK. These include the Isle of Wight Undercliff, albeit that the hazard may be somewhat understated. In some other areas, such as the Suffolk and Essex coasts, it is difficult to understand what might underlie such hazards. Coastal cliff instability, as opposed to erosion unrelated to landslides, along this SE coast is generally not such an issue until one reaches the N Suffolk and Norfolk coasts.

The assessment has been undertaken using known hotspots and a visual examination of the model at the national (UK) scale. We also note that similar to the ICG precipitation model there appear to be some data-lead artifacts which are manifest as vertical and horizontal boundaries. These are most obvious in central Wales and southern Scotland.

Similarly, the results appear to give a broadly correct regional distribution at the European scale – indeed it appears to be a textbook model of hazard areas at a European scale. One would not, however, wish to then use the model for any deeper analysis or interpretation, let alone in the context of planning for example.

11.3.6 ICG Seismic Model

The ICG seismic model shows generally low to non-existent seismic hazards in the three areas used to assess the precipitation models above. Indeed, this low level of hazard is reflected throughout the UK with only parts of north-west Scotland, parts of north-west and south Wales showing any definable, albeit low level of, hazard (Figure 17). This appears to be primarily a reflection of slope angle (unless other topographical features are used within the model) and, possibly, geology.

There is a known record of earthquakes in the Staffordshire area of England (approximately midway between Manchester and Birmingham), although we are not aware of any substantive record of earthquake-induced landslides in the area. The model does not highlight this area and this does seem to indicate, as do other aspects of the model including viewing at the European scale, that the model gives a proportionate view of hazards due to earthquakes.



Figure 17. ICG Seismic Model for UK.
Key: Green: Negligible to low hazard
Yellow/orange: Moderate hazard
Red: High hazard

11.3.7 JRC Seismic Model

The JRC seismic model shows much higher levels of hazard than the ICG model. These are relatively low in the Bervie Braes area, significantly higher in the Glen Ogle area and much higher in the Rest and be Thankful area. These hazards do not align with experience.

Indeed, the hazards as observed at a UK scale simply do not tally with experience or the recorded incidence of earthquakes, let alone earthquake-induced landslides, in Scotland and the rest of the UK (Figure 18). It is difficult to envisage a practical application to which this model might be put. Certainly as a planning tool – at any level be it local, regional or national – it seems most likely to distract from hazards that might pose more realistic risks to communities and the infrastructure by which they are served.

While unlikely to be the case it almost seems, when viewing the data at regional scale, that the ICG model takes some account of the probability of a significant seismic event while the JRC model simply considers the susceptibility to such events (i.e. taking the event as a given). Viewing at the European scale leads to a similar, but nonetheless tentative, conclusion.

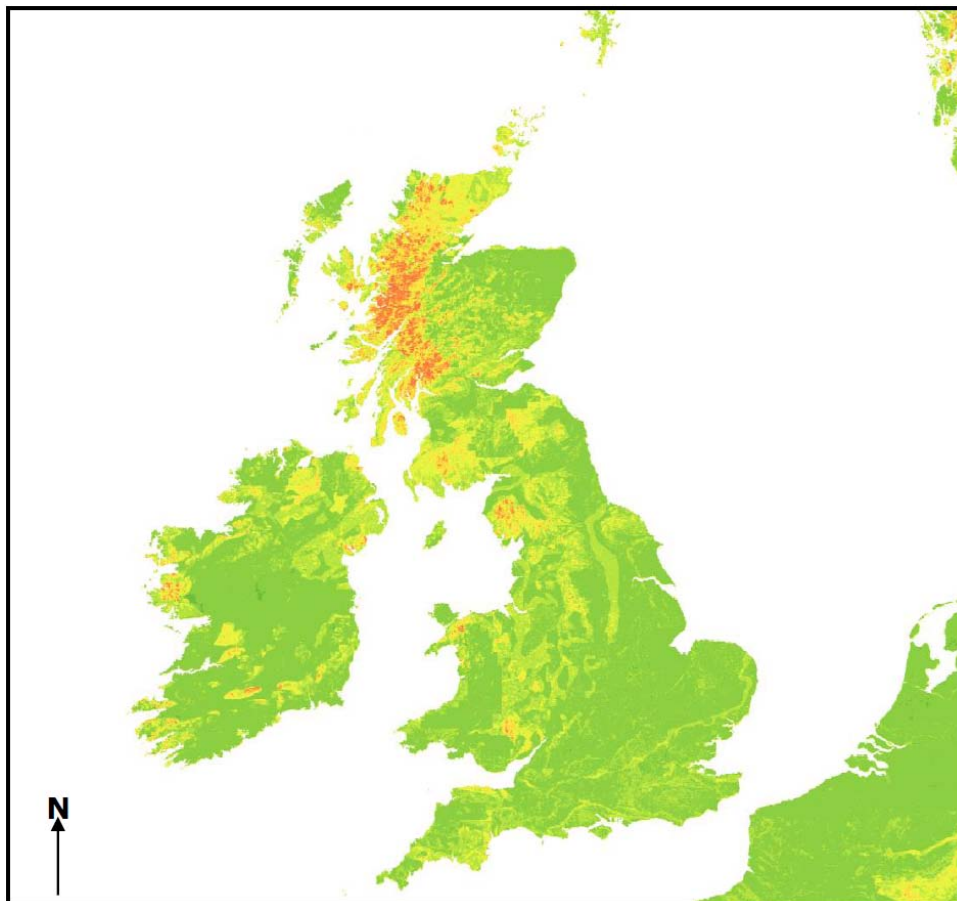


Figure 18. JRC Seismic Model for UK.
Key: Green: Negligible to low hazard
Yellow/orange: Moderate hazard
Red: High hazard

11.3.8 UNIL Rock fall Model

This is a very interesting model as intuitively it is perhaps difficult to conceive of how a continental-scale model for rock fall might be produced.

At *Glen Ogle* the rock fall events that occurred on the western side of the glen and affected the railway line until it was closed in 1965, in large part due to the risks posed by potential further rock fall, are well highlighted; those areas highlighted on the eastern side of the glen do at least coincide with rock outcrop (Figures 19 & 20). If there is a very small point to be raised regarding the model results in this area it might be in relation to whether the runout distance is a little short. This is perhaps best exemplified on the eastern flank of *Creag Mac Hanaich* (NGR NN 55000 25000) (Figure 21).

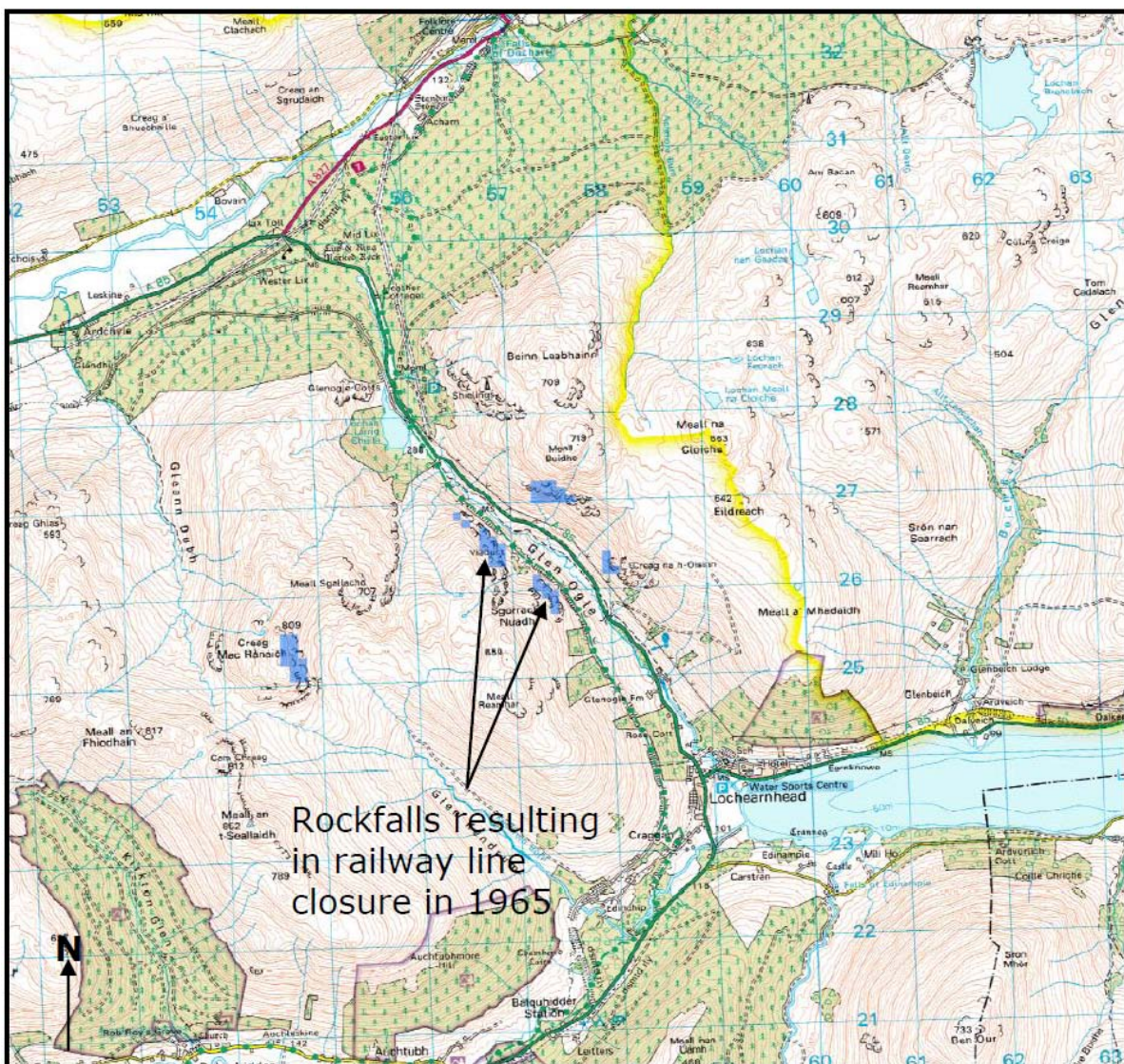


Figure 19. UNIL Rock fall Source Model for Glen Ogle (OS Data ©Crown Copyright. All rights reserved. Transport Scotland 100046668, 2010).

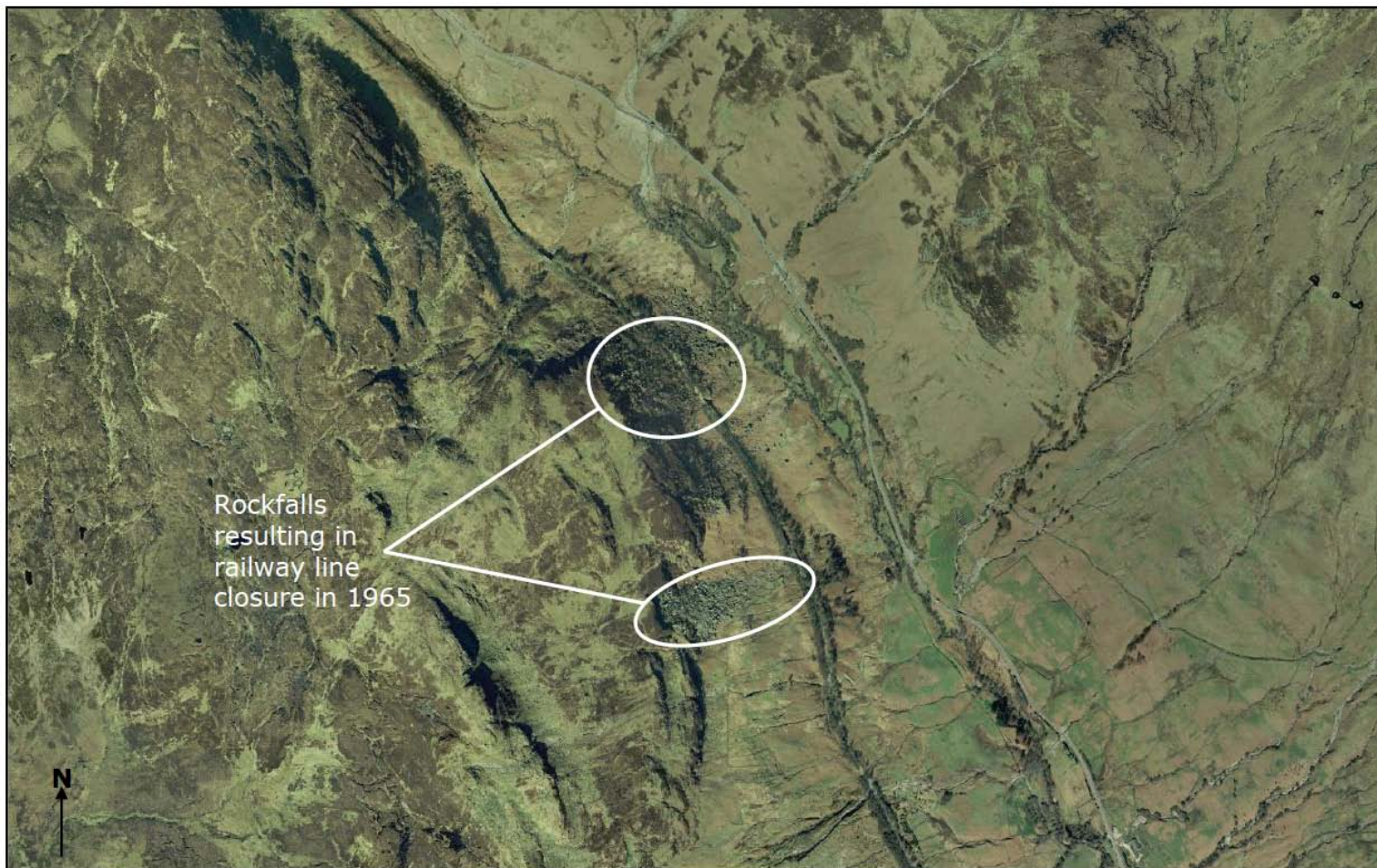


Figure 20. Aerial photograph of historic rock fall in Glen Ogle (Aerial photography imager is Licensed to Transport Scotland for PGA, through Next PerspectivesTM. Permitted use Transport Scotland business only).

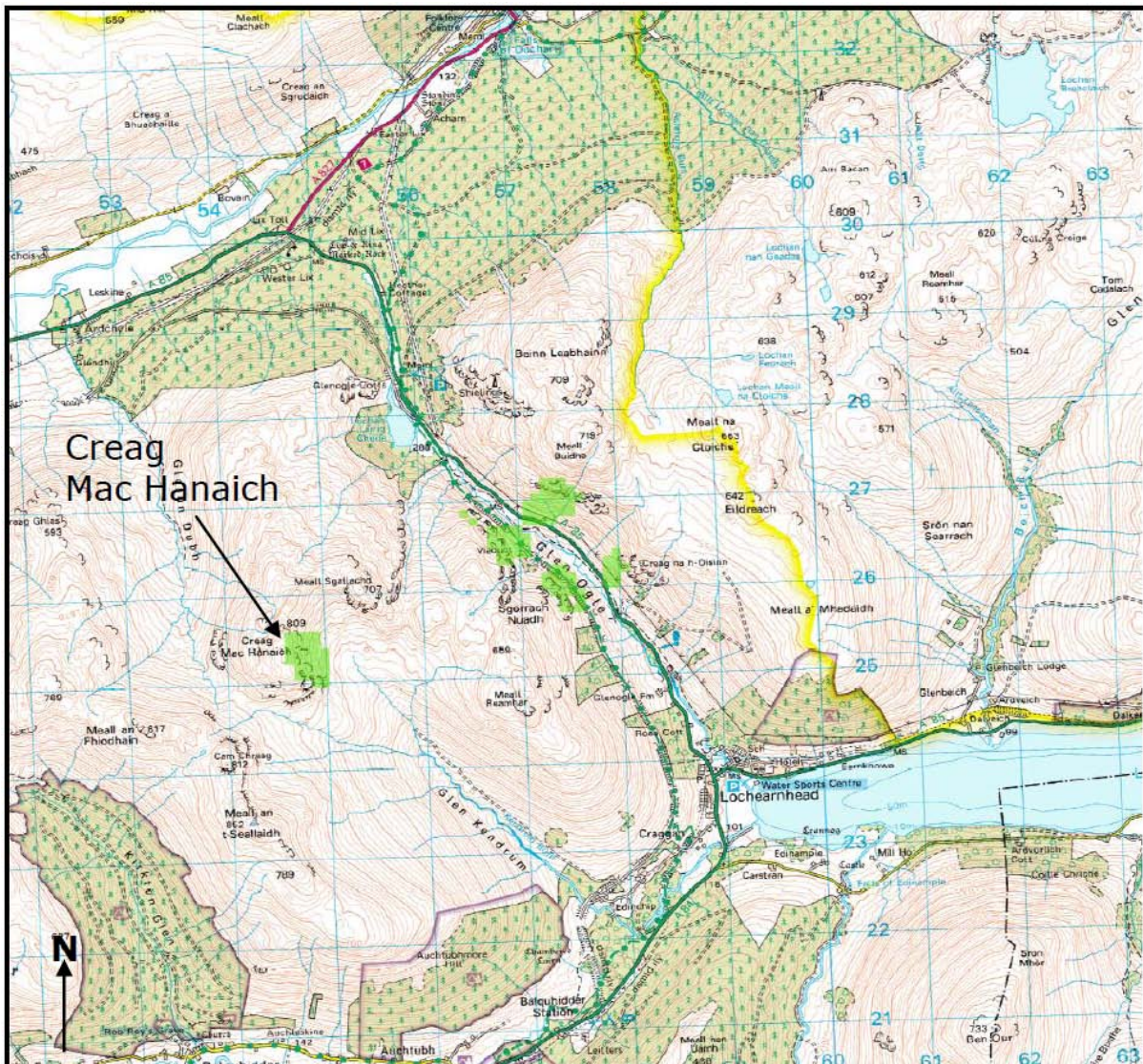


Figure 21. UNIL Rock fall Runout Model for Glen Ogle (OS Data ©Crown Copyright. All rights reserved. Transport Scotland 100046668, 2010).

In the *Rest and be Thankful* area the picture is somewhat more complex. Certainly there are a few areas, including above Glen Kinglas, where rock fall is indicated in locations where there is no outcropping present (Figures 22 & 23). As such, the runout modelling for this area is likely to give spurious results (Figures 24).

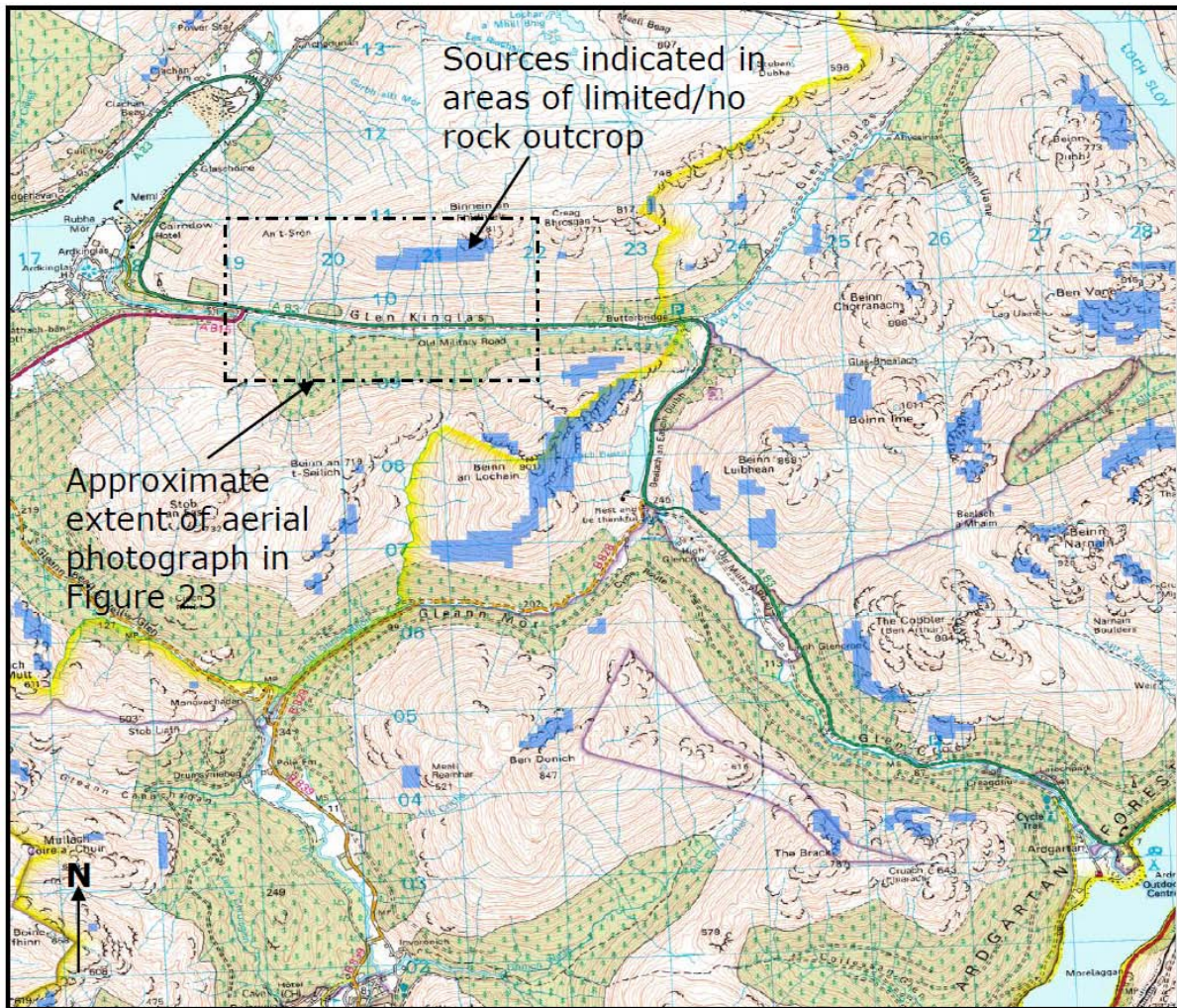


Figure 22. UNIL Rock fall Source Model for the Rest and be Thankful (OS Data ©Crown Copyright. All rights reserved. Transport Scotland 100046668, 2010).



Figure 23. Aerial photograph of Glen Kinglas showing limited to poor rock exposure (Aerial photography imager is Licensed to Transport Scotland for PGA, through Next PerspectivesTM. Permitted use Transport Scotland business only).

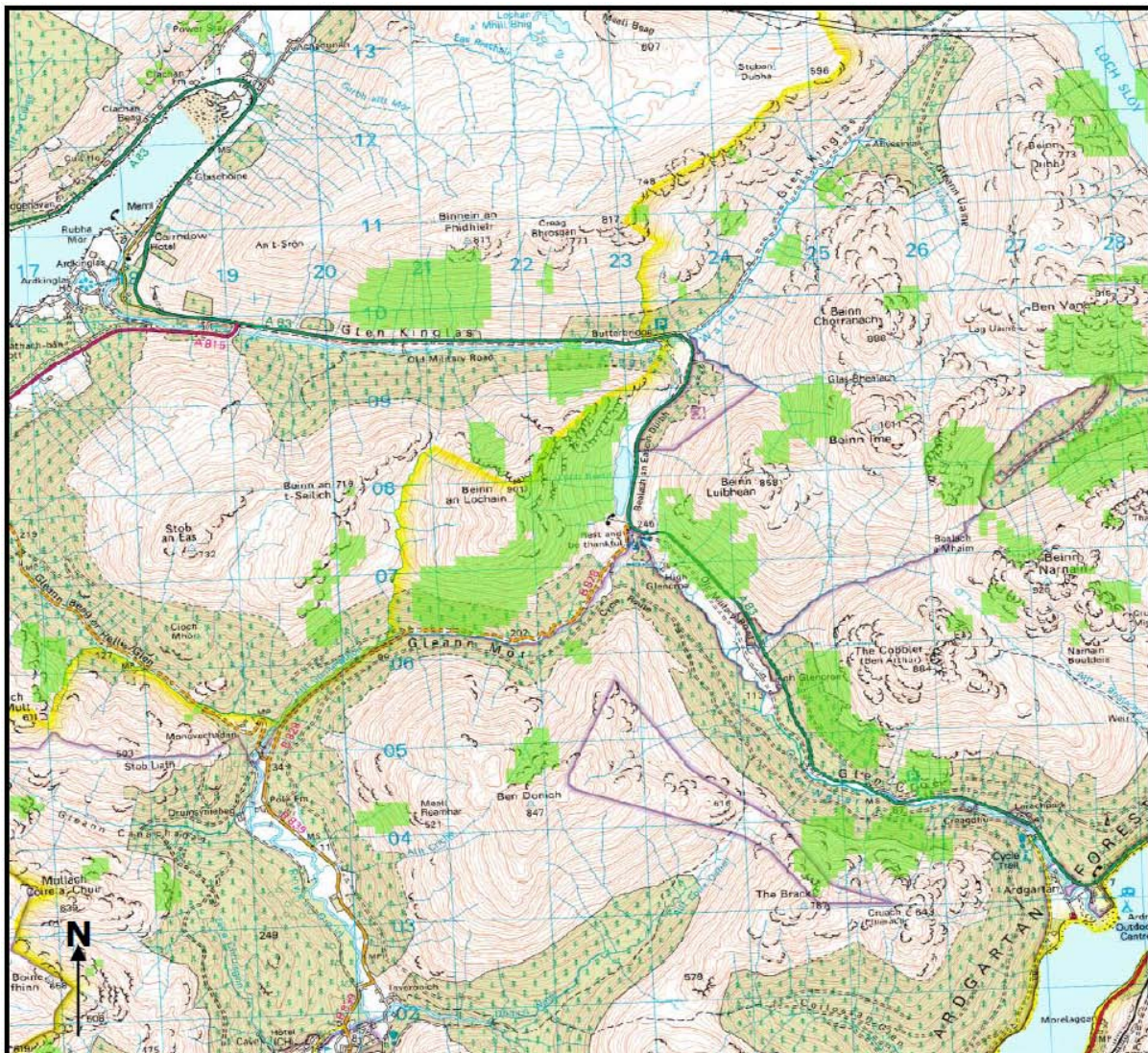


Figure 24. UNIL Rock fall Runout Model for the Rest and be Thankful (OS Data ©Crown Copyright. All rights reserved. Transport Scotland 100046668, 2010).

Unsurprisingly, the model did not highlight any potential source areas for rock fall in the area surrounding Bervie Braes, Stonehaven.

Viewed at Scotland-scale the model broadly reflects experience of rock fall in Scotland, in particular the strategic road routes that were subject to detailed hazard and risk evaluations as part of work undertaken for Transport Scotland during the 1990s. The results of the model are particularly effective along the strategic A82 between Tyndrum, Perthshire and Lochend, Inverness-Shire and along the strategic A87 from Invergarry, Inverness-Shire to Cluanie Inn, Glenmoriston, Inverness-Shire.

11.4 ANSWERS FROM NORWAY (ICG)

The validation of the model results was done by Christian Jaedicke at ICG. Generally one can see that the precipitation hazard is well represented in both models while the seismic hazard is by far overestimated in the JRC model.

- the variations in the ICG seismic data are much too small to be discussed in detail
- the JRC results show a high hazard in northern Norway (Troms), which can not be supported from observed data

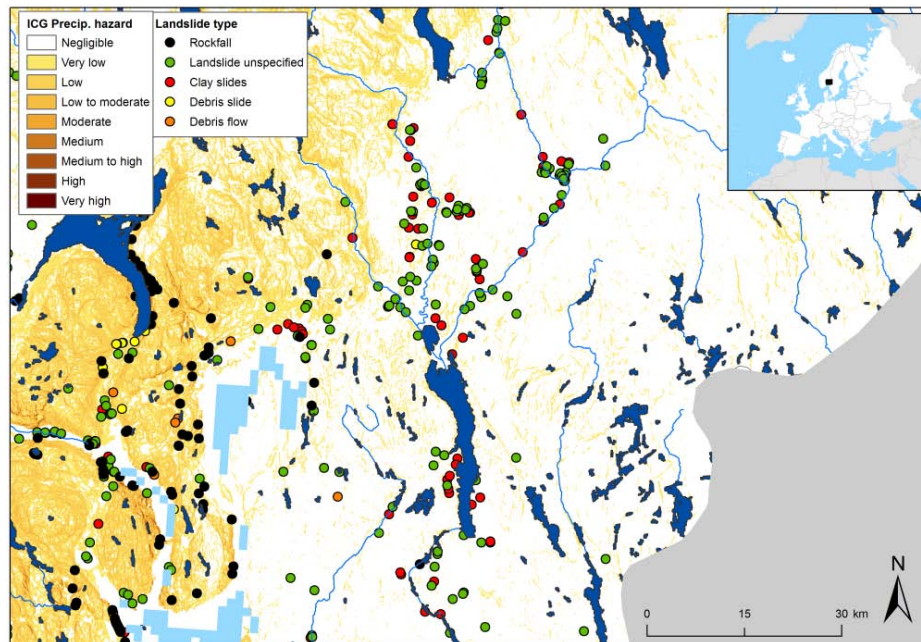


Figure 11-11: Validation of the ICG model in south eastern Norway. Slides in marine sediments in gentle terrain are not well presented in the model results

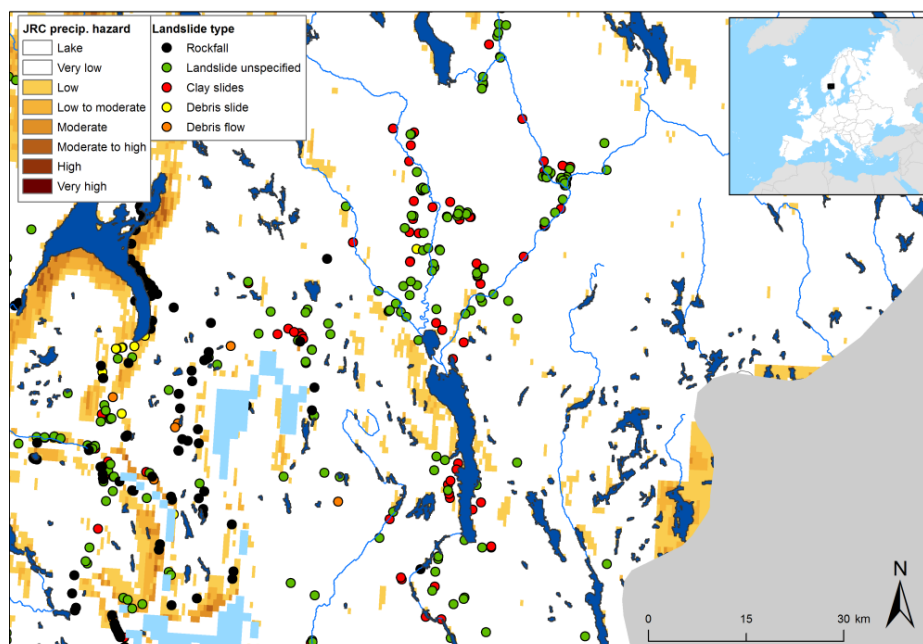


Figure 11-12: Validation of the JRC model for the same area in south eastern Norway.

The UNIL data covers only rock fall susceptibility and gives therefore somewhat less information than the other datasets. It is also limited to < 60° North

Table 11-2: Validation results for the three models' performance in Norway

No	Question	ICG (precip.)	JRC (precip.)	UNIL/ETH
1	Does the hazard map show reasonable hazard levels in the areas where you experience significant/high landslide hazard?	<ul style="list-style-type: none"> On a national scale, the results of the analysis look very good. 	<ul style="list-style-type: none"> Yes, the results fit very well 	<ul style="list-style-type: none"> The map only shows 0/1 areas susceptible to rock fall. Many of the registered rock fall coincident with the model results
2	Find examples for good fit and for areas where the results are bad. Please send us the geographical information for those areas (a shapefile with polygons covering "good areas" and a file with "bad area" polygons)	<ul style="list-style-type: none"> Good fit for rock fall Bad fit for all types of slides along Hardangerfjord and Odda Bad fit for all clay slides in marine sediments Generally less agreement for soil slides and torrents 	<ul style="list-style-type: none"> Fit is generally very good for all types of landslides along the deep fjords and dominant valleys. Hardanger and Odda much better here Seldom that there are slides registered in low hazard areas No hit for the clay slide areas 	<ul style="list-style-type: none"> The south coast from Kristiansand to Oslo is not well covered The western parts in Rogaland show a good fit Totak and Rjukan fit well
3	Do you have any explanation or suggestions why the results are different from your experience?	<ul style="list-style-type: none"> The bed geology is not the dominating factor after slope, but the quaternary geology. 	<ul style="list-style-type: none"> Again it is the missing data for the soils that causes the problems 	<ul style="list-style-type: none"> It seems that a certain minimum slope height have exist to yield rock fall in the model
4	Where are typical areas that show good results (any special geology, water ways, land cover etc.)?	<ul style="list-style-type: none"> Steep terrain, mainly bare rock, affected streets also in steep terrain 	<ul style="list-style-type: none"> Along the most relevant water ways and valleys 	<ul style="list-style-type: none"> High steep mountain sides
5	Where are typical areas that show poor results (any special geology, water ways, land cover etc.)?	<ul style="list-style-type: none"> Less steep terrain with glacier, marine and fluvial depositions 	<ul style="list-style-type: none"> Less steep terrain and coastal areas in southern Norway (mainly rock fall from very small slopes) 	<ul style="list-style-type: none"> Small and minor slopes in the south in the country
6	In total, is too much land covered by high hazard or too little? Does this even out on a national basis?	<ul style="list-style-type: none"> The marine sediment areas of south east and mid Norway are not sufficiently covered. Else, the coverage is in good agreement with the recorded events. 	<ul style="list-style-type: none"> On first glance too high hazard in many areas, but the registered events are well covered On second view, things look good also for areas with less terrain in Trøndelag 	<ul style="list-style-type: none"> Seems to cover too little of the actual hazard areas No national analysis possible
7	Do you have special hotspots in your country? Is the hazard map reasonably correct for these areas?	<ul style="list-style-type: none"> West Norway, very good fit North Norway, less good Gudbrandsdalen, ok agreement in the lower scales of hazard 	<ul style="list-style-type: none"> West Norway, very good fit North Norway, very good fit Gudbrandsdalen good Rock fall around the coast, not too good 	<ul style="list-style-type: none"> Inner parts of Rogaland are well covered
8	What is your overall impression? Are the results applicable on a European scale?	<ul style="list-style-type: none"> In Norway, most events are recorded along the transportation networks and no data is available in the terrain. The model often hits the events directly or, where the hit area is far from the release area, is close by. On a national scale, the result is good. 	<ul style="list-style-type: none"> The hazard maps look very good, also when high hazard themes to be to prominent at first glance. This model hits much more often the runout areas, where the registrations are actually done. 	<ul style="list-style-type: none"> It seems the model covers well large slopes (>200m fall height) and less well minor and small slopes that in fact produce many of the rock falls in Norway.

12 APPENDIX D – MODEL RESULTS

The results from all three models will be listed in tables for one model each. In addition a fact sheet for the most affected countries is made available here.

The same methods for counting exposed area, people and infrastructure is used applying GIS methods. It was accounted for change in pixel size due to changes in Latitude (by projecting the data on area true projections and other complications that are caused by the size of the project area. The numbers were checked against national overviews by the UN, the world fact book and wikipedia. The results of the counting are within 5% of the values from the other sources both for population and land area.

12.1 RESULTS FROM THE ICG MODEL

Nr.	Name of country	Capital	Area UN (km ²)	Population UN 2005	Density (per km ²)	Area							Population						
						Total grid (km ²)	Negligible (km ²)	Low (km ²)	Medium (km ²)	High (km ²)	Exposed (km ²)	Exposed %	Total grid	Negligible	Low	Medium	High	Exposed total	Exposed %
1	Albania	Tirana	28 748	3 111 000	108	28 733	9 837	10 293	7 635	968	4 287	14.9%	3 111 000	1 566 418	857 167	612 249	75 165	344 556	11.1%
2	Andorra	Andorra la Vella	468	80 000	171	455	333	122	0	0	12	2.7%	80 000	65 446	14 554	0	0	1 455	1.8%
3	Austria	Vienna	83 858	8 232 000	98	83 867	50 264	26 727	5 970	906	5 370	6.4%	8 232 000	6 326 796	1 488 417	338 748	78 039	328 505	4.0%
4	Belarus	Minsk	207 600	9 816 000	47	206 853	206 631	221	1	0	23	0.0%	9 816 000	9 795 914	19 655	431	0	2 095	0.0%
5	Belgium	Brussels	30 510	10 415 000	341	30 710	30 442	267	1	0	27	0.1%	10 415 000	10 358 569	56 093	338	0	5 711	0.1%
6	Bosnia and Herzegovina	Sarajevo	51 129	3 781 000	74	51 068	32 705	14 851	3 316	196	2 676	5.2%	3 781 000	2 408 099	1 093 277	263 541	16 083	204 473	5.4%
7	Bulgaria	Sofia	110 910	7 739 000	70	112 227	98 064	13 564	599	0	1 536	1.4%	7 739 000	7 001 353	704 674	32 973	0	80 359	1.0%
8	Croatia	Zagreb	56 542	4 443 000	79	56 920	42 989	9 743	3 839	349	2 475	4.3%	4 443 000	3 666 713	535 098	202 439	38 749	152 991	3.4%
9	Cyprus	Nicosia	9 251	836 000	90	9 253	6 118	1 844	1 001	290	774	8.4%	836 000	742 895	63 111	26 542	3 451	17 725	2.1%
10	Czech Republic	Prague	78 866	10 195 000	129	78 679	74 145	3 827	702	6	599	0.8%	10 195 000	9 654 202	475 170	64 928	701	67 696	0.7%
11	Denmark	Copenhagen	43 094	5 417 000	126	44 493	43 576	724	187	6	135	0.3%	5 417 000	5 379 002	31 728	6 063	207	5 199	0.1%
12	Estonia	Tallinn	45 226	1 347 000	30	45 434	45 432	2	0	0	0	0.0%	1 347 000	1 346 752	248	0	0	25	0.0%
13	Finland	Helsinki	336 593	5 244 000	16	337 245	337 233	12	0	0	1	0.0%	5 244 000	5 243 995	5	0	0	1	0.0%
14	France	Paris	547 030	61 013 000	112	549 344	481 217	50 904	15 496	1 726	11 466	2.1%	61 013 000	57 123 613	3 076 452	752 618	60 317	593 747	1.0%
15	Germany	Berlin	357 021	82 409 000	231	357 411	340 755	14 686	1 556	415	2 350	0.7%	82 409 000	79 826 353	2 382 937	163 777	35 933	323 359	0.4%
16	Greece	Athens	131 940	11 064 000	84	132 171	80 276	31 262	17 080	3 553	11 803	8.9%	11 064 000	9 241 567	1 191 415	530 471	100 547	378 830	3.4%
17	Hungary	Budapest	93 030	10 078 000	108	92 927	90 230	2 606	91	0	288	0.3%	10 078 000	9 738 591	325 439	13 970	0	36 735	0.4%
18	Iceland	Reykjavik	103 000	296 000	3	102 564	81 868	12 772	6 104	1 820	4 929	4.8%	296 000	231 087	35 269	27 226	2 418	14 113	4.8%
19	Ireland	Dublin	70 280	4 187 000	60	70 114	67 194	2 505	416	0	375	0.5%	4 187 000	4 143 394	39 314	4 292	0	5 219	0.1%
20	Italy	Rome	301 230	58 645 000	195	300 445	183 846	80 795	33 428	2 376	20 484	6.8%	58 645 000	46 277 055	8 273 475	3 676 037	418 433	2 348 592	4.0%
21	Kosovo	Pristina	10 908	1 804 000	165	10 920	7 837	2 610	466	7	407	3.7%	1 804 000	1 355 133	382 636	65 180	1 051	58 869	3.3%
22	Latvia	Riga	64 589	2 292 000	35	64 673	64 665	8	0	0	1	0.0%	2 292 000	2 291 083	917	0	0	92	0.0%
23	Liechtenstein	Vaduz	160	35 000	219	161	45	19	48	49	65	40.4%	35 000	14 415	4 314	7 686	8 585	11 322	32.3%
24	Lithuania	Vilnius	65 200	3 416 000	52	65 005	64 976	30	0	0	3	0.0%	3 416 000	3 410 399	5 551	51	0	570	0.0%
25	Luxembourg	Luxembourg	2 586	464 000	179	2 571	2 486	86	0	0	9	0.3%	464 000	448 213	15 787	0	0	1 579	0.3%
26	Republic of Macedonia	Skopje	25 713	2 035 000	79	24 827	18 012	6 473	341	0	750	3.0%	2 035 000	1 680 348	338 618	16 034	0	38 672	1.9%
27	Malta	Valletta	316	403 000	1 275	71	56	11	4	1	3	4.1%	403 000	329 151	56 120	16 403	1 326	11 859	2.9%
28	Moldova	Chişinău	33 843	3 759 000	111	33 813	32 239	1 552	22	0	162	0.5%	3 759 000	3 632 779	124 217	2 004	0	13 023	0.3%
29	Monaco	Monaco	2	32 000	16 410	15	4	3	6	1	3	22.0%	32 000	17 845	3 611	8 334	2 210	5 071	15.8%
30	Montenegro	Podgorica	13 812	625 000	45	13 326	4 615	4 692	2 979	1 040	2 403	18.0%	625 000	294 132	186 919	107 019	36 930	87 728	14.0%
31	Netherlands	Amsterdam	41 526	16 316 000	393	36 474	36 465	9	0	0	1	0.0%	16 316 000	16 310 827	5 173	0	0	5 17	0.0%
32	Norway	Oslo	324 220	4 635 000	14	351 401	302 205	42 412	6 327	457	6 596	1.9%	4 635 000	4 268 163	332 836	32 901	1 099	44 253	1.0%
33	Poland	Warsaw	312 685	38 198 000	122	312 139	305 404	6 025	701	9	822	0.3%	38 198 000	37 394 978	690 151	111 338	1 533	103 949	0.3%
34	Portugal	Lisbon	91 568	10 547 000	115	90 737	70 783	16 751	2 862	341	2 875	3.2%	10 547 000	8 885 101	1 321 745	282 001	58 153	274 928	2.6%
35	Romania	Bucharest	248 391	21 635 000	91	247 433	190 278	43 449	3 602	103	5 529	2.3%	21 635 000	19 169 386	2 278 840	181 267	5 507	287 771	1.3%
36	Russia	Moscow	3 960 000	143 170 000	36	3 847 455	3 799 600	44 038	3 713	104	5 622	0.1%	143 170 000	140 912 276	2 010 422	241 352	5 950	279 398	0.2%
37	San Marino	San Marino	61	30 000	492	61	44	16	1	0	2	3.2%	30 000	21 792	7 644	564	0	933	3.1%
38	Serbia	Belgrade	88 361	9 856 000	112	77 923	67 344	9 915	647	18	1 204	1.5%	9 856 000	8 855 861	942 568	56 111	1 460	112 550	1.1%
39	Slovakia	Bratislava	48 845	5 386 000	110	49 093	36 840	10 737	1 472	43	1 559	3.2%	5 386 000	4 401 233	836 983	143 099	4 685	131 313	2.4%
40	Slovenia	Ljubljana	20 273	2 001 000	99	19 980	11 096	6 013	2 389	482	1 800	9.0%	2 001 000	1 464 589	383 042	133 413	19 956	98 284	4.9%
41	Spain	Madrid	504 851	40 264 000	80	505 922	412 568	77 206	14 549	1 598	13 684	2.7%	40 264 000	34 220 037	4 492 791	1 286 907	264 265	1 099 616	2.7%
42	Sweden	Stockholm	449 964	9 066 000	20	449 702	446 393	3 307	2	0	331	0.1%	9 066 000	9 061 560	4 362	78	0	460	0.0%
43	Switzerland	Bern	41 290	7 441 000	180	41 355	19 421	15 771	5 671	490	3 769	9.1%	7 441 000	5 310 470	1 653 543	440 387	36 604	334 073	4.5%
44	Ukraine	Kiev	603 700	46 936 000	78	602 188	579 786	20 116	2 286	1	2 698	0.4%	46 936 000	45 338 665	1 423 839	172 956	539	194 810	0.4%
45	United Kingdom	London	244 820	60 261 000	246	245 797	224 785	17 139	3 810	62	2 919	1.2%	60 261 000	59 358 923	832 017	69 923	137	104 316	0.2%
	Europe		9 874 010	728 955 000		9 773 956	9 001 104	606 114	149 320	17 418	122 825	1.3%	728 955 000	678 585 178	38 998 141	10 091 646	1 280 035	8 207 343	1.1%

12.2 RESULTS FROM THE JRC MODEL

12.3 NATIONAL FACT SHEETS

Tables as shown in section 12.1 and 12.2 are often difficult to read. For this purpose, individual fact sheet for selected countries were made. The sheets present the total number of inhabitants, road and railway network kilometres and the number of people and infrastructure exposed to landslide hazard. The table only reproduces the results for precipitation-induced landslides, while the two maps show the precipitation as well as the earthquake-induced landslide hazard.

It is important to note that the results are highly controversial and total numbers should not be used in detailed discussions. The results are meant to give an impression of the landslide hazard and risk in each country in the order of magnitude, not in more detail.



Albania

Capital: Tirana

Areas

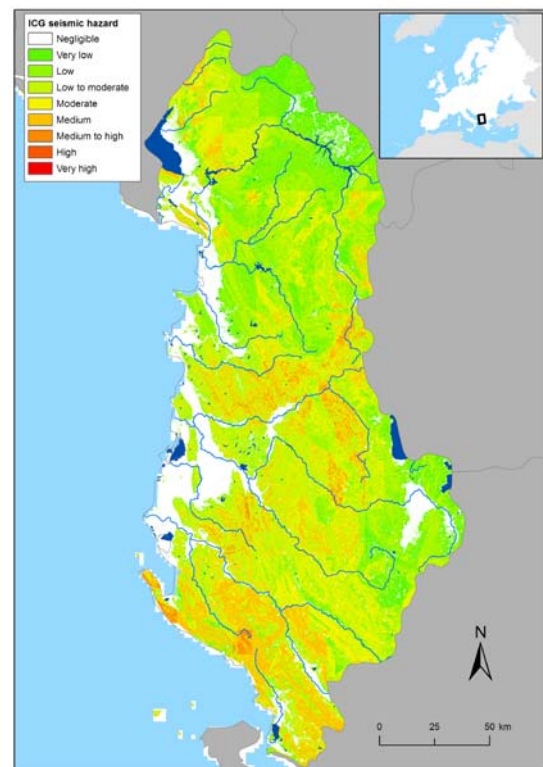
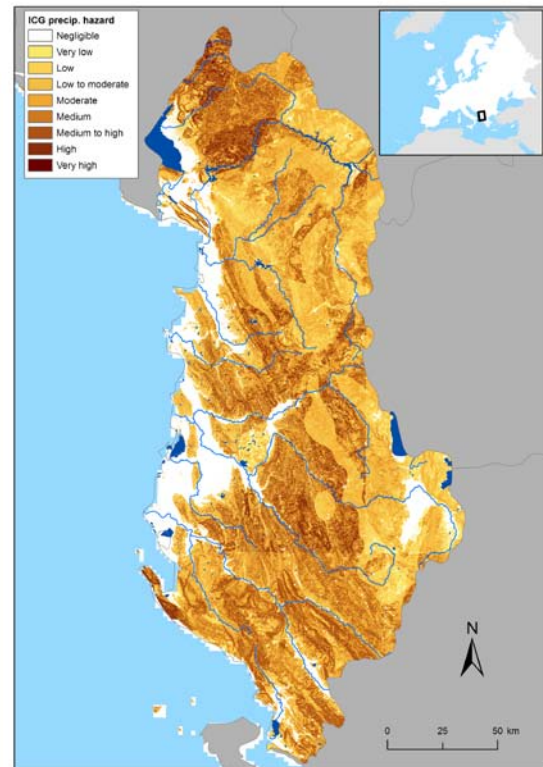
[km ²]	ICG	JRC
Total	28 700	28 300
Low hazard	10 300	9 300
Medium hazard	7 600	4 800
High hazard	1 000	2 700
Exposed	4 300	5 100
Exposed percent	14.9%	18%

Exposed population

No. people	ICG	JRC
Total population	3111000	3111000
Low hazard	857000	724000
Medium hazard	612000	311000
High hazard	75000	138000
Total exposed	345000	304000
Exposed percent	11.1%	9.8%

Infrastructure

[km]	ICG	JRC
Total roads	1 800	1 800
Roads Low hazard	600	500
Roads Medium hazard	400	300
Roads High hazard	100	100
Roads exposed percent	13.5%	12.9%
Total railways	1 000	1 000
Railways Low hazard	300	300
Railways Medium hazard	100	100
Railways High hazard	0	0
Railways exp. percent	10.6%	7.1%





Andorra

Capital: Andorra la Vella

Areas

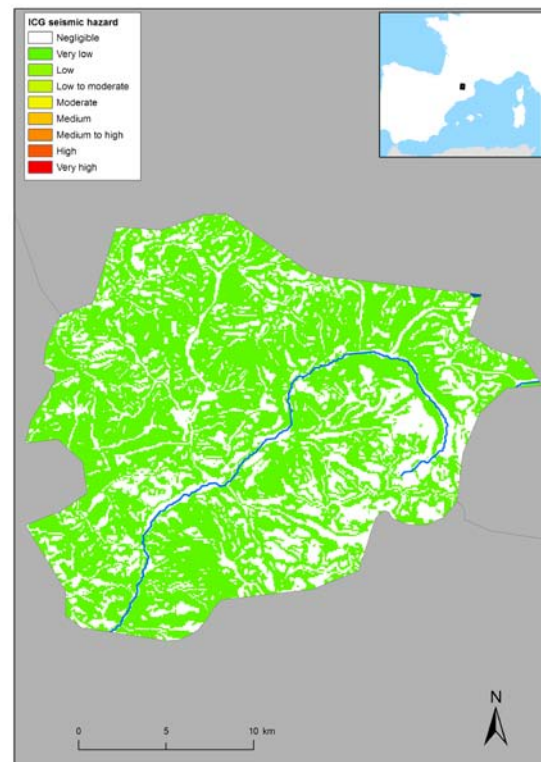
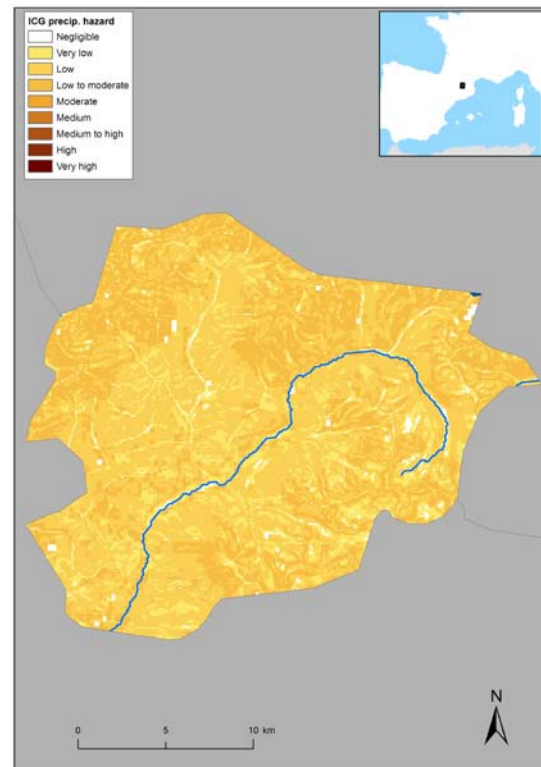
[km ²]	ICG	JRC
Total	500	500
Low hazard	100	200
Medium hazard	0	100
High hazard	0	0
Exposed	0	100
Exposed percent	2.7%	11.6%

Exposed population

No. people	ICG	JRC
Total population	80000	80000
Low hazard	15000	28000
Medium hazard	0	33000
High hazard	0	0
Total exposed	1000	13000
Exposed percent	1.8%	15.8%

Infrastructure

[km]	ICG	JRC
Total roads	200	200
Roads Low hazard	100	100
Roads Medium hazard	0	100
Roads High hazard	0	0
Roads exposed percent	5.1%	15.5%
Total railways	0	0
Railways Low hazard	0	0
Railways Medium hazard	0	0
Railways High hazard	0	0
Railways exp. percent	0%	0%





Austria

Capital: Vienna

Areas

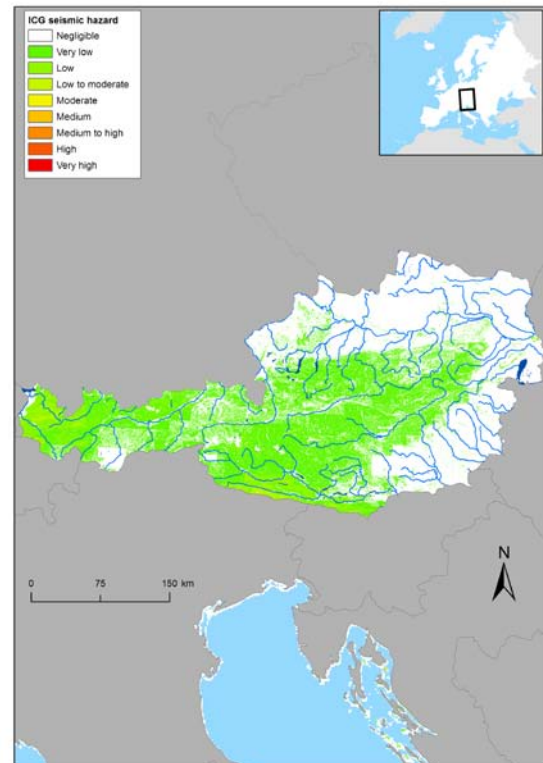
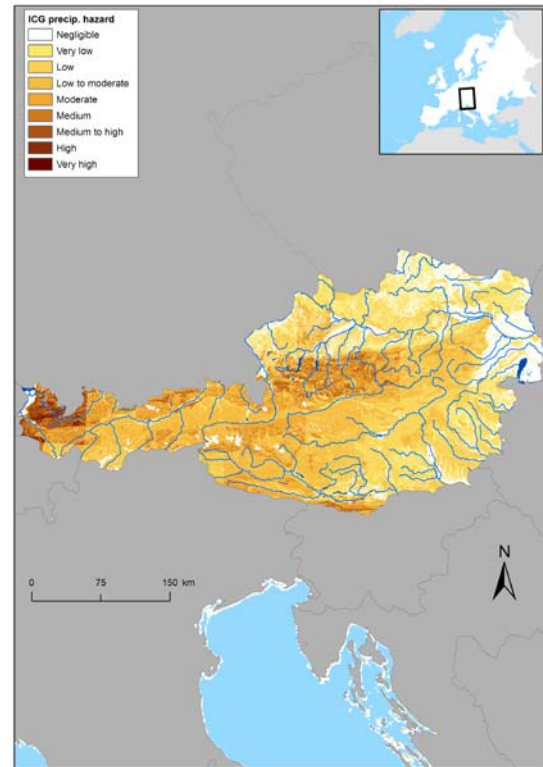
[km ²]	ICG	JRC
Total	83 900	83 900
Low hazard	26 700	23 100
Medium hazard	6 000	18 200
High hazard	900	8 300
Exposed	5 400	16 100
Exposed percent	6.4%	19.2%

Exposed population

No. people	ICG	JRC
Total population	8232000	8232000
Low hazard	1488000	1671000
Medium hazard	339000	828000
High hazard	78000	446000
Total exposed	329000	861000
Exposed percent	4%	10.5%

Infrastructure

[km]	ICG	JRC
Total roads	25 800	25 800
Roads Low hazard	8 100	6 000
Roads Medium hazard	2 100	3 400
Roads High hazard	300	1 800
Roads exposed percent	6.8%	13.3%
<hr/>		
Total railways	11 400	11 400
Railways Low hazard	3 000	2500
Railways Medium hazard	900	1500
Railways High hazard	100	800
Railways exp. percent	5.5%	13.7%





Belgium

Capital: Brussels

Areas

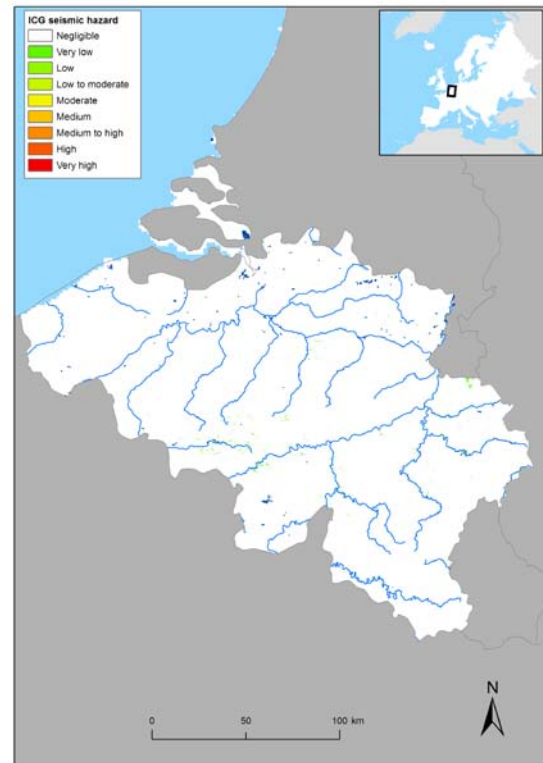
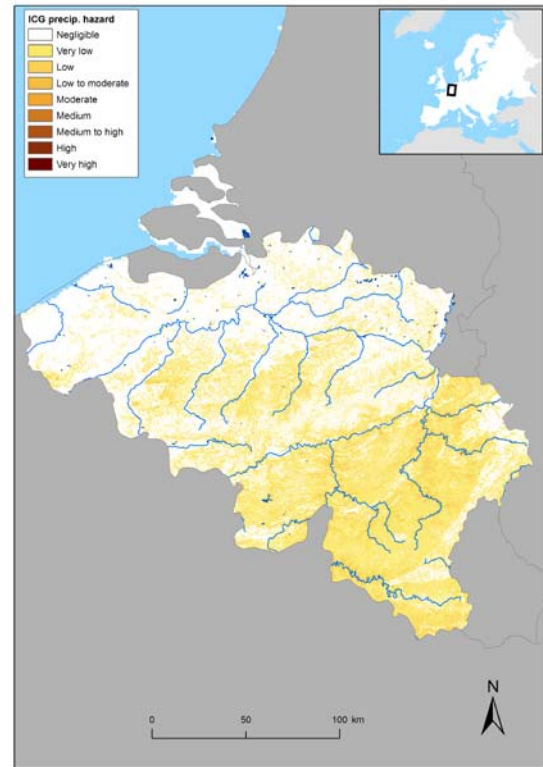
[km ²]	ICG	JRC
Total	30 700	30 700
Low hazard	300	3 800
Medium hazard	0	0
High hazard	0	0
Exposed	0	400
Exposed percent	0.1%	1.3%

Exposed population

No. people	ICG	JRC
Total population	10415000	10415000
Low hazard	56000	541000
Medium hazard	0	1000
High hazard	0	0
Total exposed	6000	54000
Exposed percent	0.1%	0.5%

Infrastructure

[km]	ICG	JRC
Total roads	15 800	15 700
Roads Low hazard	700	1 800
Roads Medium hazard	0	0
Roads High hazard	0	0
Roads exposed percent	0.4%	1.2%
Total railways	8 100	8 100
Railways Low hazard	500	800
Railways Medium hazard	0	0
Railways High hazard	0	0
Railways exp. percent	0.7%	1%



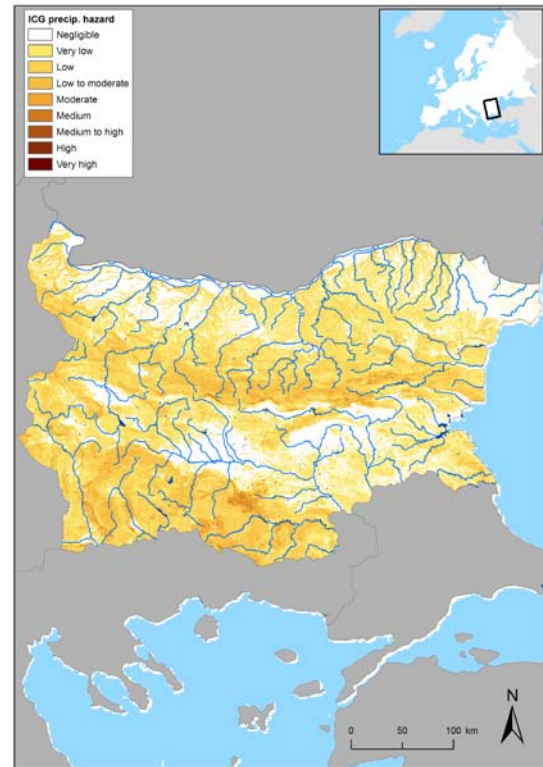


Bulgaria

Capital: Sofia

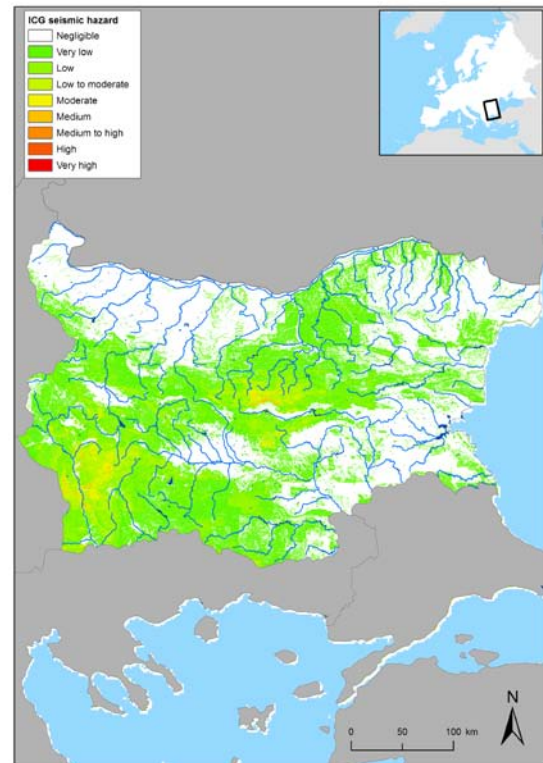
Areas

[km ²]	ICG	JRC
Total	112 200	112 100
Low hazard	13 600	31 900
Medium hazard	600	6 200
High hazard	0	0
Exposed	1 500	5 100
Exposed percent	1.4%	4.5%



Exposed population

No. people	ICG	JRC
Total population	7739000	7739000
Low hazard	705000	1591000
Medium hazard	33000	366000
High hazard	0	0
Total exposed	80000	269000
Exposed percent	1%	3.5%



Infrastructure

[km]	ICG	JRC
Total roads	7 700	7 700
Roads Low hazard	1 100	1 600
Roads Medium hazard	100	200
Roads High hazard	0	0
Roads exposed percent	1.8%	3%
Total railways	8 600	8 600
Railways Low hazard	1 200	1500
Railways Medium hazard	100	100
Railways High hazard	0	0
Railways exp. percent	1.7%	2.2%



Czech Republic

Capital: Prague

Areas

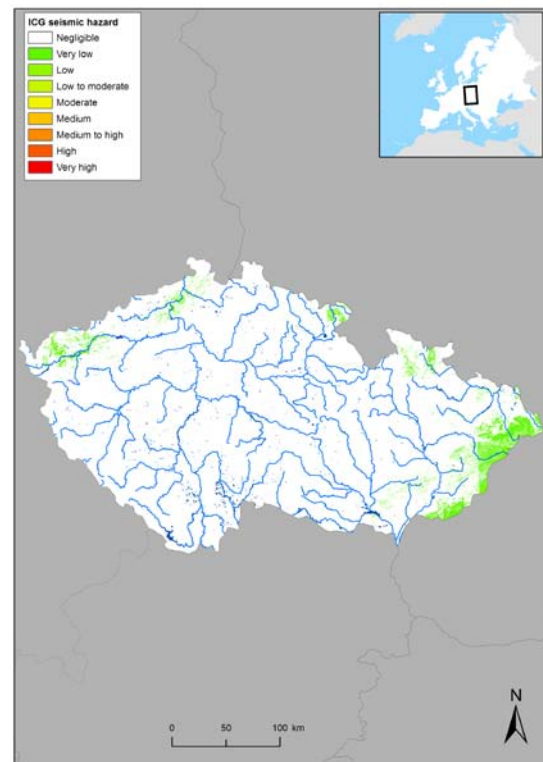
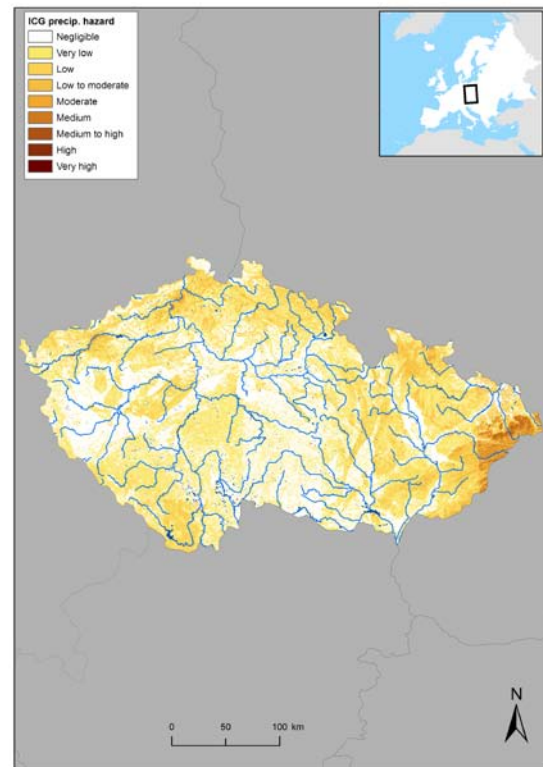
[km ²]	ICG	JRC
Total	78 700	78 700
Low hazard	3 800	20 100
Medium hazard	700	700
High hazard	0	0
Exposed	600	2 200
Exposed percent	0.8%	2.8%

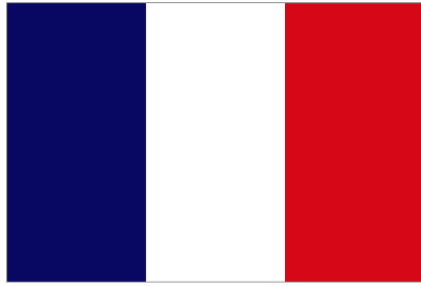
Exposed population

No. people	ICG	JRC
Total population	10195000	10195000
Low hazard	475000	2476000
Medium hazard	65000	57000
High hazard	1000	0
Total exposed	68000	265000
Exposed percent	0.7%	2.6%

Infrastructure

[km]	ICG	JRC
Total roads	23 500	23 500
Roads Low hazard	2 100	5 600
Roads Medium hazard	200	100
Roads High hazard	0	0
Roads exposed percent	1.2%	2.5%
Total railways	20 500	20 500
Railways Low hazard	2 500	5300
Railways Medium hazard	300	100
Railways High hazard	0	0
Railways exp. percent	1.7%	2.8%





France

Capital: Paris

Areas

[km ²]	ICG	JRC
Total	549 300	547 400
Low hazard	50 900	80 800
Medium hazard	15 500	25 800
High hazard	1 700	8 500
Exposed	11 500	24 300
Exposed percent	2.1%	4.4%



Exposed population

No. people	ICG	JRC
Total population	61013000	61013000
Low hazard	3076000	6713000
Medium hazard	753000	915000
High hazard	60000	270000
Total exposed	594000	1216000
Exposed percent	1%	2%



Infrastructure

[km]	ICG	JRC
Total roads	151 100	150 400
Roads Low hazard	19 200	22 400
Roads Medium hazard	6 500	4 500
Roads High hazard	700	1 700
Roads exposed percent	3%	3.5%
Total railways	66 800	66 600
Railways Low hazard	7 700	9500
Railways Medium hazard	1 900	1400
Railways High hazard	200	600
Railways exp. percent	2.4%	3%



Germany

Capital: Berlin

Areas

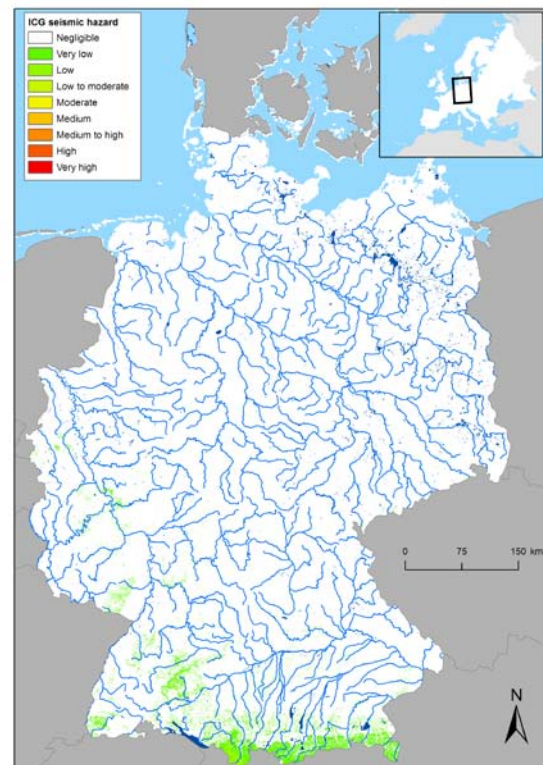
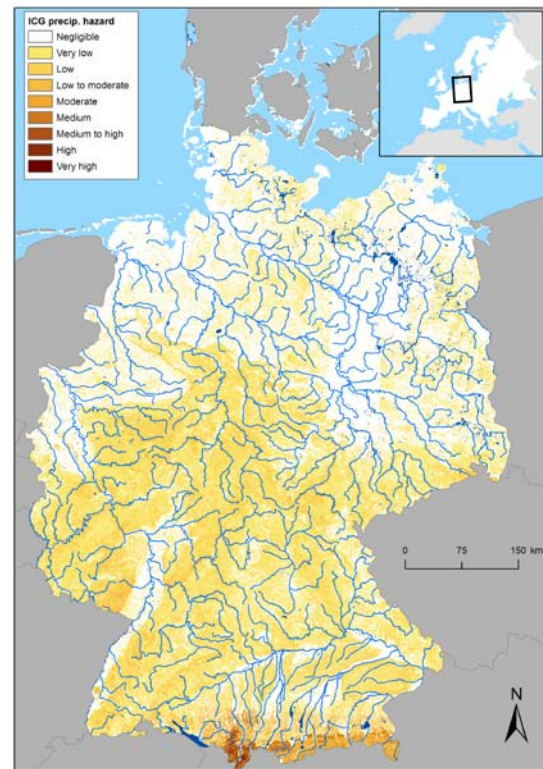
[km ²]	ICG	JRC
Total	357 400	356 300
Low hazard	14 700	29 400
Medium hazard	1 600	2 400
High hazard	400	800
Exposed	2 400	4 500
Exposed percent	0.7%	1.3%

Exposed population

No. people	ICG	JRC
Total population	82409000	82409000
Low hazard	2383000	5481000
Medium hazard	164000	225000
High hazard	36000	81000
Total exposed	323000	696000
Exposed percent	0.4%	0.8%

Infrastructure

[km]	ICG	JRC
Total roads	170 200	170 100
Roads Low hazard	18 200	14 700
Roads Medium hazard	1 000	500
Roads High hazard	200	100
Roads exposed percent	1.3%	1%
Total railways	84 300	84 300
Railways Low hazard	9 500	7100
Railways Medium hazard	500	200
Railways High hazard	100	100
Railways exp. percent	1.4%	1%





Greece

Capital: Athens

Areas

[km ²]	ICG	JRC
Total	132 200	128 500
Low hazard	31 300	50 200
Medium hazard	17 100	21 400
High hazard	3 600	2 900
Exposed	11 800	14 300
Exposed percent	8.9%	11.2%

Exposed population

No. people	ICG	JRC
Total population	11064000	11064000
Low hazard	1191000	2628000
Medium hazard	530000	732000
High hazard	101000	74000
Total exposed	379000	557000
Exposed percent	3.4%	5%

Infrastructure

[km]	ICG	JRC
Total roads	19 600	18 800
Roads Low hazard	3 800	6 200
Roads Medium hazard	2 600	2 100
Roads High hazard	900	300
Roads exposed percent	10.4%	8.2%
Total railways	4 900	4 700
Railways Low hazard	500	800
Railways Medium hazard	200	200
Railways High hazard	0	0
Railways exp. percent	3.3%	3.2%





Italy

Capital: Rome

Areas

[km ²]	ICG	JRC
Total	300 400	297 900
Low hazard	80 800	84 200
Medium hazard	33 400	45 200
High hazard	2 400	19 100
Exposed	20 500	41 000
Exposed percent	6.8%	13.8%



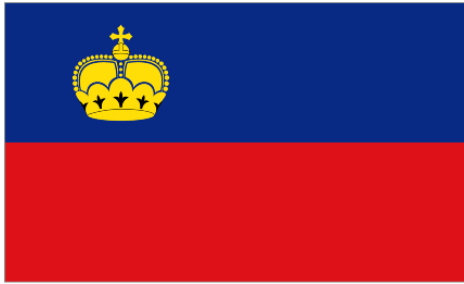
Exposed population

No. people	ICG	JRC
Total population	58645000	58645000
Low hazard	8273000	10584000
Medium hazard	3676000	4062000
High hazard	418000	1411000
Total exposed	2349000	3688000
Exposed percent	4%	6.3%



Infrastructure

[km]	ICG	JRC
Total roads	75 700	74 800
Roads Low hazard	17 100	17 400
Roads Medium hazard	11 600	8 000
Roads High hazard	1 400	3 600
Roads exposed percent	8.7%	10.3%
Total railways	35 800	35 100
Railways Low hazard	6 100	7200
Railways Medium hazard	3 700	2700
Railways High hazard	600	1200
Railways exp. percent	6.4%	7.8%

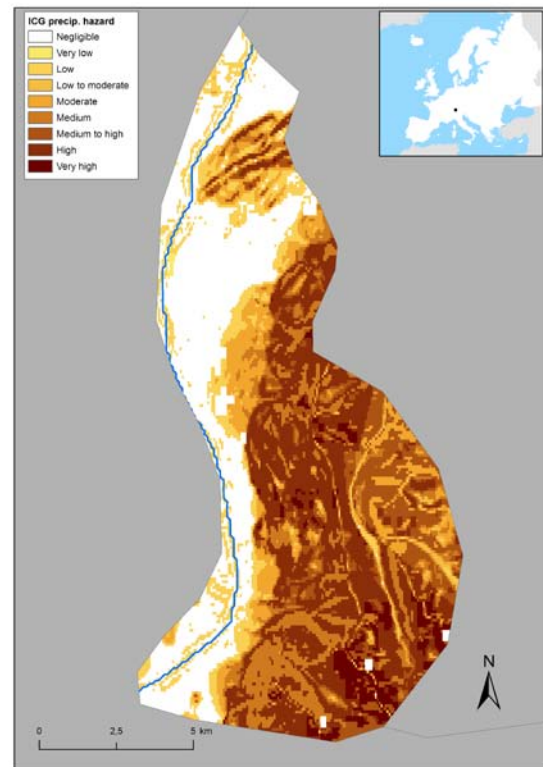


Liechtenstein

Capital: Vaduz

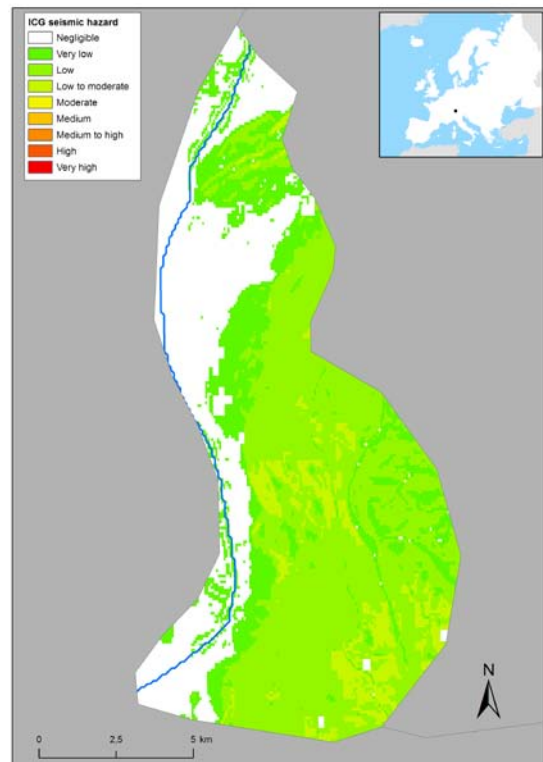
Areas

[km ²]	ICG	JRC
Total	200	200
Low hazard	0	0
Medium hazard	0	0
High hazard	0	100
Exposed	100	100
Exposed percent	40.4%	65%



Exposed population

No. people	ICG	JRC
Total population	35000	35000
Low hazard	4000	9000
Medium hazard	8000	4000
High hazard	9000	20000
Total exposed	11000	22000
Exposed percent	32.3%	64.3%



Infrastructure

[km]	ICG	JRC
Total roads	100	100
Roads Low hazard	0	0
Roads Medium hazard	0	0
Roads High hazard	0	0
Roads exposed percent	16.4%	48.1%
Total railways	0	0
Railways Low hazard	0	0
Railways Medium hazard	0	0
Railways High hazard	0	0
Railways exp. percent	13.8%	74.5%



Montenegro

Capital: Podgorica

Areas

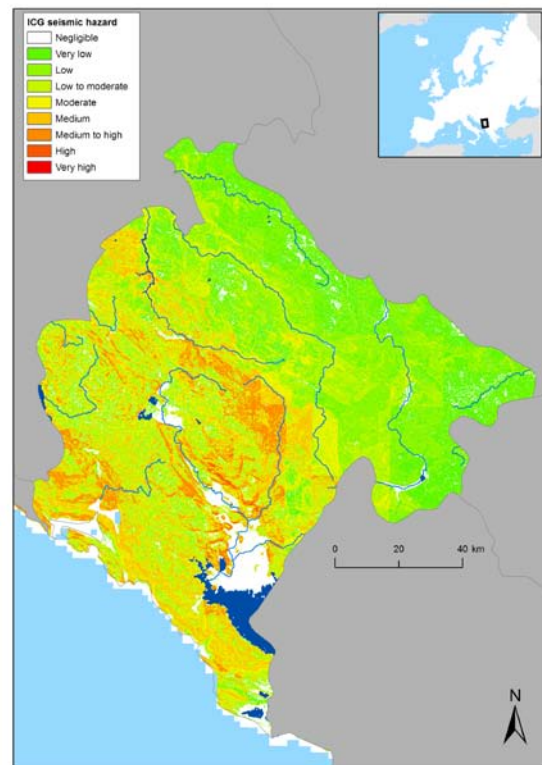
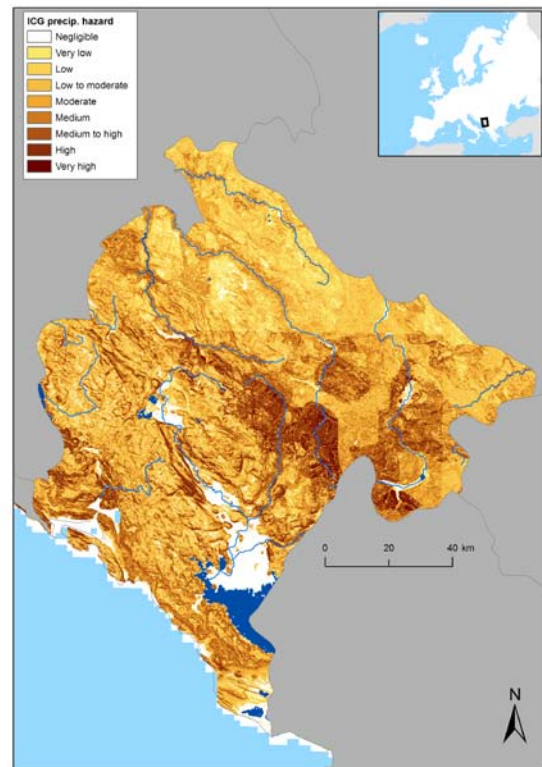
[km ²]	ICG	JRC
Total	13 300	13 200
Low hazard	4 700	7 400
Medium hazard	3 000	2 700
High hazard	1 000	2 000
Exposed	2 400	3 600
Exposed percent	18%	27.2%

Exposed population

No. people	ICG	JRC
Total population	625000	625000
Low hazard	187000	373000
Medium hazard	107000	84000
High hazard	37000	62000
Total exposed	88000	125000
Exposed percent	14%	20%

Infrastructure

[km]	ICG	JRC
Total roads	1 100	1 100
Roads Low hazard	200	600
Roads Medium hazard	400	200
Roads High hazard	200	200
Roads exposed percent	33.6%	30.5%
Total railways	800	800
Railways Low hazard	100	400
Railways Medium hazard	200	200
Railways High hazard	200	200
Railways exp. percent	40%	33.4%





Netherlands

Capital: Amsterdam

Areas

[km ²]	ICG	JRC
Total	36 500	34 900
Low hazard	0	200
Medium hazard	0	0
High hazard	0	0
Exposed	0	0
Exposed percent	0%	0%



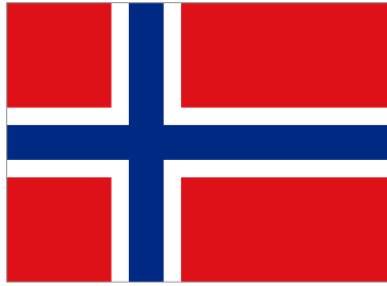
Exposed population

No. people	ICG	JRC
Total population	16316000	16316000
Low hazard	5000	18000
Medium hazard	0	0
High hazard	0	0
Total exposed	1000	2000
Exposed percent	0%	0%



Infrastructure

[km]	ICG	JRC
Total roads	29 600	29 200
Roads Low hazard	0	100
Roads Medium hazard	0	0
Roads High hazard	0	0
Roads exposed percent	0%	0%
Total railways	5 500	5 500
Railways Low hazard	0	0
Railways Medium hazard	0	0
Railways High hazard	0	0
Railways exp. percent	0%	0%



Norway

Capital: Oslo

Areas

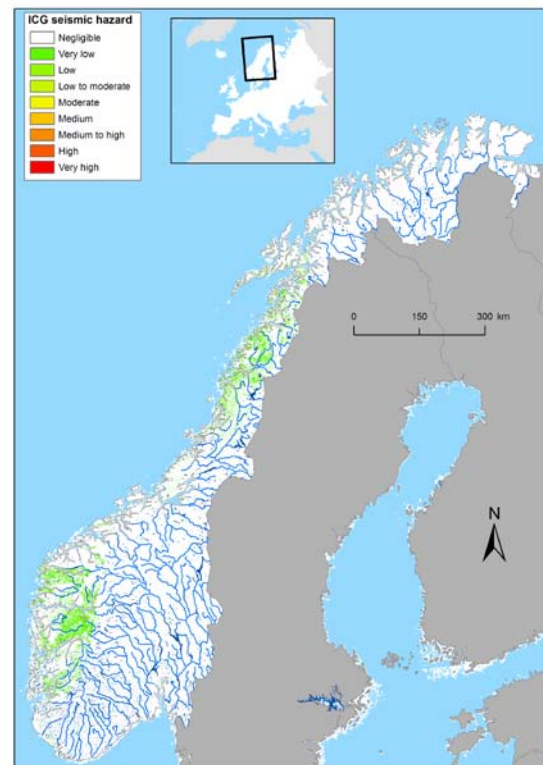
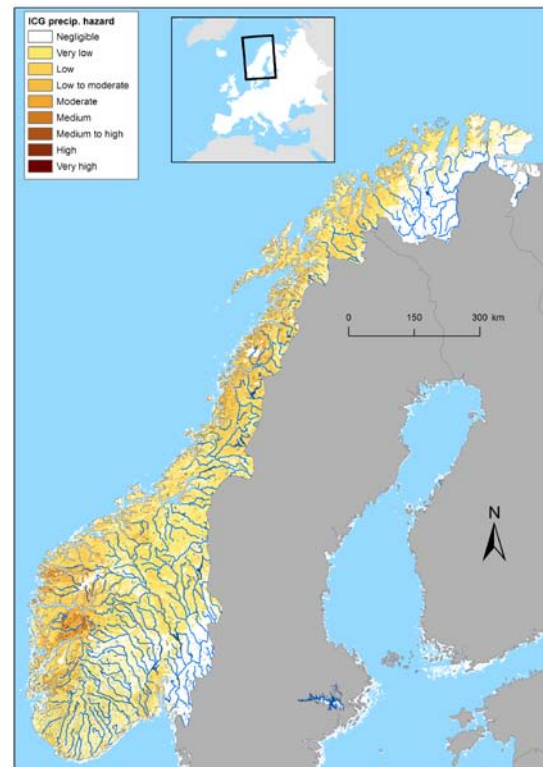
[km ²]	ICG	JRC
Total	351 400	316 500
Low hazard	42 400	120 300
Medium hazard	6 300	43 900
High hazard	500	15 500
Exposed	6 600	40 700
Exposed percent	1.9%	12.9%

Exposed population

No. people	ICG	JRC
Total population	4635000	4635000
Low hazard	333000	1046000
Medium hazard	33000	263000
High hazard	1000	92000
Total exposed	44000	276000
Exposed percent	1%	6%

Infrastructure

[km]	ICG	JRC
Total roads	48 300	37 900
Roads Low hazard	5 400	11 500
Roads Medium hazard	800	4 500
Roads High hazard	0	3 100
Roads exposed percent	2.2%	14.7%
Total railways	10 200	9 300
Railways Low hazard	1 300	2600
Railways Medium hazard	300	1400
Railways High hazard	100	400
Railways exp. percent	2.8%	11.7%





Portugal

Capital: Lisbon

Areas

[km ²]	ICG	JRC
Total	90 700	91 000
Low hazard	16 800	8 300
Medium hazard	2 900	800
High hazard	300	300
Exposed	2 900	1 300
Exposed percent	3.2%	1.5%

Exposed population

No. people	ICG	JRC
Total population	10547000	10547000
Low hazard	1322000	560000
Medium hazard	282000	130000
High hazard	58000	48000
Total exposed	275000	143000
Exposed percent	2.6%	1.4%

Infrastructure

[km]	ICG	JRC
Total roads	15 800	15 300
Roads Low hazard	4 500	1 100
Roads Medium hazard	1 300	200
Roads High hazard	300	100
Roads exposed percent	7.5%	2.1%
Total railways	6 500	6 400
Railways Low hazard	1 500	400
Railways Medium hazard	600	0
Railways High hazard	0	0
Railways exp. percent	5.5%	0.6%





Romania

Capital: Bucharest

Areas

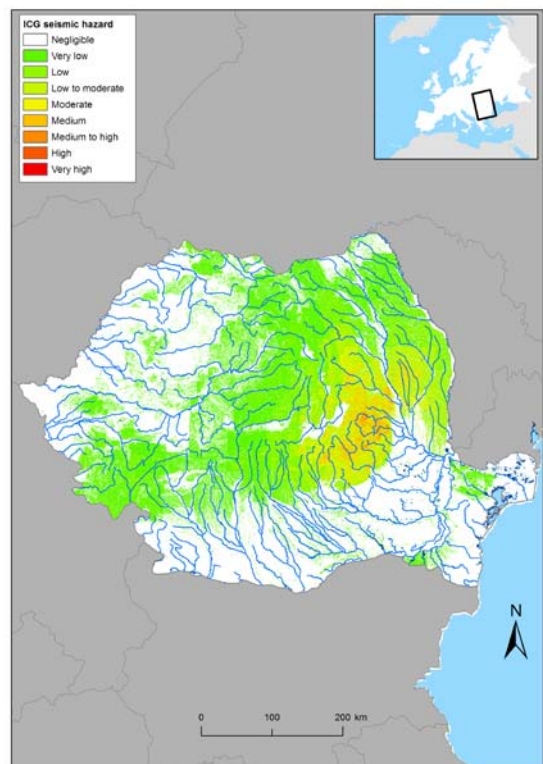
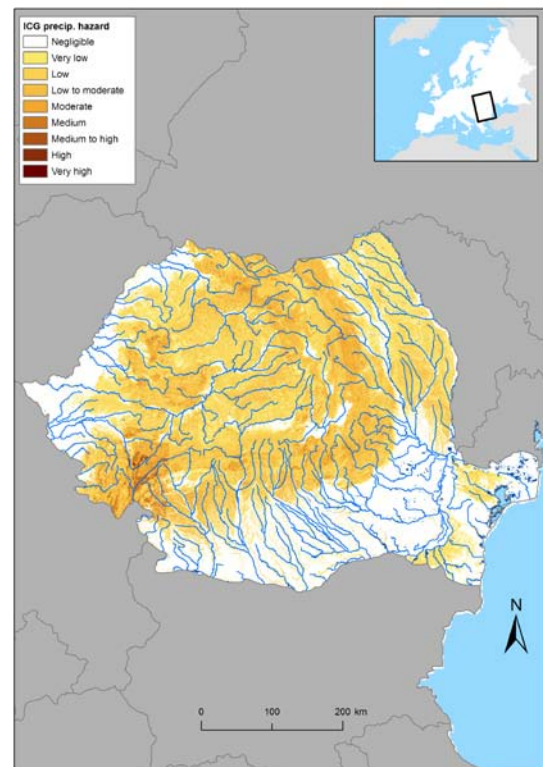
[km ²]	ICG	JRC
Total	237 400	237 300
Low hazard	43 400	44 600
Medium hazard	3 600	10 700
High hazard	100	100
Exposed	5 500	7 700
Exposed percent	2.3%	3.3%

Exposed population

No. people	ICG	JRC
Total population	21635000	21635000
Low hazard	2279000	2165000
Medium hazard	181000	454000
High hazard	6000	1000
Total exposed	288000	354000
Exposed percent	1.3%	1.6%

Infrastructure

[km]	ICG	JRC
Total roads	31 900	31 900
Roads Low hazard	6 200	4 500
Roads Medium hazard	1 000	1 000
Roads High hazard	100	0
Roads exposed percent	3.1%	2.4%
Total railways	23 500	23 500
Railways Low hazard	3 700	3200
Railways Medium hazard	800	700
Railways High hazard	0	0
Railways exp. percent	2.7%	2.2%





Slovakia

Capital: Bratislava

Areas

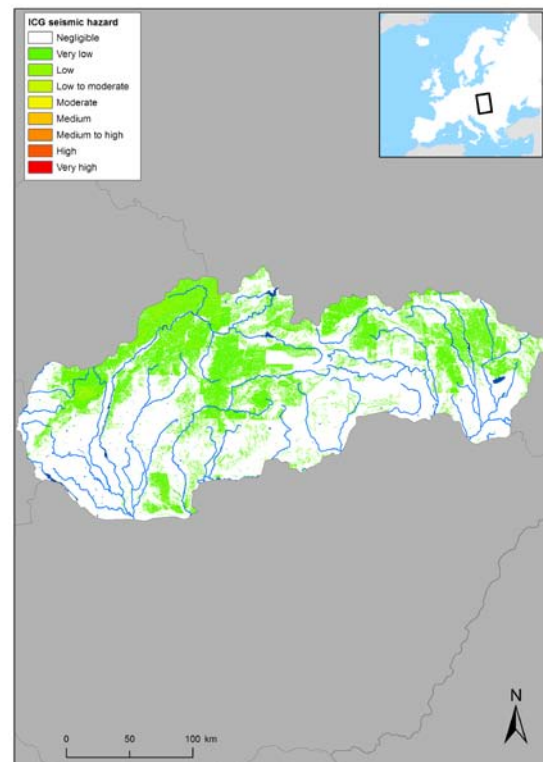
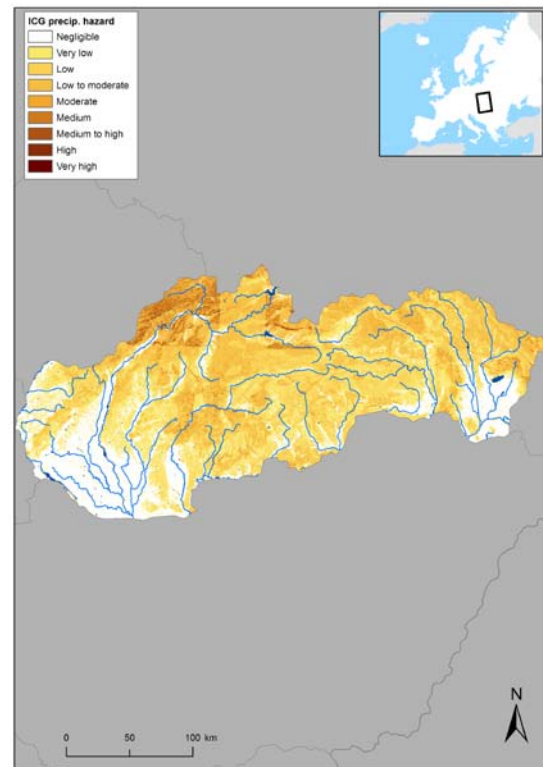
[km ²]	ICG	JRC
Total	49 100	49 100
Low hazard	10 700	20 300
Medium hazard	1 500	3 200
High hazard	0	0
Exposed	1 600	3 000
Exposed percent	3.2%	6.2%

Exposed population

No. people	ICG	JRC
Total population	5386000	5386000
Low hazard	837000	1664000
Medium hazard	143000	190000
High hazard	5000	1000
Total exposed	131000	224000
Exposed percent	2.4%	4.2%

Infrastructure

[km]	ICG	JRC
Total roads	7 800	7 800
Roads Low hazard	1 700	2 600
Roads Medium hazard	400	300
Roads High hazard	0	0
Roads exposed percent	4.1%	4.6%
Total railways	7 500	7 500
Railways Low hazard	1 300	2200
Railways Medium hazard	300	300
Railways High hazard	0	0
Railways exp. percent	3.3%	4.2%





Slovenia

Capital: Ljubljana

Areas

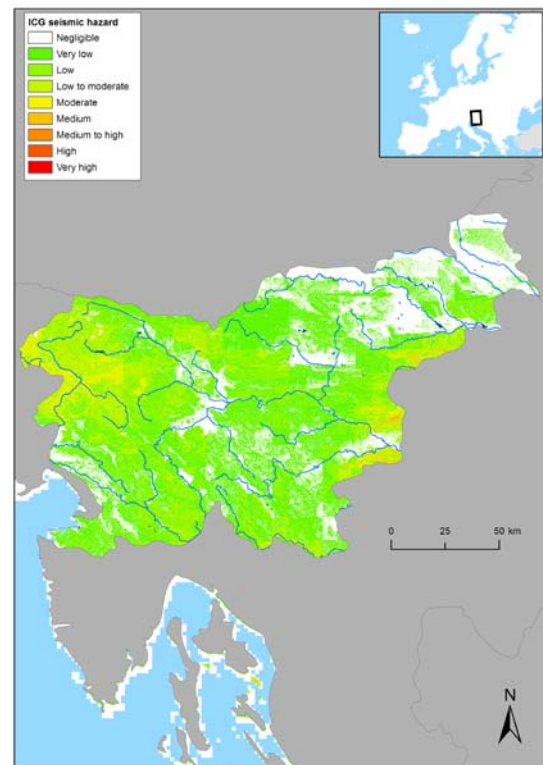
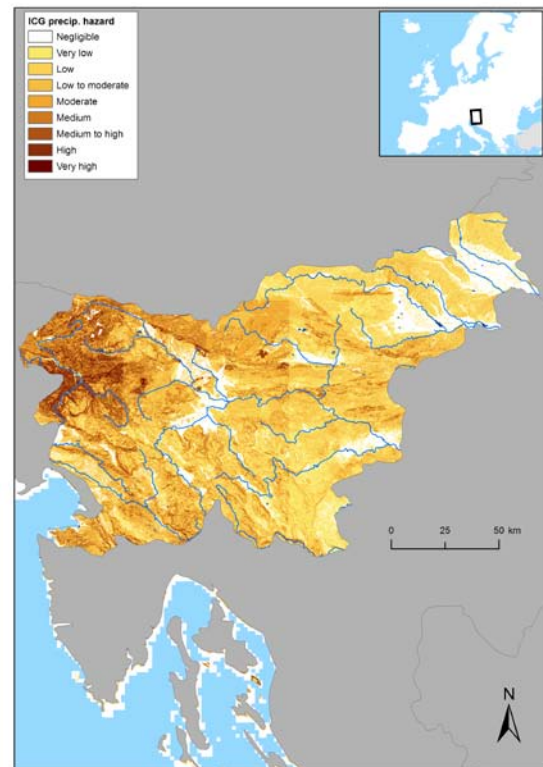
[km ²]	ICG	JRC
Total	20 000	20 000
Low hazard	6 000	8 600
Medium hazard	2 400	2 700
High hazard	500	2 000
Exposed	1 800	3 700
Exposed percent	9%	18.3%

Exposed population

No. people	ICG	JRC
Total population	2001000	2001000
Low hazard	383000	675000
Medium hazard	133000	123000
High hazard	20000	71000
Total exposed	98000	176000
Exposed percent	4.9%	8.8%

Infrastructure

[km]	ICG	JRC
Total roads	4 600	4 600
Roads Low hazard	1 500	1 800
Roads Medium hazard	900	400
Roads High hazard	200	300
Roads exposed percent	13%	13.4%
Total railways	2 500	2 500
Railways Low hazard	800	1000
Railways Medium hazard	400	200
Railways High hazard	100	100
Railways exp. percent	13.6%	10.5%





Spain

Capital: Madrid

Areas

[km ²]	ICG	JRC
Total	505 900	503 900
Low hazard	77 200	61 300
Medium hazard	14 500	20 900
High hazard	1 600	2 800
Exposed	13 700	15 200
Exposed percent	2.7%	3%



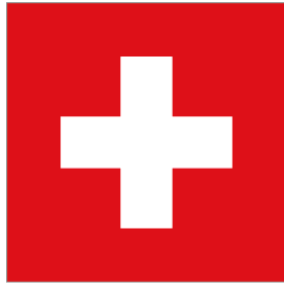
Exposed population

No. people	ICG	JRC
Total population	40264000	40264000
Low hazard	4493000	4457000
Medium hazard	1287000	1099000
High hazard	264000	165000
Total exposed	1100000	940000
Exposed percent	2.7%	2.3%



Infrastructure

[km]	ICG	JRC
Total roads	86 900	86 200
Roads Low hazard	16 300	10 400
Roads Medium hazard	4 400	3 300
Roads High hazard	800	500
Roads exposed percent	4.3%	2.9%
<hr/>		
Total railways	30 000	29 900
Railways Low hazard	4 700	3400
Railways Medium hazard	1 100	1000
Railways High hazard	100	100
Railways exp. percent	2.9%	2.5%



Switzerland

Capital: Bern

Areas

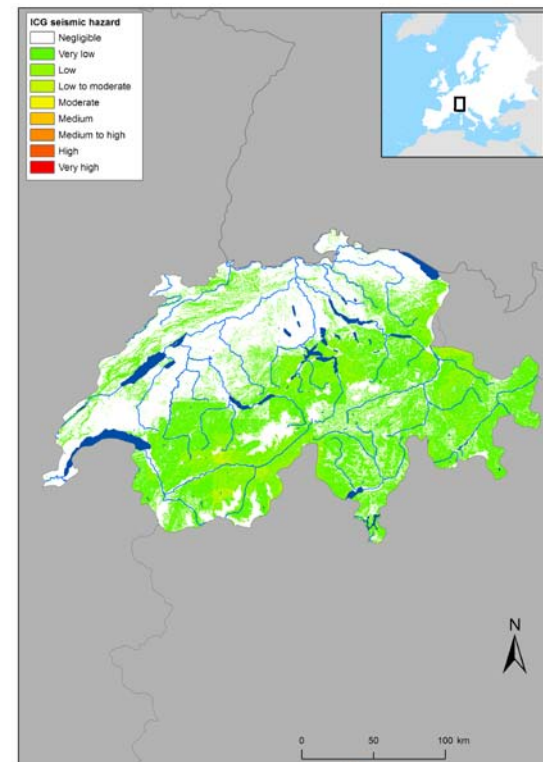
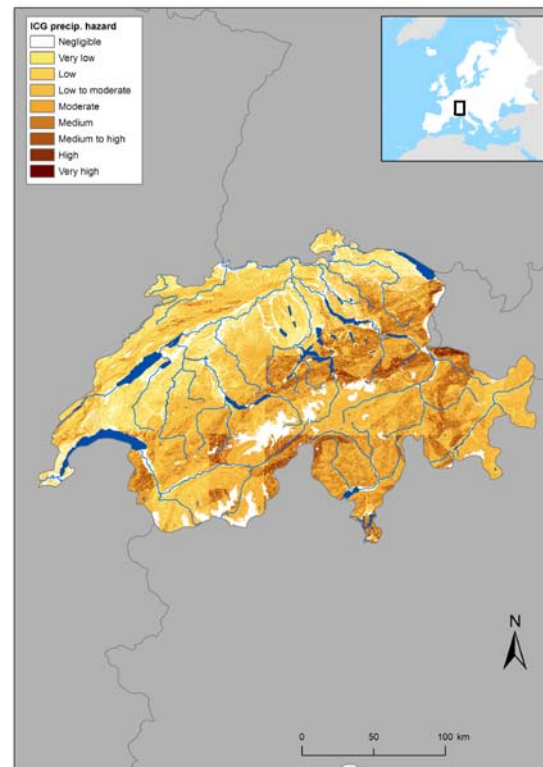
[km ²]	ICG	JRC
Total	41 400	41 400
Low hazard	15 800	10 700
Medium hazard	5 700	11 400
High hazard	500	10 100
Exposed	3 800	14 600
Exposed percent	9.1%	35.3%

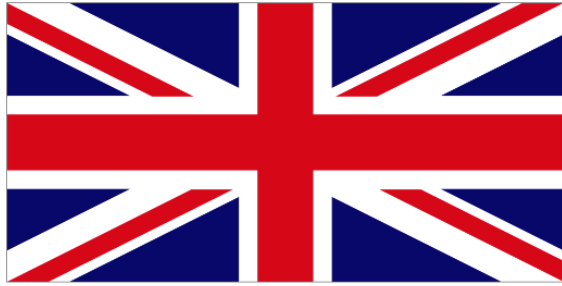
Exposed population

No. people	ICG	JRC
Total population	7441000	7441000
Low hazard	1654000	2478000
Medium hazard	440000	810000
High hazard	37000	522000
Total exposed	334000	1013000
Exposed percent	4.5%	13.6%

Infrastructure

[km]	ICG	JRC
Total roads	13 200	13 200
Roads Low hazard	4 600	4 400
Roads Medium hazard	1 900	2 000
Roads High hazard	100	2 000
Roads exposed percent	8.9%	23%
Total railways	9 500	9 500
Railways Low hazard	3 400	3100
Railways Medium hazard	1 400	1800
Railways High hazard	100	1600
Railways exp. percent	9%	25.3%





United Kingdom

Capital: London

Areas

[km ²]	ICG	JRC
Total	245 800	241 100
Low hazard	17 100	47 300
Medium hazard	3 800	7 000
High hazard	100	2 900
Exposed	2 900	9 700
Exposed percent	1.2%	4%

Exposed population

No. people	ICG	JRC
Total population	60261000	60261000
Low hazard	832000	4520000
Medium hazard	70000	90000
High hazard	0	11000
Total exposed	104000	490000
Exposed percent	0.2%	0.8%

Infrastructure

[km]	ICG	JRC
Total roads	97 200	96 400
Roads Low hazard	6 500	14 100
Roads Medium hazard	1 400	1 100
Roads High hazard	0	500
Roads exposed percent	1.1%	2.3%
Total railways	37 700	37 300
Railways Low hazard	2 100	4500
Railways Medium hazard	600	400
Railways High hazard	0	200
Railways exp. percent	1%	2%

